A NOVEL METHOD OF DETECTING GALLING AND OTHER FORMS OF CATASTROPHIC ADHESION IN TRIBOTESTS

by

Gregory Michael Dalton

A thesis submitted in partial fulfillment
of the requirements for the degree of

Doctor of Philosophy (PhD) in Natural Resources Engineering

The School of Graduate Studies
Laurentian University
Sudbury, Ontario, Canada

THESIS DEFENCE COMMITTEE/COMITÉ DE SOUTENANCE DE THÈSE

Laurentian Université/Université Laurentienne
School of Graduate Studies/École des études supérieures

Title of Thesis Titre de la thèse	A NOVEL METHOD OF DETECTING GALLING AND OTHER FORMS OF CATASTROPHIC ADHESION IN TRIBOTESTS
Name of Candidate Nom du candidat	Dalton, Gregory Michael
Degree Diplôme	Doctor of Philosophy

Department/Program Département/Programme	Natural Resources Engineering	Date of Defence Date de la soutenance	May 15, 2014

APPROVED/APPROUVÉ

Thesis Examiners/Examinateurs de thèse:

Dr. Markus Timusk
(Supervisor/Directeur de thèse)

Dr. Krishna Challagulla
(Committee member/Membre du comité)

Dr. Joy Gray-Munro
(Committee member/Membre du comité)

Dr. Marnie Ham
(External Examiner/Examinatrice externe)

Dr. Louis Mercier
(Internal Examiner/Examinateur interne)

Approved for the School of Graduate Studies
Approuvé pour l'École des études supérieures
Dr. David Lesbarrères
M. David LesbarrèresDr. Louis Mercier
Director, School of Graduate Studies
Directeur, École des études supérieures

ACCESSIBILITY CLAUSE AND PERMISSION TO USE

I, **Gregory Michael Dalton**, hereby grant to Laurentian University and/or its agents the non-exclusive license to archive and make accessible my thesis, dissertation, or project report in whole or in part in all forms of media, now or for the duration of my copyright ownership. I retain all other ownership rights to the copyright of the thesis, dissertation or project report. I also reserve the right to use in future works (such as articles or books) all or part of this thesis, dissertation, or project report. I further agree that permission for copying of this thesis in any manner, in whole or in part, for scholarly purposes may be granted by the professor or professors who supervised my thesis work or, in their absence, by the Head of the Department in which my thesis work was done. It is understood that any copying or publication or use of this thesis or parts thereof for financial gain shall not be allowed without my written permission. It is also understood that this copy is being made available in this form by the authority of the copyright owner solely for the purpose of private study and research and may not be copied or reproduced except as permitted by the copyright laws without written authority from the copyright owner.

Abstract

Tribotests are used to evaluate the performance of lubricants and surface treatments intended for use in industrial applications. They are invaluable tools for lubricant development since many lubricant parameters can be screened in the laboratory with only the best going on to production trials. Friction force or coefficient of friction is often used as an indicator of lubricant performance with sudden increases in friction coefficient indicating failure through catastrophic adhesion. Under some conditions the identification of the point of failure can be a subjective process. This raises the question: Are there better methods for identifying lubricant failure due to catastrophic adhesion that would be beneficial in the evaluation of lubricants? The hypothesis of this research states that a combination of data from various sensors measuring the real-time response of a tribotest provides better detection of adhesive wear than the coefficient of friction alone.

In this investigation an industrial tribotester (the Twist Compression Test) was instrumented with a variety of sensors to record: vibrations along two axes, acoustic emissions, electrical resistance, as well as transmitted torsional force and normal force. The signals were collected at 10 kHz for the duration of the tests. In the main study D2 tool steel annular specimens were tested on cold-rolled sheet steel at 100 MPa contact pressure in flat sliding at 0.01 m/s. The effects of lubricant viscosity and lubricant chemistry on the adhesive properties of the surface were examined. Tests results were analyzed to establish the apparent point of failure based on the traditional friction criteria. Extended tests of one condition were run to various points up to and after this point and the results analyzed to correlate sensor data with the test specimen surfaces. Sensor data features were used to identify adhesive wear as a continuous process. In particular an increase “friction amplitude” related to a form of stick-slip was used as a key indicator of the occurrence of

galling. The findings of this research forms a knowledge base for the development of a decision support system (DSS) to identify lubricant failure based on industrial application requirements.

Key Words

Abrasive wear

Acoustic Emission (AE).

Adhesive wear

Apparent contact area

Apparent interface pressure

Asperity

Catastrophic Adhesion

Coefficient of friction

Cold-rolled steel

Decision Support System (DSS)

EP additive

Friction

Galling

Lubricant

Real contact area

Tribotest

Twist Compression Test (TCT)

The above terms are used to describe phenomena particularly relevant to this research. The meanings of these words are explained when they are first used in this document. Definitions of many of these and other terms used in this document can be found in the ASTM Standard G40.

Acknowledgements

The completion of this dissertation marks the end of a long and winding path that started many years ago. Along that path I encountered many people and events that motivated me and influenced the research that forms the basis of this work.

My late mother, Catherine Dalton, deserves the credit for believing in me and getting me started in engineering. The late Prof. John Schey, Waterloo, recognized my potential as a tribologist and mentored me in both my academic and industrial research.

I am very grateful to have found in my PhD supervisor, Prof. Markus Timusk, someone who understands complex systems and was able to provide the guidance and tools to achieve our objective. My fellow graduate students, Greg Lakanen, Jeff Pagnutti, and Dr. Jordan McBain, helped immensely with the instrumentation and data manipulation.

This research was funded by TribSys Inc. and was initiated in response to questions I received from clients over many years. The research could not have been done without the knowledge and skill of Ted McClure, TribSys LLC, Valparaiso, Indiana, USA. Ted's abilities in formulating lubricants produced a rare collection of experimental lubricants that could be used to reveal the fundamental role of lubricants in adhesive wear. Ted also conducted the experiments of the preliminary study to help establish a baseline with an industrial tribotest.

I struggle to find words to express how much my spouse, Dr. Philippa Spoel, has contributed to this achievement. Her roles as an avid supporter, an advisor, an academic role model, and a friend are, without a doubt, the reason this dissertation exists today.

To my father,

the late William Joseph Dalton, PhD, who showed me what is possible.

and my children,

Aidan and Bridget, who inspire me to seek it.

"If he is indeed wise he does not bid you enter the house of his wisdom,

but rather leads you to the threshold of your own mind."

— Khalil Gibran, The Prophet

Table of Contents

List of Tables

List of Figures

Chapter 1

1 Introduction

1.1 Motivation and aim of this work

In transportation and resource industries, the various costs associated with equipment assets represent a large percentage of the total operating cost. These costs include the direct cost of equipment procurement, scheduled maintenance, and repair, as well as the indirect costs and reduced capacity associated with both scheduled and unscheduled downtime. Reducing any of these costs contribute directly to profitability but perhaps the greatest impact is realized with reducing unscheduled downtime.

> *"It's estimated that the total cost of unscheduled downtime can be as much as 15 times that of a scheduled event."* [1]

Industry relies on machines for every aspect of their activities from transportation to manufacturing. These machines have rolling and sliding components that eventually fail and require repair or replacement so that the machine continues to function. While the machine is nonfunctional, production capacity is impaired and other equipment and personnel may be idled until the machine is returned to operation. Both the cost of machinery repair or replacement and the lost opportunity of idle resources must be considered in the overall cost of equipment downtime.

Companies recognize the economic importance of keeping critical machines operating and devote considerable resources to that end. For example, in the mining industry, it is estimated that 50% of the cost of operating a mine is related to capital equipment maintenance and replacement [2]. Many unplanned failures in industry are attributed to lubricant breakdown

resulting in adhesive wear. Adhesive wear has many, sometimes confusing, names, it is commonly referred to as galling, scuffing, and pick-up, in this work the term "catastrophic adhesion" is used to include all forms of adhesive wear that have an irreversible, negative impact on the contacting surfaces.

Catastrophic adhesion occurs when two surfaces come into intimate contact and form junctions (also known as cold-welding). The formation and separation of these junctions result in unpredictable contact conditions. These conditions change the magnitude and distribution of contact stresses which may cause friction to rise and components to fail.

The likelihood of catastrophic adhesion occurring can be reduced by one or more of the following options: 1) selecting materials that have a low affinity for one another, 2) applying a surface treatment such as a coating (usually to one surface), 3) choosing a reactive lubricant that forms a separating film on the contacting surfaces, or 4) engineering the texture of the surfaces to retain lubricant (for example, very smooth surfaces are prone to adhesion [3]). While these solutions seem straightforward, solving the problem of adhesion is not easy. Generations of tribologists have failed to come up with a reliable model for predicting catastrophic adhesion. In 2006 Vitos and Larsen wrote:

"*In spite of the extensive research on galling throughout the years, today there is still a lack of understanding of the physical and chemical mechanisms that determine the adhesive and sliding behavior of metallic materials"*[4]

As a consequence of this lack of understanding, the engineer whose job it is to specify a lubricant or surface treatment must rely on previous experience, vendor knowledge (and bias), or trial and error to choose an appropriate course of action. Unfortunately, catastrophic adhesion (and the

resulting equipment failure) is stochastic in nature and the successful application of a lubricant can only be measured upon failure of the lubricant. A reliable method is needed for evaluating the ability of a lubricant or surface treatment to prevent catastrophic adhesion. The evaluation method must produce failure in each lubricant in order to compare the performance of candidate lubricants. The ideal system would also permit for the detection of catastrophic adhesion in real time allowing the test to be stopped thus preserving surface features of specimens at the point of lubricant failure. This would allow post-test analyses and help build a better understanding of lubricant mechanisms. The research presented here addresses the issue of lubricant and surface treatment selection using a systematic approach in developing a decision support system for lubricant and surface treatment evaluation.

The terms: lubricant, lubricating and surface treatment have many meanings. For the purpose of this study the following definitions are used:

- ***lubricant***, *n "a substance used for lubricating an engine or component, such as oil or grease"* [5]
- ***lubricating***, *adj "make (a process) run smoothly"* [6]
- ***surface treatment (finishing),*** *n "a broad range of industrial processes that alter the surface of a manufactured item to achieve a certain property. Finishing processes may be employed to: improve appearance, adhesion or wettability, solderability, corrosion resistance, tarnish resistance, chemical resistance, wear resistance, hardness, modify electrical conductivity, remove burrs and other surface flaws, and control the surface friction.* [7]

1.1.1 Decision support systems

The analyses of data from complex systems such as tribotesting may require computer algorithms to aid in data manipulation and pattern recognition. These systems are known as Decision Support Systems (DSS).

According to the U.S. Department of Education:

> *(A)"decision support system" is defined as a cohesive, integrated hardware and software system designed specifically to manipulate data and enable users to distill and compile useful information from disparate sources of raw data to support problem solving and decision making.* [8]

Decision support systems are being used in areas that have relied on expert interpretation and in areas where complex data sets cannot be accurately represented by traditional mathematical models. Their applications have varied widely from predicting consumer behavior to diagnosing and prescribing treatment in medical settings. Zalounina et al (2004) used a DSS to diagnose and treat infections and showed the power of DSS' by comparing models with and without cross-resistance to infection [9]. Studies on implementation of DSS into engineering applications show that DSS's are being used for their diagnosis and predicative capability in applications such as electrical power grid vulnerability and predicting equipment failure in a condition monitoring application. Stein et al (2003) [10] used a commercially available DSS platform to develop a fault detection system for a group of electron beams used in melting titanium. Prior to the implementation of the DSS the quality of the melting process relied on operator expertise to identify improper melting. With the DSS operating, the overall fault diagnosis improved and new operator training time was reduced from 2-4 years to 1-2 years.

Intelligent decision support systems serve engineers in many areas. For example, condition monitoring systems on aircraft engines interpret complex multidimensional transducers signals to detect incipient faults before they evolve into costly catastrophic failures. A key first step to producing such system involves understanding the mechanisms of failure and being able to reliably configure transducers, collect and process signals, extract features and reduce dimensionality of the data set. The system must also be insensitive to noise, be robust in nature, and be able to maintain data integrity (minimal filtering and optimal sampling rate) while being sensitive to the event that it is designed to detect.

Central to the task of building a DSS are three activities:

1. collecting the right data;
2. identifying the critical data features;
3. correlating those features to the outcome (knowledge acquisition).

Pechenizky *et al* called the process of knowledge acquisition *"among the most challenging tasks related to the development of a DSS"* [11].

This research embodies that knowledge acquisition process in the development of a DSS for lubricant evaluation by: 1) collecting multiple sensor data, 2) identifying the critical data features of adhesive failure, and 3) correlating these features to observed adhesive failure in industrial applications.

1.2 Background – Lubricant Formulation

It is important before discussing the details of this research that the workings of the lubricant industry be understood. For the most part, lubricant companies employ chemists who formulate lubricants for equipment and processes designed by mechanical engineers. These two disciplines have very little overlap and as a result there are few opportunities for communication and when it does occur is often not productive. Most of the problems arise during the lubricant development cycle when the chemist relies on a tribotest to provide a measure of the effectiveness of the lubricant in a complex mechanism or process. This section examines the context for, and issues related to, lubricant evaluation in the lubricant development cycle. Figure 1 shows the process of lubricant development starting with the impetus (drivers) for change and leading through to production trials. The process involves various information sources and feedback from the testing that takes place throughout the development cycle. This cycle takes months and years and cost hundreds of thousands of dollars so the importance of testing in achieving a successful product cannot be overstated.

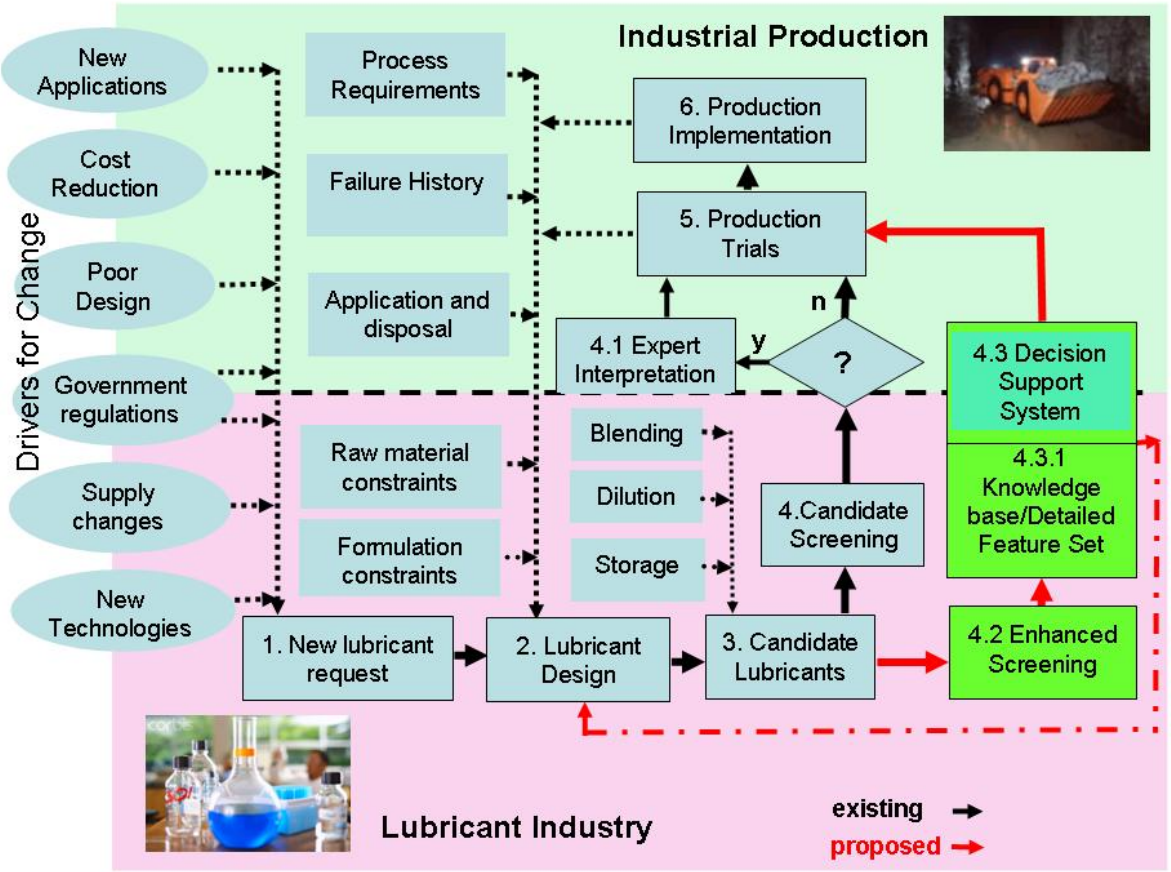

Figure 1: The Lubricant Development Cycle (black arrows)

1.2.1 New Lubricant Request – Drivers for Change

The drivers for change that lead to new lubricant requests originate from industrial production, government, or the lubricant industry itself. Production drivers include new applications, cost reduction, and poorly designed equipment. Governments may force change by setting regulations or requiring reporting of hazardous substances. The lubricant industry may drive change in trying to adapt to raw material supply or to gain a competitive edge using new technologies. These drivers for change are the primary reasons why new lubricant formulations are developed. It is important to understand the drivers for change in order to understand the lubricant development process. These drivers are explained in more detail in Sub-section I-VI.

I. New Applications

One expects that most new applications involve components similar to existing applications and therefore would use the same lubricants. While this is often true, many new applications are a complete departure from existing knowledge and it is not assumed that conditions are the same. This is particularly true with new tool materials where in some applications (i.e. high speed machining) the use of lubricants has been minimized or eliminated. Other applications, such as hydroforming (where pressurized fluid is used to form a component from a sheet or tube blank), involve process conditions that go beyond established practice. For example, in tube hydroforming, a steel tube is expanded into a cavity with water pressure that can exceed 350 MPa. The lubricant must allow the metal to move along the cavity wall or the tube will split. Furthermore, the lubricant must be compatible with the high pressure water pumps since contamination is unavoidable. Hydroforming and other novel processes usually require extensive lubricant development programs to fully understand lubricant requirements.

II. Cost Reduction

During process commissioning and startup, little attention is paid to the cost associated with consumables. Often a lubricant is chosen to solve a particular problem with little regard for cost. This is especially true in metal forming processes where in some cases polyethylene sheets are used to produce good parts. However, once a process is operating effectively, attention turns to maximizing profitability especially focusing on reducing the cost of consumables such as lubricants. Lubricants are a particularly attractive target since there is the cost of procurement and the cost of waste treatment and disposal.

III. Poor Design of a Part or Process

Some equipment or process designs are prone to failure because they are poorly designed. The failure of the equipment or process to achieve design specifications often leads to warranty and recall issues. In some cases the equipment or process operates outside of the design specifications. Once the equipment is onsite and operational it is usually easier to achieve improvement by trying a new lubricant than by changing the design.

IV. Government Regulations

Recognition by government that certain industrial chemicals are harmful to the environment or are hazardous to human health has led to restrictions on lubricant additives and cleaners. For example, since the late 1980's the lubricant industry has been under pressure to find alternatives for chlorinated paraffin (an additive that is used extensively to prevent catastrophic adhesion). Another example of how government regulations have driven the need for development of new lubricants is the elimination of chlorinated organic solvents and their replacement with water-based degreasers [12]. This necessitated a major effort by all lubricant companies to develop lubricants compatible with the new cleaning processes.

V. Supply Changes

The lubricant industry relies on the byproducts of oil distillation and is subject to variations in supply depending on the oil source and the end product demand. For instance, the characteristics of sulfonates (a multipurpose additive used as a rust preventative and an emulsifier) depend on the source of the crude oil. Synthetic sulfonates are much more

expensive but provide consistent characteristics. Bio-lubricants are suited for use in areas where lubricant is released in the environment. For example research and industrial trials are underway at the University of Northern Iowa to evaluate the effectiveness of bio-based greases for railway rails [13].

VI. New Technologies

New lubricant base oil and additive technologies provide opportunities for lubricant developers to gain a competitive edge by developing lubricants with superior properties to existing lubricants. Advances in nano-particles have opened up possibilities for lubricants with dispersions of nano-particles that increase the load carrying capacity of the base oil. The particles are small enough to remain in suspension during storage yet large enough to keep the surfaces from intimate contact in boundary lubrication [14].

1.2.2 Process Requirements – complex tribological relationships

Lubricants are formulated to control friction and temperature, and to minimize wear. However, all aspects of the process including facility cleanliness and health and safety must be considered in the design of the lubricant. While the design of a lubricant must first start with its intended purpose, the specific requirements of the process and downstream implications must be understood and addressed for a lubricant to be truly effective. Often conflicts arise between the various desired characteristics of a lubricant. For example, increasing lubricant viscosity may improve gear life for a piece of equipment but the increase in friction associated with the higher viscosity could increase energy consumption (the relationship between viscosity and friction is nonlinear). Likewise, in metalworking, improving lubricants with reactive additives for

improved component production may cause reactive surface films that cause downstream problems for welding and painting.

Tribology (the science of contacting surfaces in relative motion) provides a systematic approach to understanding the factors governing surface interaction in machinery. Mechanical devices rely on the movement of components in order to perform functions. The surfaces of the contacting components along with the lubricant separating them and the operating conditions (the machine's duty cycle) form a tribological system. This relationship is illustrated in Figure 2.

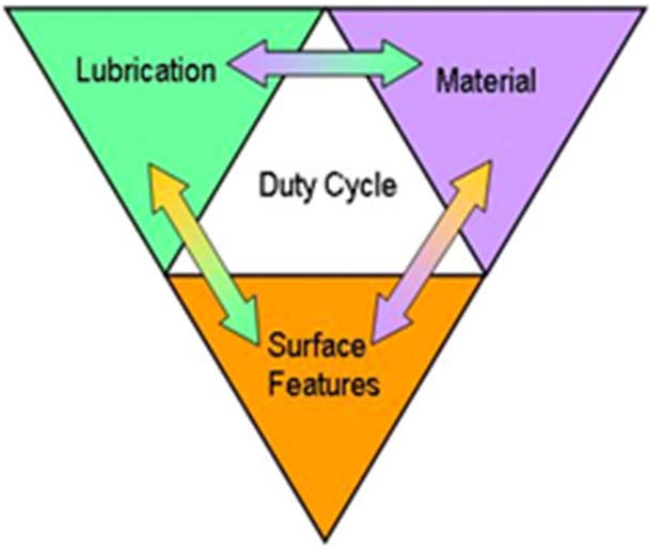

Figure 2: The components of a tribological system

I. **Material** refers to the bulk physical properties including: composition, hardness, strength, and elastic moduli features of each of the contacting surfaces.

II. **Surface Features** also refers to the properties of the contacting surfaces but is restricted to those features that lie on or near the surface including various roughness features, coatings, or modifications (chemical or thermal).

III. **Lubrication** refers to the action of any substance that is applied to one or both contacting surfaces including any reaction that modifies a surface physically or chemically.

IV. Duty Cycle includes system characteristics such as velocity of the surfaces, applied forces, start-stop or continuous timing, and the operating environment (e.g. temperature and atmosphere).

The complexity of a tribological system arises from the many interrelated factors as well as the diverse scientific disciplines at work. These disciplines include but are not limited to: physics, chemistry, dynamics, material science, solid mechanics, thermodynamics, and fluid mechanics.

One example of a tribological system found in the mining industry is the action of a scoop tram's bucket. The loaded bucket pivots on pins and bushings as it is lifted. A thin film of lubricant separates the bushing from the pin allowing the two surfaces to move relative to one another under the weight of the bucket and ore. In normal operations, this may happen thousands of times without failure. However, a single incident that is out of the ordinary (perhaps colder or hotter ambient temperatures) can cause the lubricant film to fail and the two surfaces to come into direct contact with one another. If conditions are right, catastrophic adhesion results and equipment failure follows soon after. The failure of a bucket's pivots is a common occurrence and a major contributor to equipment downtime (Figure 3).

Figure 3: Catastrophic adhesive failure of a scoop bucket pivot bushings necessitates rebuilding of the bucket pivots with mobile line-boring equipment. [15]

Similarly, catastrophic adhesion in the metal forming industry leads to downtime and failure of production equipment and manufactured components. Figure 4 shows the failure of a tube bending mandrel through catastrophic adhesion and the resulting failure of the pipe being bent. The factors contributing to failures should be considered in new lubricant design.

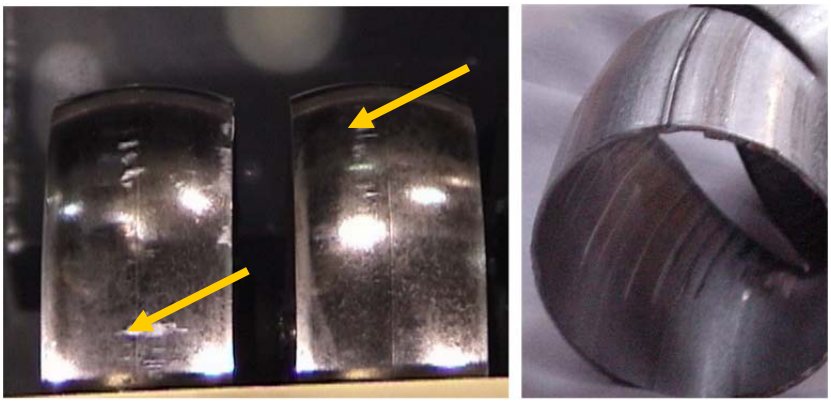

Figure 4: Adhesion on a bending mandrel and the resulting damage to the pipe (scoring and splitting)

1.2.3. Lubricant Failure

An important step in the development of lubricants is to consider previous process history, particularly lubricant failures. The immediate driver for change is cost reduction but perhaps there were previous failures that led to the adoption of a high price lubricant. The best way to understand lubricant failure is to examine failed components for the dominant wear mechanisms. Schey identified five modes of wear: abrasion, adhesion, erosion, fatigue, and chemical wear emphasizing that they rarely occur individually in isolation [16]. It is important to distinguish between the gradual wear associated with abrasion and erosion and catastrophic failure associated with adhesion. Abrasion and erosion are most often related to normal service life and as a result are predictable [17] and generally result in a gradual loss of functionality. Adhesion is unpredictable and usually results in unscheduled equipment downtime and component failure.

This thesis is intended to address the issues related to developing lubricants that are effective in reducing adhesive wear and its related cost. The discussion is begun in Chapter 2 by describing specific examples of catastrophic adhesion in a variety of industrial applications from mining to transportation and manufacturing. The theory of adhesive wear and how it relates to friction is then discussed in detail followed by an examination of the role of tribotests in modeling and measuring friction and wear. Advancements in data analysis using decision support systems (DSS) are introduced including a strategy for their application to tribotest data. Chapter 3 describes the experimental methodology for a preliminary study using a standard commercial TCT and a main and extended study using a highly-instrumented TCT to explore adhesive wear. Chapter 4 presents the results of the preliminary study where the suitability of the variables for the main study was evaluated. Chapter 5 presents the finding of the main and extended studies with post-test analyses of the test specimens. Finally the results are discussed in Chapter 6 with

the objective of answering the question: Are there better methods for identifying lubricant failure due to catastrophic adhesion that are beneficial in the evaluation of lubricants?

Chapter 2

2. Adhesive Wear - Costly and Unpredictable

This chapter outlines the issues and opportunities related to adhesive wear in various industries. The root causes of adhesive wear, and techniques used by the lubricant industry to mitigate this unpredictable and catastrophic form of wear are also reviewed. The final two sections examine how industry has attempted to evaluate adhesive wear mitigation strategies in the laboratory and how new analytical techniques are used to improve laboratory performance.

2.1. The Role of Adhesive Wear in Industry

2.1.1. Reduced productivity and profitability

Industrial equipment and processes, like consumer goods, have a designed service life. The startup or introduction period of a new process or product has a higher risk of failure early on than once the product is mature. As the product ages, it enters a period where material limitations increase failures often through gradual wear processes of erosion, abrasion and fatigue. The "bathtub" curve describes this typical product life cycle (Figure 5).

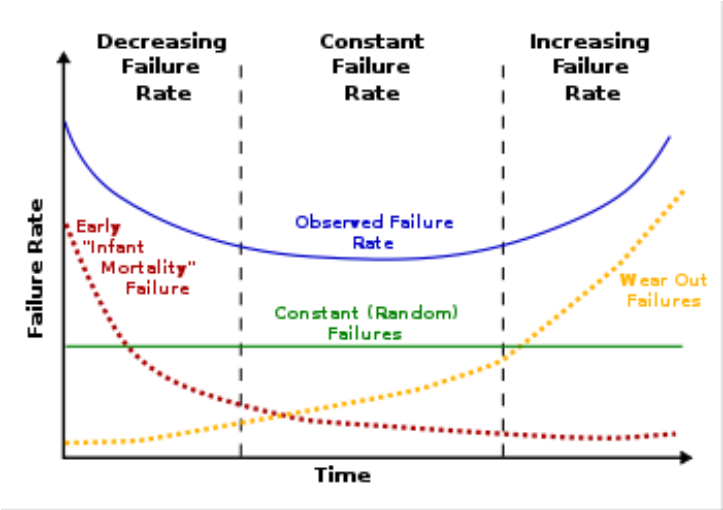

Figure 5: The Bathtub Curve and Product Failure Behavior [18]

If one considers the impact of a product on a manufacturer or mining company the capital costs of equipment (as well as other costs) are recovered during the life of the product or mine otherwise profit is impacted. It is critical for companies to control equipment downtime to achieve productivity and profitability. The best way to control equipment downtime is to understand the factors affecting component life cycle and to take measures to maximize service life while minimizing maintenance costs. In a 1995 study, Runciman and Vayenas found that preventative maintenance on scoops "consumed large amounts of repair time and contributed greatly to total downtime of all scoops under consideration." They recommended "better maintenance schedules (based on actual operating time) and reasoning of failures"[19].

2.1.2. Wear and maintenance

Wear is recognized and accepted as a limiting factor in the longevity and durability of equipment. The capacity and availability of equipment are critical factors in achieving productivity and profitability. Various studies have attempted to estimate the cost of wear to industry, in a 1987 study, Zum Gahr reported:

> *"Estimated direct and consequential annual loss to industries in the USA due to wear is approximately 1-2% of GDP"* [20].

Most companies track equipment breakdowns and try to minimize wear-related downtime on critical machines. Numerous strategies for minimizing wear-related downtime have evolved including scheduled (preventative) maintenance, predictive maintenance, and condition monitoring of lubricants and components to reduce downtime. The use of regular maintenance intervals based on a calendar schedule results in unnecessary downtime and part replacement for equipment that saw fewer hours of use than anticipated. Strategies that base scheduled maintenance on actual machine usage reduce downtime and maintenance costs. Condition

monitoring of oil detect oil deterioration and debris that indicate the need for maintenance. Condition monitoring of components for vibration or loading indicates wear and impending failure.

When components fail prematurely it is not just a matter of replacing the failed component but it is also important to determine the root cause of the failure and address it so that premature failure is avoided in the future. Premature failure can be defined as a failure mode that was unanticipated or occurred in a shorter period of time than anticipated at the time of design [21]. Determining the cause of failure is difficult since multiple wear modes are often present at the time of failure.

Adhesive wear, due to its stochastic nature is often the first wear mode to appear. Adhesive wear is easily identified as the root cause when the component fails due to seizure. However, other failures are not so obviously related to adhesive wear. Debris from adhesive wear may cause valves or seals to function improperly. Another failure related to adhesive wear is fatigue failure of a shaft originating at a stress concentration (scoring) caused by adhesive wear.

2.1.3. Impact of Adhesive Wear on Various Industries

The role of adhesive wear in premature failure is attributed to particular conditions typical of certain products and processes. These conditions usually involve sliding of contacting surfaces (rather than pure rolling), thin lubricant films, and high contact stresses. In some cases the designer recognizes the tendency for adhesive wear and includes measures such as special lubricant formulations or surface treatments. In other cases actual conditions are more severe than the designer anticipated. Such conditions are created by temperature extremes, frequent start-stop operation, and localized stresses from variable surface roughness. The following

examples illustrate the severity and serious nature of adhesive wear on a variety of engineering applications:

I. Automotive manufacturing – metal stamping is a high volume process that forms the backbone of automotive manufacturing. Metal stamping dies are required to run for duration of platform life (usually 5 to 7 years) to ensure economic feasibility [22]. Billions of dollars are spent annually on lubricants and surface treatments to prevent adhesive wear. Adhesive wear in metal stamping has a negative impact on productivity and profitability by reducing part quality, increasing die maintenance, and reducing die life. Figure 6 shows the effect of adhesive wear on the surface quality of a stamped steel hinge for a truck. The scoring of the metal was deep enough to cause premature failure concerns.

Figure 6: Galling of a truck door hinge rendering the part unusable. The white arrow indicates severe adhesive wear (galling) affecting part quality.

II. Wind Power Generation – The move into wind power using massive HAWT (horizontal axis wind turbine) designs saw thousands of these units being installed around the world over a relatively short period of time. Cost analysis of the projects was based on a 20 year life of the turbine. In a 2006 Sandia Labs report [23] entitled *Wind Turbine Reliability: Understanding and Minimizing Wind Turbine Operation and Maintenance Costs*, Christopher Walford reported:

"The costs can be separated into the broad categories of operations, scheduled maintenance and unscheduled maintenance. The portion of O&M costs associated with unscheduled maintenance – the area most difficult to predict – is between 30% and 60% of the total"

Much of this unscheduled maintenance was a result of higher rate of gearbox failure than anticipated. Ribrant [24] found that most of the premature gearbox failures were attributable to wear of mechanical components. Furthermore, failure of the gearbox in these large turbines results in more downtime than for other types of failure. Gearbox failure not only increases maintenance costs but is a major cause of downtime since the wind turbines are often located in remote, inaccessible areas and the gearbox components require cranes and other specialized equipment for repair or replacement. While the type of wear in the Ribrant study was not discussed, others have related factors such as load and speed contribute to the occurrence of scoring on the gear tooth face in power generating equipment.

III. Mining – The severe environment (dust, high humidity and other harsh conditions) encountered in typical mining operations results in accelerated wear of components. For underground mining those particularly susceptible to adhesive wear are:

- **Scoops** - The bucket bushings on scoops are particularly susceptible to galling due to the highly localized stresses (during lifting of a loaded bucket) and long sliding distances (60-90 degrees of rotation) where the lube is squeezed from the contact zone.

- **Wire ropes for hoists** - Wire ropes require frequent application of lubricant with extreme pressure (EP) additives to prevent adhesive wear between the drum and the wires and between the wires themselves. The ropes are suspended in shafts where they are subjected to moisture and dust. Intermittent service of wire ropes results in poor lubrication in areas where the lubricant has dried or migrated away [25].
- **Hoist gears** - Hoist gears like wind turbine gears suffer from intermittent use. During stoppages lubricant migrates from the gear teeth interface leaving areas that are unprotected at startup. Operating speeds below design specifications leads to poor lubricant splash up from the rotating gears. While this problem is addressed by pumping or misting the lubricant directly onto the gears, most systems still rely on splash lubrication [26].
- **Hydraulic components** – Heavily loaded equipment results in adhesive wear of sliding and rotating hydraulic components.

IV. Transportation – While adhesive wear is problematic in many areas of the transportation industry, this discussion focuses on some of the more relevant examples with respect to both economic cost and passenger safety.

- **Railways** – In North America large volumes of freight are moved every day by rail. Rail is an efficient means of transportation due to the low friction losses of the steel wheel rolling on the steel rail. Unfortunately, when the wheels slide, either laterally while cornering or longitudinally during braking or hill climbing, the probability of adhesive wear is high. In a 2006 study Reddy estimated that, in the US alone, the cost of ineffective lubrication at the wheel-rail interface was in excess of US$2 billion annually [27]. A startling case is one studied by the author where a rail collapsed under a static normal load and a spinning (sliding) wheel (Figure

7). Adhesive wear and thermal softening combined to undermine the structural integrity of the rail resulting in its collapse.

Figure 7: Image showing damage to a rail from adhesive wear action of a spinning rail wheel (photo courtesy Ontario MNR)

- **Aircraft** – In the aircraft industry there is a high probability of fatal crashes when critical components fail. As a result, product testing and safety procedures are more stringent than in other industries. A recent helicopter crash in Canada highlighted the problem of predicting the occurrence of catastrophic adhesive wear.

The crash of a Sikorsky helicopter off of the coast of Newfoundland resulted in the tragic loss of 17 lives when the oil pressure in the gearbox dropped due to a broken stud. With the loss of pressure the gearbox faced a run-dry condition that, under design specifications, it could endure for 30 minutes. Being only 54 miles from the St. Johns Airport the pilots opted to return to base rather than ditching in the sea. The gearbox seized and the helicopter crashed after only 10

minutes. The pilots were forced to ditch from 800 feet resulting in the deaths of 17 of the 18 passengers and crew. In the ensuing investigation it was found that the gearbox had failed the 30 minute run-dry test but was certified by the FAA since they considered the likelihood of a total loss of oil to be remote. In the crash report, the Transportation Safety Board of Canada recommended (among other things) that the FAA reassess the exemption it granted Sikorsky on the 30 minute "run dry" requirement for the gearbox [28].

The stochastic nature of adhesive wear testing leads engineers to the belief that these tests are not reliable. However, adhesive wear results show that time to failure is dependent on complex, poorly understood variables. Adhesive wear tests are valuable in providing failure data when they compare two lubricants or coatings.

2.1.4. Origins of Adhesive Wear

Adhesive wear as the name suggests has its origins in the adhesion between surfaces. While adhesion alone between surfaces is not sufficient to cause wear, it is the root of the problem.

The role of adhesion in friction was disputed for many years with camps split between those who believed friction results from asperity interaction (roughness features) and those who believed that friction was a result of the adhesive attraction of surfaces. Advances in surface analysis (particularly the atomic force microscope, AFM) have shown that both asperity interaction and adhesion play a role in friction and adhesive wear. This role is critical to the understanding of lubricant failure and will be discussed at length in the next section.

2.2. Friction and Adhesive Wear

2.2.1. Overview

This section explores the relationship between friction and adhesive wear. This exploration is a necessary part of this investigation because many wear researchers use friction as an indicator of adhesive wear. Often the relative value of the COF (coefficient of friction) or a sudden rise in the COF is used to indicate that adhesive wear has occurred. Given the close relationship that is assumed between friction and adhesive wear it is important to examine the origins and validity of this assumption.

One might expect that friction (documented as early as the building of the pyramids) has been thoroughly researched and well understood with comprehensive mathematical models to calculate friction for a given pair of contacting surfaces. Unfortunately, despite several centuries of effort, the ability to characterize friction with theoretical models is possible for only the simplest of cases. Friction values for most real-life contacts (i.e. in the presence of surface oxidation, lubricants, and high stress levels) must be determined empirically.

2.2.2. Early Friction Theories

Scientific writings for the past 500 years beginning with Leonardo Da Vinci (1452-1519) have identified the properties of friction in order to arrive at a general theory of friction. Da Vinci presented two laws of friction: 1) that friction was independent of apparent contact area, and 2) the friction force was proportional to the normal force [29]. His theory that the resistance to sliding came from the roughness of the surfaces and that smoother surfaces had lower friction continues to be disputed and debated.

Like Da Vinci, Amontons (1663-1705) and Coulomb (1736-1806) believed that friction arose from the work required to separate surface roughness features or, alternatively, to wear or deform the surfaces [30]. The model in Figure 8 shows two simple asperities colliding. They must shear off, deform, or separate in order to continue moving.

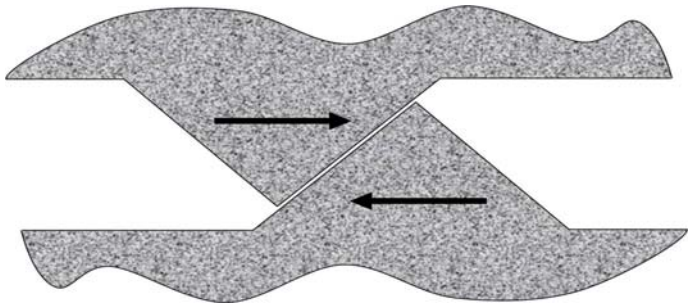

Figure 8: Asperities on opposing surfaces must shear, deform, or separate when they encounter.

The model shown in Figure 9 illustrates how the frictional force is independent of the apparent area of contact when only the separation of asperities is considered. The weight of a block resting on it small face has less asperities engaged than when it is resting on its large face but, assuming the roughness of the surfaces are the same, the amount of work to lift its weight clear of the asperities is the same. However, if shearing or deformation of the asperities is considered than the fewer asperities (smaller contact area) requires less force to deform or shear. The result is a lower frictional force with a smaller area.

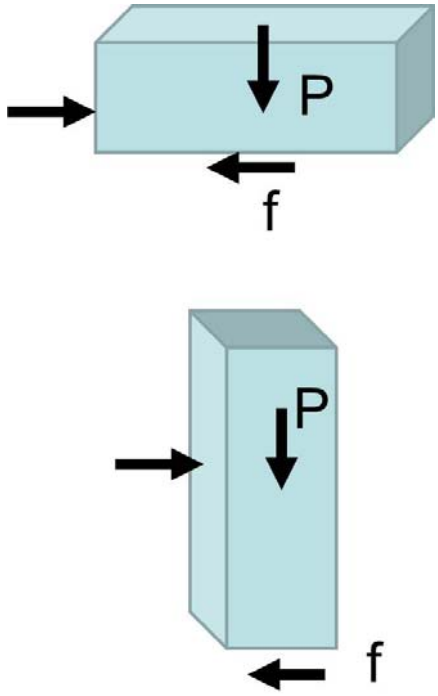

Figure 9: Friction independent of apparent contact area in the asperity interaction model of friction.

These early laws of friction lead to the definition of a non-dimensional measure of friction known as the coefficient of friction (COF or μ), the ratio of the frictional force (f) to the normal force (P):

$$\mu = f/P \qquad \textbf{Equation 1}$$

The coefficient of friction is a convenient measure of the relative ease of sliding two surfaces against one another. The COF, however, has limited value since the usually complex conditions of sliding are reduced to a single ratio. These complexities include oxidation of the surface, preparation technique, contamination from process lubricants, and environmental considerations (temperature, humidity). Despite its lack of usefulness, the static and kinetic COF values for material couples in dry contact and in some cases lubricated contact are still presented in

engineering handbooks. The limitations of these tabulated values are acknowledged in the preface to the table:

> *"Extreme care is needed in using friction coefficients and additional independent references should be used. For any specific application the ideal method of determining the coefficient of friction is by trials."* [31]

Amonton surmised that friction force arose from the work required to lift the load and unlock the asperities (Figure 9). He concluded that the friction force for all surfaces was a constant ratio of friction force to normal load of 1:3 [32].

For more than 150 years these views were supported by investigations of scientists such as Euler and Coulomb. Deviations from the 1/3 ratio were explained by fracture and deformation of asperities [33]. One expects that in the absence of asperities on a surface (such as with glass or liquid) friction is minimal; however, the opposite was found to be true.

Rayleigh, Beilby, and later Tomlison (1929) investigated the friction force between smooth surfaces and concluded that molecular attraction between surfaces was the source of friction between smooth surfaces [34].

2.2.3. Modern friction theories – asperities and adhesion in sliding friction

Bowden and Tabor's examination in 1950 of the Amonton/Coulomb Laws of Friction showed that these laws worked relatively well for many contacts for reasons unknown to their originators [35]. They found that friction is dependent on real contact area and that as normal load increased asperity interaction increased and with it the shear force required to maintain motion. This finding showed conditions where friction is independent of apparent contact area and illuminated the mechanism for the proportionality between normal force and frictional force. They found that these laws held for surfaces where the real area of contact grows with increasing normal load

including boundary lubricated surfaces (discussed in the next section). There are many cases where the real area of contact does not grow with increasing load and the friction laws do not hold. Bowden and Tabor point out that the laws are no longer valid for thin metallic coatings, soft metals, and oxide films. Other mechanisms that block the increase in real contact area are work-hardening of the surface with plastic deformation, merging of the asperities under very heavy normal loads, and the presence of reactive lubricant films.

At the biennial congress of the International Deep Drawing Research Group in Dearborn Michigan, Dalton modeled asperity fields using polyethylene foam showing how the real area of contact of a surface could stabilize when asperities merge forming closed lubricant reservoirs [36].

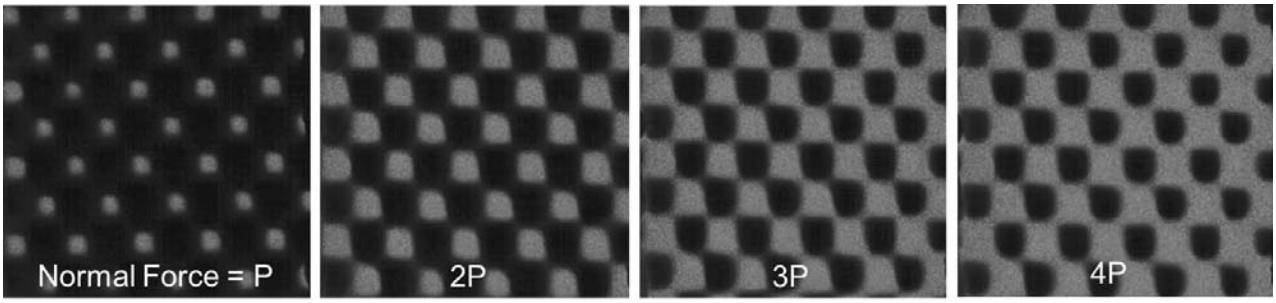

Figure 10: Foam model photos showing the formation of closed pockets (dark areas) as asperities (light areas) merge with increasing load. [36]

Later, in two different studies, Dalton showed how the coefficient of friction decreased with increasing normal force (at least initially) in lubricated flat annular contact using the Twist Compression Test (TCT). The two studies showed the transient nature of friction during flat sliding and the effect of viscosity on friction Figure 11 [37] and Figure 12 [38]. The lubricant used for the two studies varied widely over a range of viscosities with the lubricant for the data

depicted in Figure 11 being a high viscosity 90 cSt gear oil while the lubricant used in Fig 12 study was a 23 cSt oil.

a.

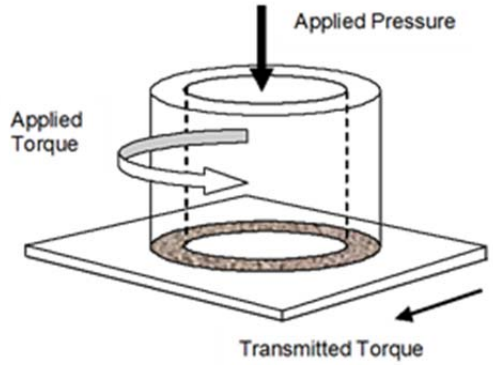

b.

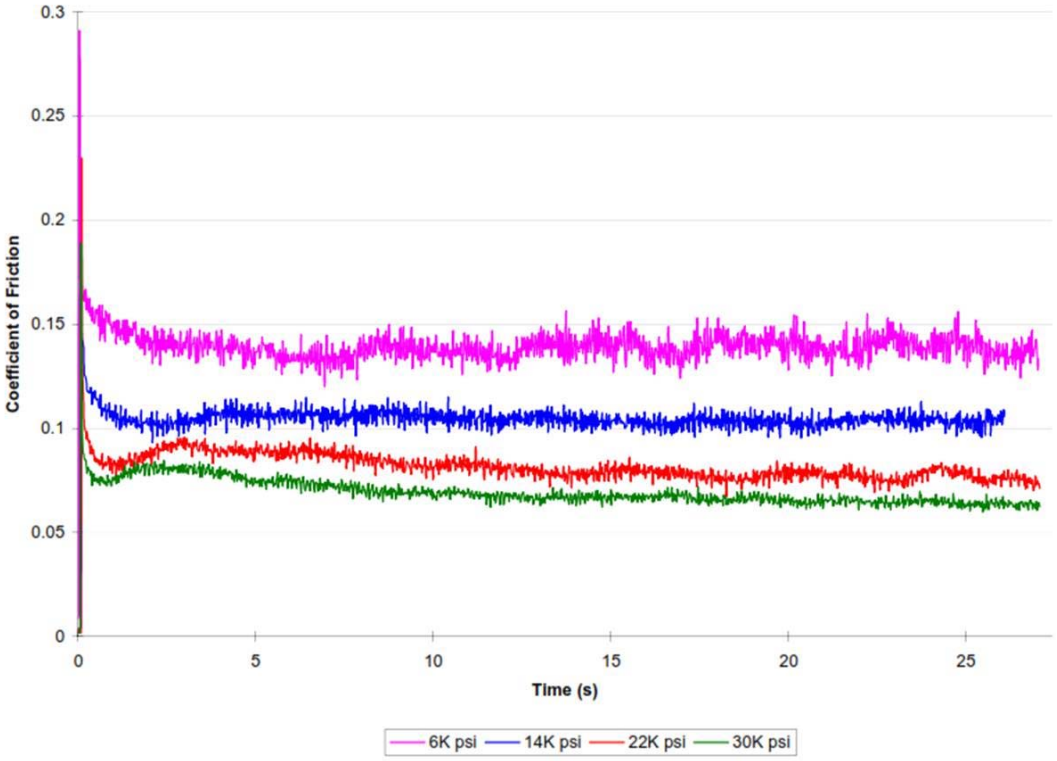

Figure 11: (a) The contact area (shaded) between the upper annular specimen and lower flat sheet in the Twist Compression Test (TCT). (b) TCT results showing decreasing friction with increasing contact pressure with all other factors held constant. (courtesy TribSys Inc.)

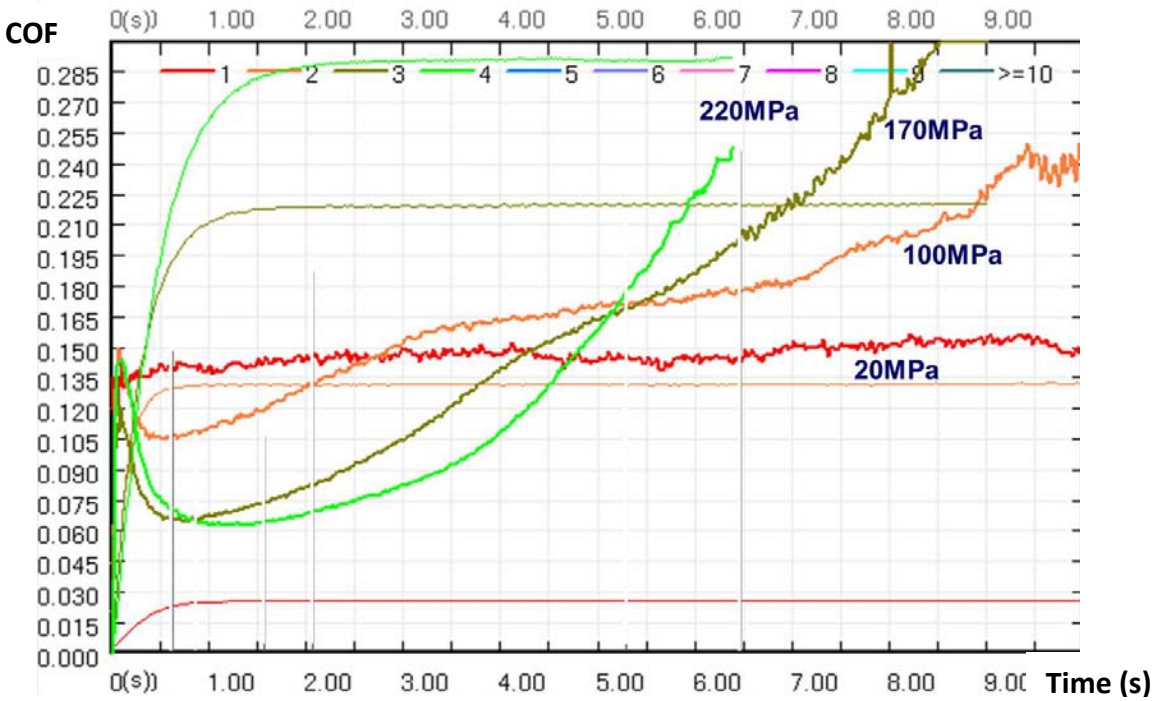

Figure 12: Friction response (μ versus time (s) of a lubricated steel on steel contact at different apparent contact pressure for TCT results)

Note:

- The lighter coloured curves show the instantaneous apparent contact pressure corresponding to the friction curves of the same colour
- The lowest friction values are achieved at the highest apparent contact pressure (light green curve).
- Apparent contact pressure is calculated using the measured normal force divided by the apparent area of contact shown in the schematic (Figure 11a).

2.2.4. Lubricants and Friction

Rotating shafts were common during the industrial revolution as steam energy was harnessed using pistons and crankshafts. The high speed of rotation and large forces required shaft supports to allow the shaft to turn with low wear and minimal friction losses. Near the end of the 19th century Reynolds described how under the right conditions a rotating shaft is supported on a

lubricant film. This was accomplished with journal bearings. Journal bearings support rotating shafts by generating a pressurized lubricant film to support the shaft (Figure 13).

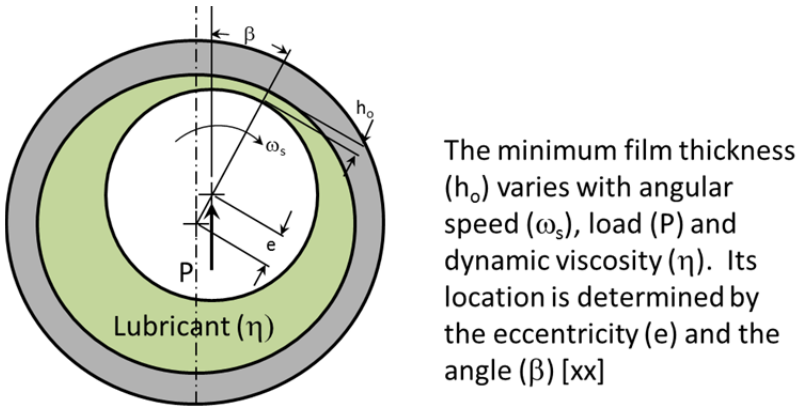

Figure 13: Journal Bearing illustrating Reynolds' parameters [39]

In 1902 Stribeck published curves (Figure 14) showing the relationship for the phenomenon described by Reynolds and later Hersey related velocity, viscosity, and interface pressure to the film thickness and the coefficient of friction in journal bearings where:

> *"the minimum film thickness (h_o) varies with angular speed (ω_s), Load (P) and dynamic viscosity (η). Its location is determined by the eccentricity € and the angle (β)"* [39]

Stribeck's model showed how speeds, viscosity lubricants, and load affect film thickness. With low viscosity, low speed, and high loads the film was not sufficient to separate the surfaces and the load was borne at the contacting asperities (boundary regime). This is the startup condition for most equipment and the surfaces must be able to survive the highly localized stresses. As the speed or viscosity increased (or the load dropped) the film thickness increased and the surfaces began to separate. Friction decreased linearly as the fraction of the apparent contact area supported by the lubricant grew (mixed film regime). Once full separation between the surfaces was established further increase of the Hersey parameter ($\eta * \omega/\beta$) resulted in an increase in friction due to viscous drag.

Stribeck's model was well-received then and over one hundred years later the Stribeck curve is still used to describe many lubricated contacts. It is cited extensively in tribology studies far removed from journal bearings. A search of the past 5 years of *Tribology International* publications reveals forty-two scholarly references ranging from a new friction model for metal stamping lubricant based on the Stribeck curve to an investigation on the effect of saliva viscosity on tribological behaviour of tooth enamel.

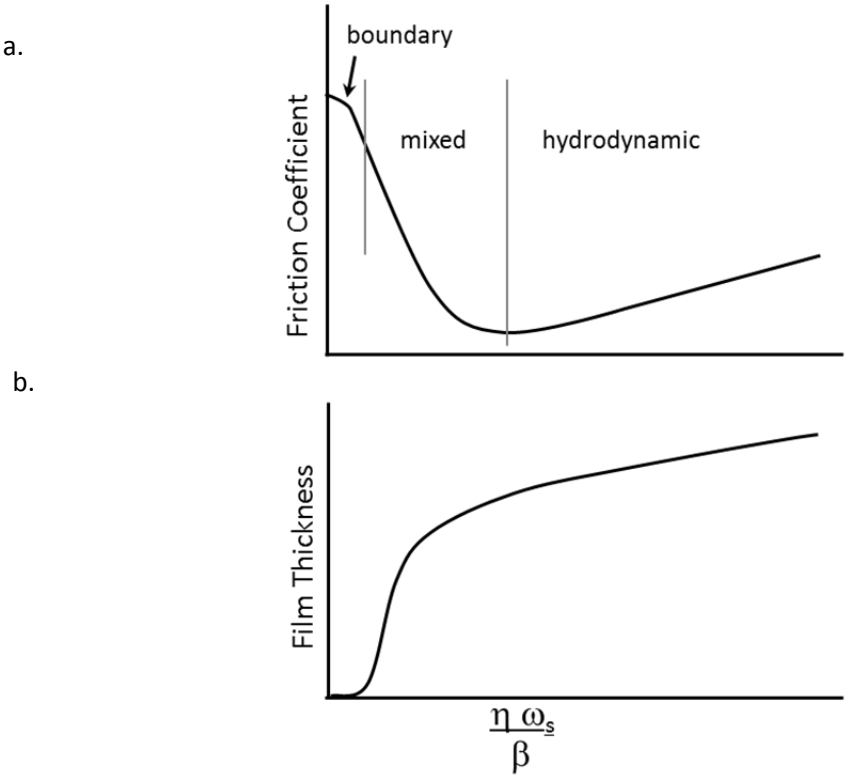

Figure 14: Stribeck curves showing the variation of (a) friction and (b) film thickness with the non-dimensional Sommerfeld parameter.

Schey recognized the limitations of the Stribeck curve for the extreme contact stress of many metal forming operations [40]. He suggested a modified 3 axis relationship (Figure 15) with the ratio of contact stress (p) to flow stress (σ_f). The complexity of his model was necessary to

encompass lubricant additives and plastically deforming metals but unfortunately these complications limited its widespread acceptance.

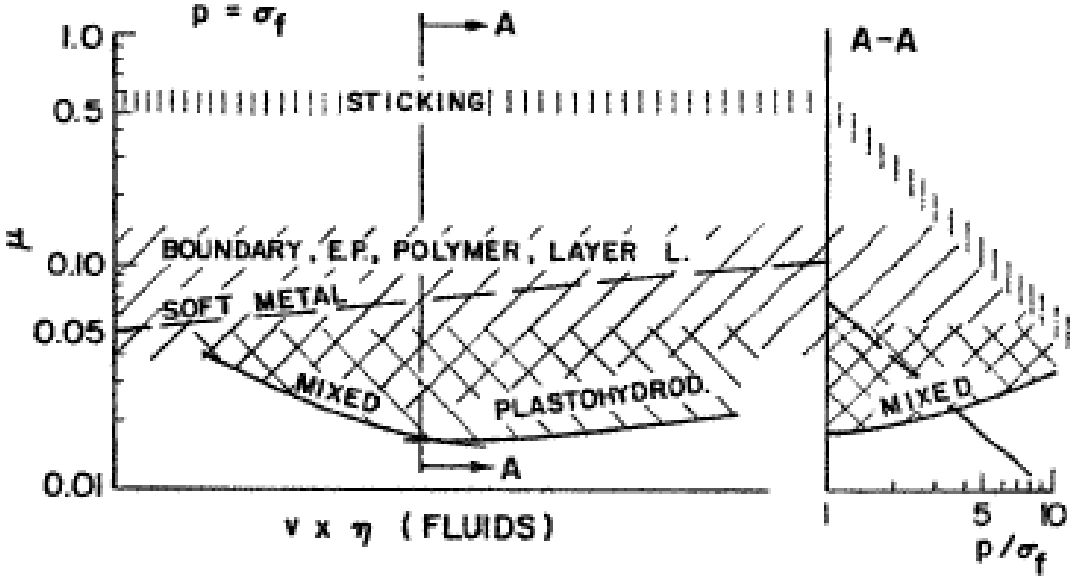

Figure 15: Modified Stribeck curve for metalworking *(from Schey, Tribology in Metalworking)* [40].

2.2.5. Sliding contact

In their 1950 landmark text "The Friction and Lubrication of Solids" Bowden and Tabor tackled the question of the origins of friction [41]. They observed that previous theories of the source of friction were confined only to surface phenomena such as sliding and molecular attraction and that these theories ignored the massive distortion and deformation of sliding surfaces:

> *"Obviously the physical processes that occur during sliding are too complex to yield easily to a simple mathematical treatment, but the experiments show that, under the intense pressure which acts at the summits of the surface irregularities, a localized adhesion and welding together of the metal surfaces occurs. When sliding takes place, work is required to shear these welded junctions and also to plough out the metal."* [41]

Bowden and Tabor suggested that finding a quantitative model of the friction force is not realistic and instead proposed a general friction model to provide an understanding of the contributing factors. In their model friction is the sum of two terms: a shearing term and a ploughing term. The shearing term is a function of the shear stress (s) acting over the real area of contact (A). The ploughing term is a function of the pressure required to displace the material (p') in front of a hemispherical asperity and the cross-sectional area (A') of the portion of the asperity that is below the surface (Figure 16). The total frictional force is given as:

$$F = S + P = As + A'p' \qquad \textbf{Equation 2}$$

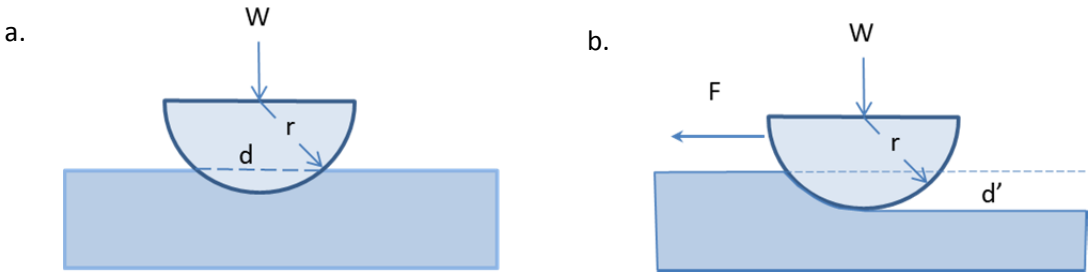

Figure 16: Bowden and Tabor's model of a hard asperity in contact with a soft surface: (a) shows the contribution due to shearing (S) and (b) shows the contribution due to ploughing (P).

Schey [42] suggested that for metal forming the ploughing term should be dropped since quality considerations would preclude that condition and the process should be stopped. He showed how the Bowden-Tabor friction model for the shearing component at the point where asperity deformation stabilizes ($P=A_rH$) would be reduce to:

$$COF = S/P = A_r*k/A_r*H = k/H \qquad \textbf{Equation 3}$$

According to Von Mises, $k=0.577\ \sigma_f$ and with H estimated as $3\sigma_f$, maximum friction values would be about 1/5. Higher friction values are common and result when the combined shear and normal stress are considered. The reason for the higher friction is that pressure required for flow

(σ_f) drops and the real area of contact increases and with it the required shear stress to break the junctions.

The shaping of metal involves processes that impose high stresses in order to exceed the elastic limit and achieve plasticity for a given metallic material. Metal forming processes are complicated by metal properties that vary dynamically with strain-rate sensitivity, work hardening, and dynamic recrystallization. The surfaces of these metals are also undergoing surface roughness changes in some cases roughening and others flattening of asperities as well as extreme thermodynamic events.

However, these changes to the surfaces are not limited to metal forming. Plastic deformation is a common event in many surface interactions when lubricant films do not fully separate two surfaces. When sliding is initiated, a frictional shear stress is superimposed on the normal stress and the combined stress results in further deformation of the asperities. The combination of sliding, high contact forces and newly formed (nascent) surfaces gives rise to the ideal conditions for adhesive junctions to form (cold welding). These junctions either cause the sliding to cease (seizure) or shear at the weakest point. If the shear line is below the original surface then metal is transferred to the opposite (harder) surface. During subsequent sliding the transferred metal may act like a plow damaging the softer surface or be re-transferred to the other surface where the process continues. This process, known as adhesive wear, is present to some extent in all contacts that are in intimate contact (i.e. bearings and gears during starting and stopping, wire rope when it is wound on a drum) and can become catastrophic (reducing the expected service life) if not controlled.

2.2.6. Controlling Adhesive Wear with Lubricants and Surface Modification.

There are many ways to reduce adhesive wear between contacting surfaces, especially if these methods are introduced during the design stage of a process or mechanism. In most cases the issue of adhesive wear is not recognized until after commissioning when productivity is affected. The issue is then left for production and maintenance engineers to address. The two most common tools that they have for controlling adhesive wear are lubrication and surface modification.

The most effective method of reducing adhesive wear is by completely separating the contacting surfaces with a lubricant. However in most cases contact is unavoidable and adhesive wear is inevitable. The severity of the adhesive wear event depends on the nature of the contact and the properties of the surfaces.

Another method of controlling the severity of adhesive wear is to introduce a reactive element into the area of metal to metal contact. Typically there are three elements used in this manner they are: phosphorus, chlorine, and sulfur and are known as EP additives [43]. EP stands for "extreme pressure" but the name is a misnomer since it is not pressure but temperature that activates EP additives [44] (Figure 17). This figure also indicates the limit of effectiveness of these additives (i.e. temperature at which desorption or decomposition occurs).

Cameron also observed the temperature sensitivity of lubricant additives [45]. He found that regardless of the lubricant film thickness, gears became scuffed when the surface temperature reached a critical temperature between 150 and 200 degrees Celsius. He found that below this temperature boundary additive molecules were adsorbed on the surfaces. He wrote:

"As soon as the temperature of the surfaces reaches the critical value the molecules desorb and the surfaces are clean. Any adventitious bridging of the surfaces, either due to high spots touching or to a piece of metallic wear debris, causes them to weld together. On parting a chunk is torn out and next time round this welding and tearing gets worse till the surfaces are completely torn and scored."[45]

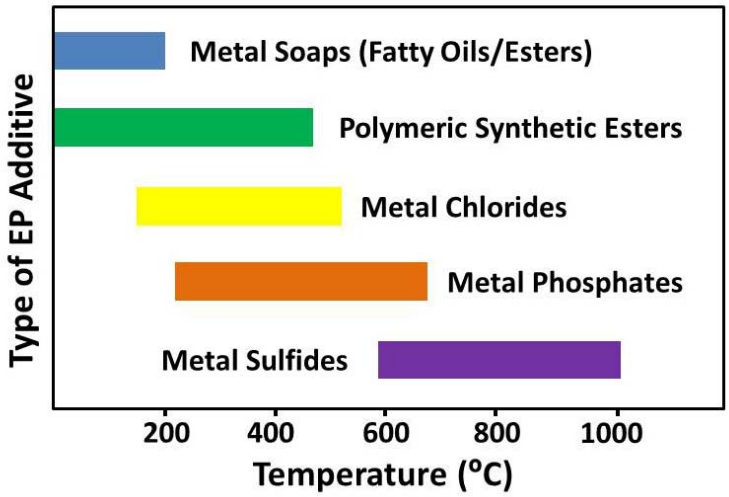

Figure 17: Temperature of activation and decomposition for lubricant additives [44].

Cameron describes two classes of additives, antiwear and antiweld as protection against adhesive wear. The antiwear additives adhere more tenaciously to the surface than boundary additives and are not as affected by temperature. In fact, a study by Grew and Cameron [46] found that the antiwear additive was blocked from adhering to a surface in the presence of cetylamine (a boundary additive) until the critical temperature was reached whereupon the amine desorbed and the sulfur compound was able to access the surface and reduce scuffing. The antiwear additive, while more strongly bonded to the surface and more resistant to heat than the boundary additive, is however removed by the rubbing of asperities.

Antiweld compounds are described by Cameron [47] as reactive compounds that form chlorides and sulfides rapidly on exposed metal surfaces. Their action reduces adhesive wear but results in the formation of a sacrificial compound on one or both of the surfaces (chemical wear). This is

particularly true of copper alloys where the corrosion and discolouration of the surfaces caused by EP additives may be unacceptable.

Surface modification is an effective method to control adhesive wear. Increasing hardness increases the melting point and as a consequence should reduce adhesion. Increasing the hardness of surface may lead to disruption of a protective oxide on the other surface resulting in an increase in adhesion. Work hardening of a surface may cause an increase in wear particle size since shear of junctions takes place in the substrate rather than in the harder material closer to the surface. Other factors provide powerful mechanisms for controlling adhesive wear but generalizations are difficult to make [47]. These mechanisms include: choosing dissimilar metals, use of coatings particularly ceramics, and using textures to retain lubricants.

2.2.6.1. Surface Coating For Low Affinity Between Surfaces

Numerous researchers have shown that the affinity between metallic pairs is a powerful factor in adhesive wear [48, 49, 50, 51]. In general those materials that have a high solid solubility exhibit a greater tendency for adhesive wear. Stainless steel with its high chromium content has reduced adhesion with copper alloys than with iron alloys. Draw dies for stainless steel components are typically made of high strength aluminum bronze. Aluminum has a high solid solubility with many metals so ceramic coatings (such as titanium nitride) are often used to reduce adhesive wear. Obviously the effectiveness of a lubricant additive is affected by a surface coating or other treatment however this aspect is frequently overlooked and unnecessary additives are applied to the detriment of the profitability and the environment.

2.2.6.2. Surface texture

Automotive researchers more than 30 years ago studied the effect of surface texture on the sheet metal forming process. They were trying to solve the problem of how to describe the qualities of a sheet surface that produce the optimal properties for painting (not too rough but not so smooth as to produce galling during forming [52].

The sheet surface parameters most commonly recorded are [53]:

- Ra - Centre line average (CLA) or arithmetic average roughness
- Rq – Root mean square (RMS) average roughness

These measures alone have little meaning since that lack information on spatial structure or difference in peaks and valleys [54]. Thus very different surfaces can have the same Ra or Rq. The use of peak density (Pc) and the skewness of the peaks above or below the mean line (Rsk) are used to improve the description of the sheet surface texture. Pc can be used as an indication of the size of the lubricant pockets (higher Pc relates to smaller lubricant pockets) while Rsk can be used as an indication of propensity for adhesive wear (galling). A positive Rsk indicates low volume (sharp peaks) above the centerline compared to a negative Rsk where the surface is characterized by plateaux that distribute the normal force over a larger area.

The type of filter used to remove the waviness (long wavelength features) of the surface will have an effect on these parameters. A 0.8mm cutoff is commonly used for automotive sheet. Choice of a shorter cutoff length would result in the filtering of larger scale roughness features process [55] such as those imparted during the rolling process.

The outcome of the investigation into the effect of sheet roughness on galling behavior, described above, was to define an optimal process window for automotive sheet metal stamping using two parameters: roughness (Ra) and peak density (Pc). These optimal parameters were achieved by cold-rolling the automotive sheet with shot blast rolls [56].

2.2.7. Friction Instabilities

A major barrier to detection of lubricant failure using friction values is a phenomenon known as stick-slip. Stick-slip arises from the elastic properties of the surfaces and are modeled as a mass, spring, and damper. Various contact conditions produce a range of stick slip responses [57]. Cameron found a transition from smooth sliding to stick slip at some critical temperature [58]. Halling [59] devoted an entire chapter to friction instability and remarked that a prolonged "stick" phase results in a higher friction value as slip begins than with a shorter stick phase. He observed that under some conditions the breakaway friction increased with successive sticking phases. Berman suggested that three types of stick-slip models be used to identify the type of stick-slip friction [60]:

Surface topology model - the stick arises from encounters between asperities (DaVinci) and the slip occurs as they disengage. Friction force amplitude depends on surface roughness parameters.

Distance-dependent model – the adhesion two asperities increases after some time and then resist separation during a "creep" phase before slipping. Static friction increases to saturation and friction force amplitude decreases with sliding distance.

Rate and state models – used with lubricated surfaces where static lubricant properties differ from dynamic properties. Friction amplitude remains constant with velocity in the over-damped regime.

It is important to recognize that instabilities in the friction force are important indications of the type of sliding friction and are useful in identifying lubricant failure.

2.2.8. Identifying Lubricant Failure

The goal of this research is to improve the ability of the lubricant developer to evaluate different formulations to determine the candidates with the greatest chance of success in a process or mechanism. In other words, which lubricant formulations are least likely to show tendency to produce adhesive wear.

Considering the lubricant's role to maximize the tribological compatibility between contacting surfaces Fox-Rabinovich et al [61] wrote:

> *"Tribological compatibility can be evaluated as a specific criterion of the frictional bodies' interaction using the temperature of the seizure initiation. The seizure threshold is normally observed visually, but this method is time consuming and its accuracy is low. A more accurate method of evaluation of tribological compatibility for the HLTS [heavily loaded tribosystems] is needed. This criterion has to be more accurate when compared to the visual observations and should correspond to the specific working conditions. To realize this idea, the phenomenon of seizure (galling) formation has to be considered. The seizure initiation during friction indicates that an external friction transforms to an internal one."*

Schey [62] suggested that the rise of the ploughing term in Bowden and Tabor's friction model is considered as the point of failure in most metal forming processes.

The ASTM G40 definition of galling which is used as a criterion for failure in the standards G98 and G196 states:

> *"Galling is a form of surface damage arising between sliding solids, distinguished by macroscopic, usually localized, roughening and creation of protrusions, above the original surface".*[63]

This criterion (as pointed out earlier in this section in the quote by Fox-Rabinovich) is inaccurate and expensive since successive tests are run until failure is observed.

Many researchers have attempted to identify lubricant failure with data other than friction force. These data include electrical conductivity, surface temperature, acoustic emissions, and vibration. They are discussed later.

2.3. Using Tribotests to Evaluate Adhesive Wear Reduction Strategies

The screening of lubricant candidates for effectiveness in an industrial application is a necessary part of the lubricant development cycle [64]. This screening, conducted at various stages in the development cycle, identify individual additive characteristics as well as synergistic effects between additives. In some cases additive combinations have negative effects. The presence of boundary additives or viscosity improvers can block the action of EP additives. Screening with an appropriate bench test help developers identify the sensitivity of the additives to the process parameters and to narrow the field of candidate lubricants for a particular application.

There are many factors to consider when choosing an appropriate tribotest for lubricant or surface treatment evaluation. John Schey [65] summarized those for metalworking processes in a single chart (Figure 18).

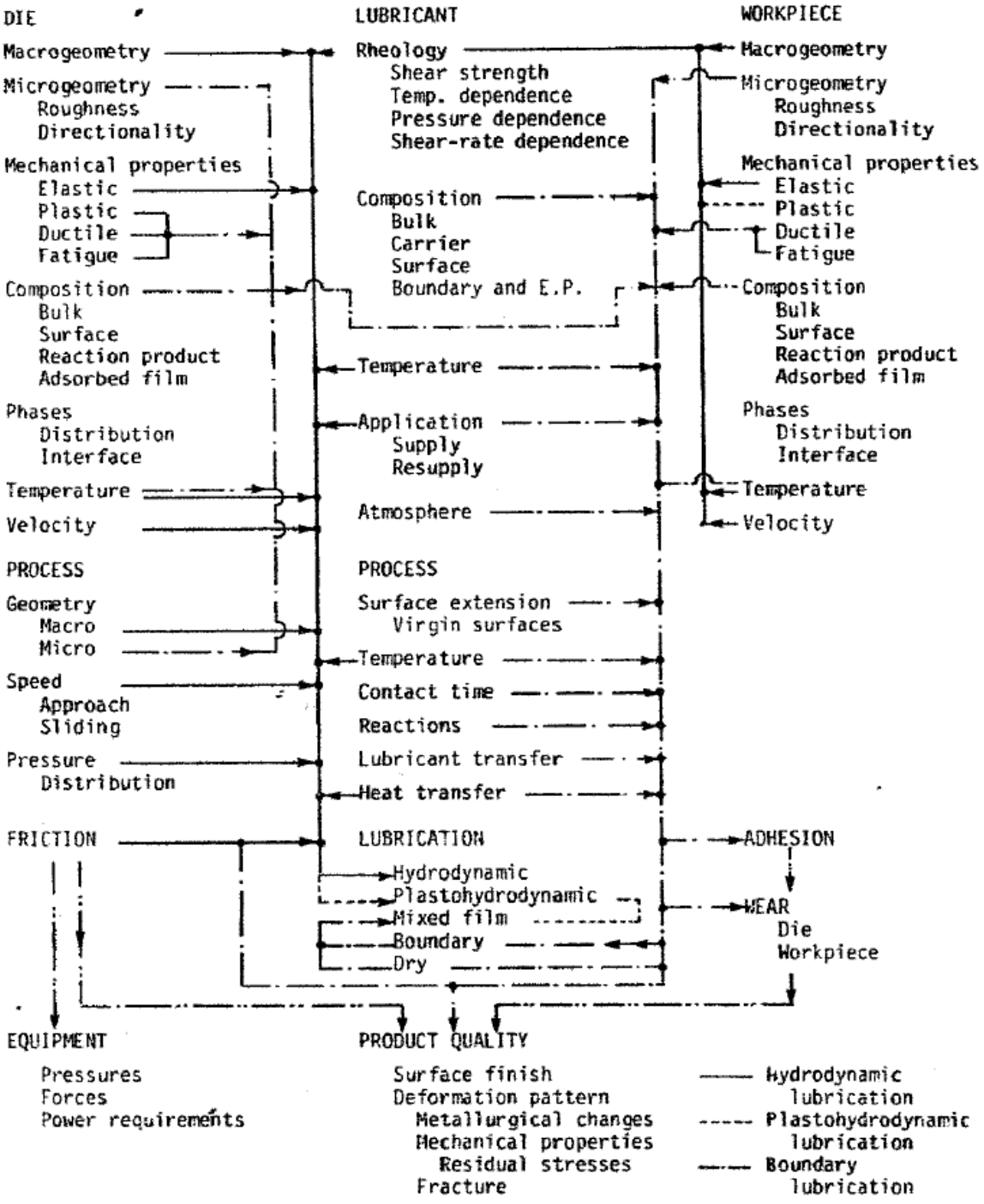

Figure 18: Elements of a metalworking lubrication system. (*from J. A. Schey Tribology In Metalworking*)[65]

This chart shows that there are a myriad of interactions to consider when designing a lubricant for a metalworking process. Other lubrication applications are not as complex but are still sufficiently complex to require a good understanding of what tribotest is most appropriate. Often the choice of lubricant is based on finding an optimal region between two desired but conflicting parameters. An effective tribotest is able to produce a response curve over a range of values for the parameters to find this process window (Figure 19).

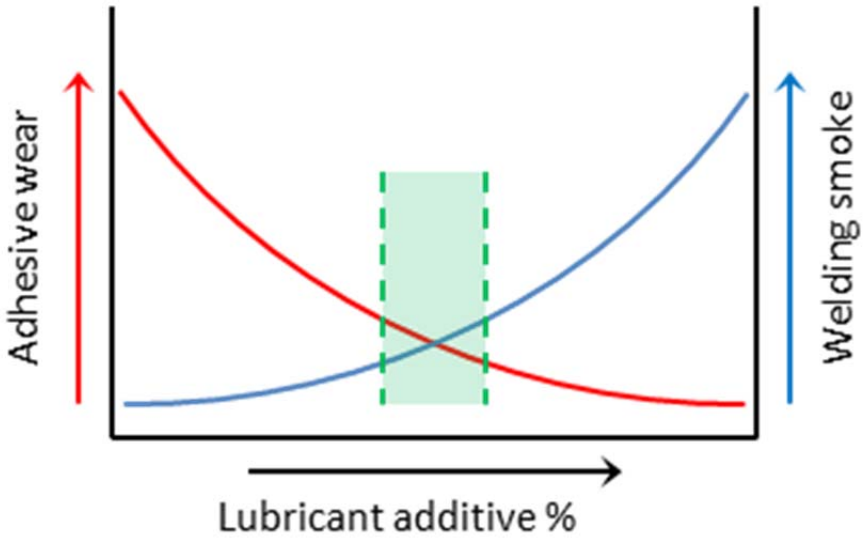

Figure 19: Optimal lubricant additive range (green) to achieve minimal wear and minimal welding smoke

The tribologist must understand how the choice of tribotest affects the correlation of the data obtained to the application. A bench test is simple and allows many parameters to be studied in a fundamental way but has the disadvantage of being remote from the process. Production trials are ideal from the perspective of relevance but they are costly and difficult to interpret other than pass/fail. The advantages and disadvantage of different analysis methodologies is shown in Figure 20.

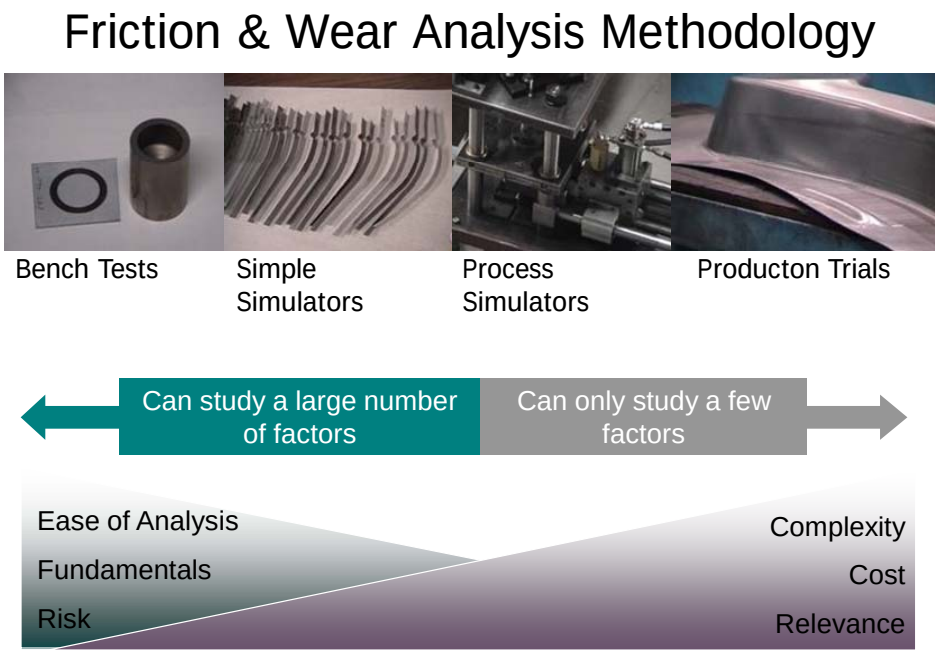

Figure 20: Advantages and disadvantages of different friction and wear analysis methodologies (*adapted from Schey* [66]).

The chemist may formulate several different lubricant candidates and produce various dilutions of each candidate. The objective of the lubricant chemist is to find the optimal concentration of an additive and the correct dilution of the final formulation. This is accomplished using an appropriate tribotest.

Another important consideration in the effectiveness of a lubricant is its shelf life. Lubricant candidates are often retained and periodically assessed to determine changes in effectiveness due to storage duration or conditions. Assessing the influence of formulation and storage on the effectiveness of a lubricant is done easily in a controlled tribotest once a baseline is established.

Finally, lubricant companies attempt to avoid the risk of failure in production trials by selecting the best lubricant from a field of candidates. In most cases, the production trials include one or two lubricants from each company with no chance for a second attempt. Screening for process-suitability is carried out using a tribotest to measure the tribological properties (friction and wear) for comparison with the lubricant currently in use. The candidate screening procedure practiced by most TCT users is shown in Figure 21.

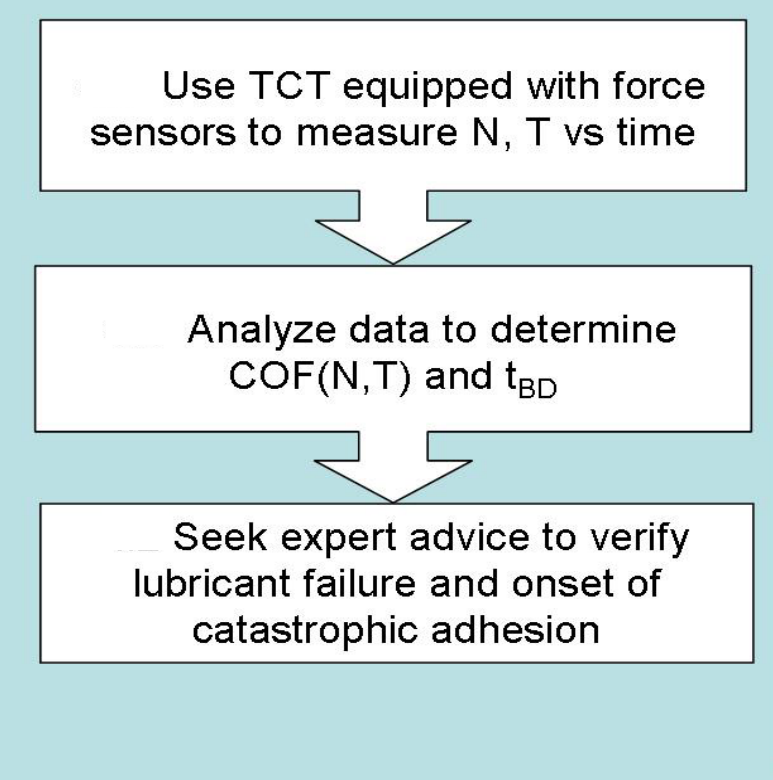

Figure 21: Typical lubricant screening methodology

2.3.1. Factors to Consider in Choosing an Appropriate Tribotest

In choosing an appropriate tribotest one must consider how the tribotest relates to the industrial application in terms of contact geometry, lubrication regime, and finally what type of response will be produced by the tribotest.

2.3.1.1. Contact Geometry

An appropriate tribotest with the correct contact geometry closely resembling the application is used to evaluate the characteristics of the lubricant required in the process application. The type of contact geometry is an important consideration in determining the contact stress and the lubricant film thickness. Figure 22 shows a simplified schematic of the effect of different contact geometries on these parameters. If the wrong contact geometry is chosen then a tribotest results are misleading or erroneous. For example the Pin on Disk test (ASTM G99) involves a stationary point contact pressed against a rotating disk (Figure 22 – sphere /flat). The resulting wear is observed and measured both on the pin and on the counter face. While it said that the test measures the adhesive nature of the two surfaces [67], the major drawback of this method is that the point of contact is not big enough to develop a field of asperity interactions or the formation of lubricant pockets between asperities (microscopic surface features). A further complication is that the contact mechanics of a sphere on flat changes rapidly as the contact zone grows initially with deformation and then wear.

A cylinder on flat produces a line contact where new lubricant enters the contact through a converging gap. As with point contact, lubricant replenishment inherent with line contact means that depletion cannot be achieved.

In flat-on-flat contact the characteristics of the asperities and the valleys dictate the lubricant film thickness and the resulting lubrication regime (Figure 23). However, the geometry of the entry condition also controls the lubricant film thickness. Any geometry that allows a lubricant wedge to form prevents conformance of the two surfaces and lubricant depletion is not achieved (Figure 22 –Flat (rounded edge)/Flat).

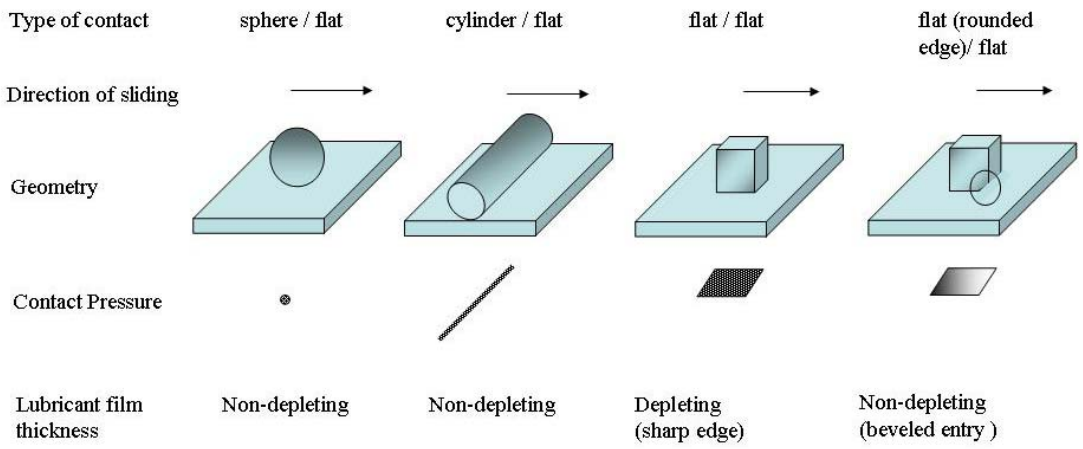

Figure 22: Schematic showing simplified contact geometries and effect on film thickness.

Since adhesion is most likely to occur with the minimum film thickness, the tribotest must be able to achieve lubricant depletion in order to effectively evaluate anti-adhesion properties of a lubricant.

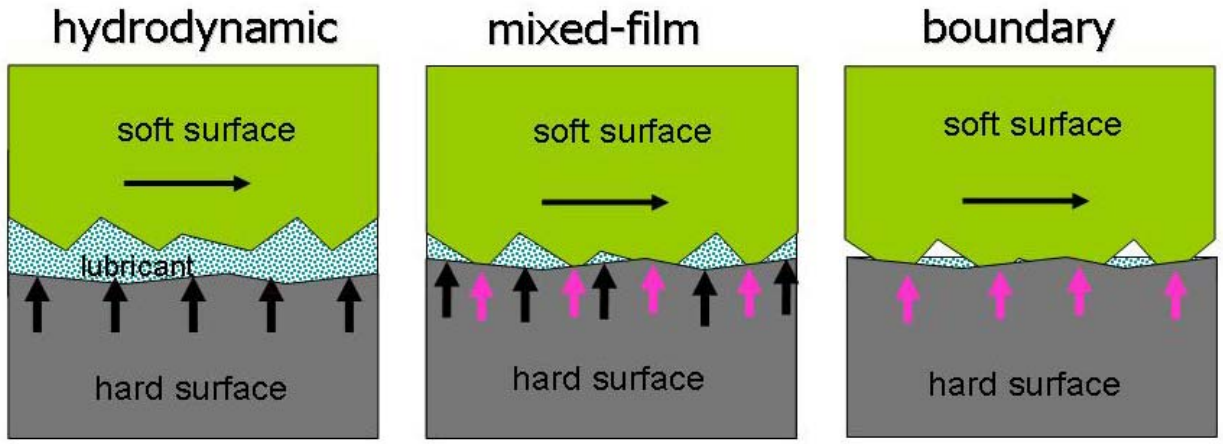

Figure 23: Lubrication regimes dark arrows indicate lubricant support, light arrows direct contact.

2.3.1.2. Lubrication Regime

Early flat-on-flat tribotests attempted to prevent tilting of the surfaces and prevent an entry gap by making the tribotest more rigid. This proved almost impossible due to the small deflections needed to achieve a lubricant wedge and limitations in machining tolerances [68]. Modern tribotests ensure flat-on-flat contact through the use of self-aligning specimen holders.

Consider Figure 24, if the block is not perfectly flat or the load is not applied evenly then a converging gap occurs and the pressure of the lubricant and entrainment of fresh lubricant produces what is known as ***hydrodynamic lubrication***. The surfaces are kept separate and the severe conditions leading to lubricant failure is not achieved. While this is often the goal for the product or process adhesive wear occurs when the conditions fail to achieve hydrodynamic lubrication. The goal of the tribotest as a method of evaluating adhesive wear is not to reproduce ideal lubricant conditions but to reproduce conditions of failure.

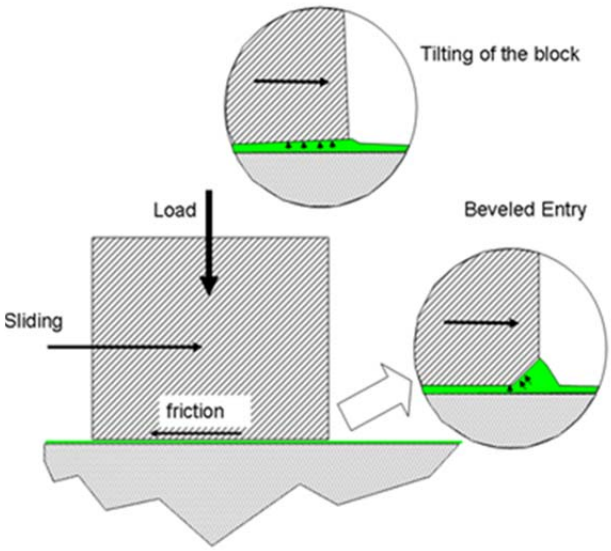

Figure 24: Entry condition producing hydrodynamic lubrication regime

In ***mixed film lubrication*** the normal load is supported by a "mix" of pressurized lubricant

pockets and boundary lubricated asperities. The pressurized lubricant pockets provide both a reduction in stress at the asperities but also act as reservoirs of lubricant for the metal on metal contact at the asperities (Figure 23). With extended sliding, the reservoirs are exhausted and both the support and the supply to the interface are lost resulting in a change of lubricant regime to boundary lubrication. Some friction tests such as the drawbead simulator are designed to operate exclusively in the mixed-film regime. Their aim is not to evaluate adhesive wear resistance but to determine entry conditions (friction values) for process control and numerical modelling.

Boundary lubrication is a condition that occurs when lubricant pockets are depleted and the entire load of the contacting surfaces is borne by a single layer of adsorbed lubricant molecules. Obviously, the conditions of boundary lubrication are tenuous and the protection provided a single molecular layer fleeting, but the protection may be enough in applications where the lubricant supply is only briefly interrupted.

2.3.2. The Twist Compression Test

One particular tribotest, the Twist Compression Test (TCT) was developed in the 1960's by Dr. John Schey (Figure 25). Designed to achieve lubrication depletion, the TCT applies a high normal stress to a flat-on-flat contact while maintaining alignment of the two surfaces. This alignment is critical to ensure the film thickness is reduced throughout the test.

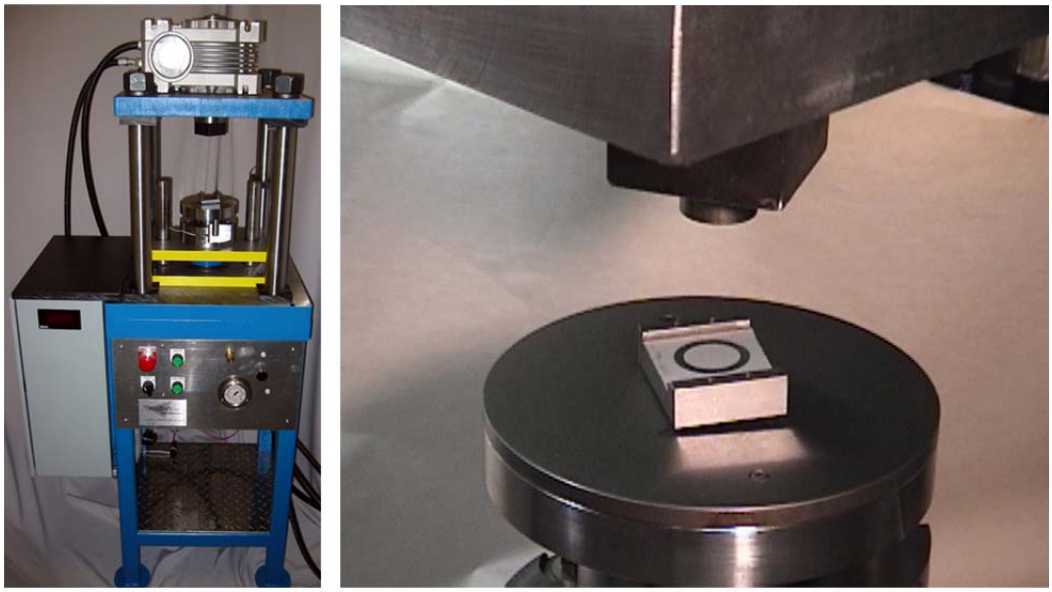

Figure 25: The TribSys Twist Compression Test (left) with detail on the upper and lower specimen holders (right).

The TCT is used to evaluate a lubricant's performance in the boundary regime by running the test until the lubricant is depleted and failure (adhesive wear) occurs.

The depletion of lubricants in the TCT is accomplished with a rotating flat annular specimen in contact with a flat specimen. The rotation of the annulus eliminates the entry gap and provides the opportunity for long sliding distances through multiple rotations (Figure 26).

The following sequence describes the procedure for testing a lubricant/substrate combination using the described apparatus.

1. A rotating annular tool (die specimen) contacts the lubricated sheet specimen (alternatively, rotation can be initiated after contact).
2. A suite of sensors collect relevant signals including transmitted torsional force, vibration, temperature, and electrical resistance between the contacting surfaces.

3. Continued contact and rotation leads to lubricant breakdown which in some cases is marked by a sudden increase in friction and chatter due to stick-slip.

TCT Variables and Lubricant Regime

Lubricant regimes are determined primarily by three variables: viscosity of the lubricant, velocity of the surfaces, and interface pressure. The annular shape of the specimen is important. The annular contact area rather than solid circular contact area eliminates the zero velocity condition at the centre of the circular contact (Figure 27). The zero velocity condition produces a velocity gradient from the centre to the outside radius that leads to varying lubrication regimes across the contact area resulting in complex, difficult to analyse conditions.

Figure 26: TCT test specimens - flat (left), annular (right)

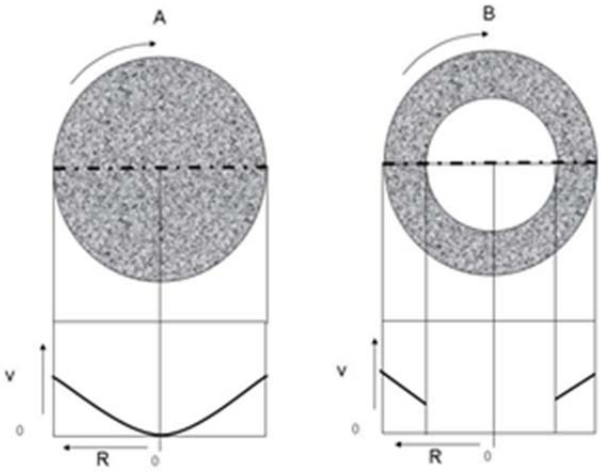

Figure 27: Zero velocity (v) condition with solid specimen (A) compared to annular specimen (B)

The TCT applies a torque to one specimen under an applied compressive load and measures the resulting torque transmitted through the interface to a second specimen (Figure 28). The ratio of these forces produces a non-dimensional parameter, the coefficient of friction (COF), for the surfaces (Figure 29).

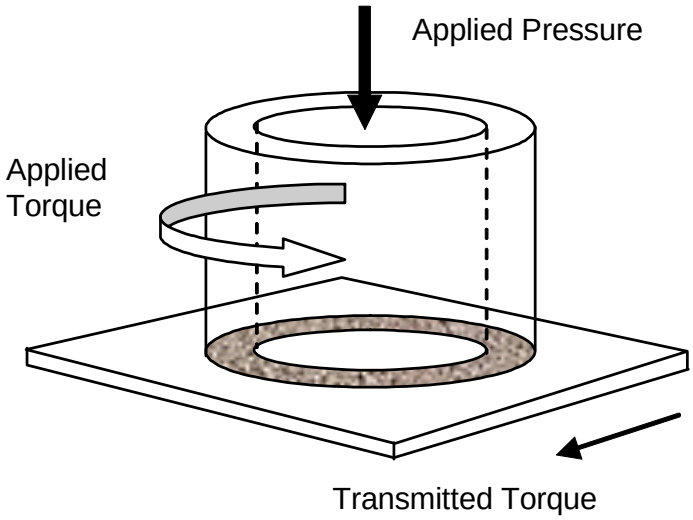

Figure 28: Schematic of contacting surfaces in the TCT.

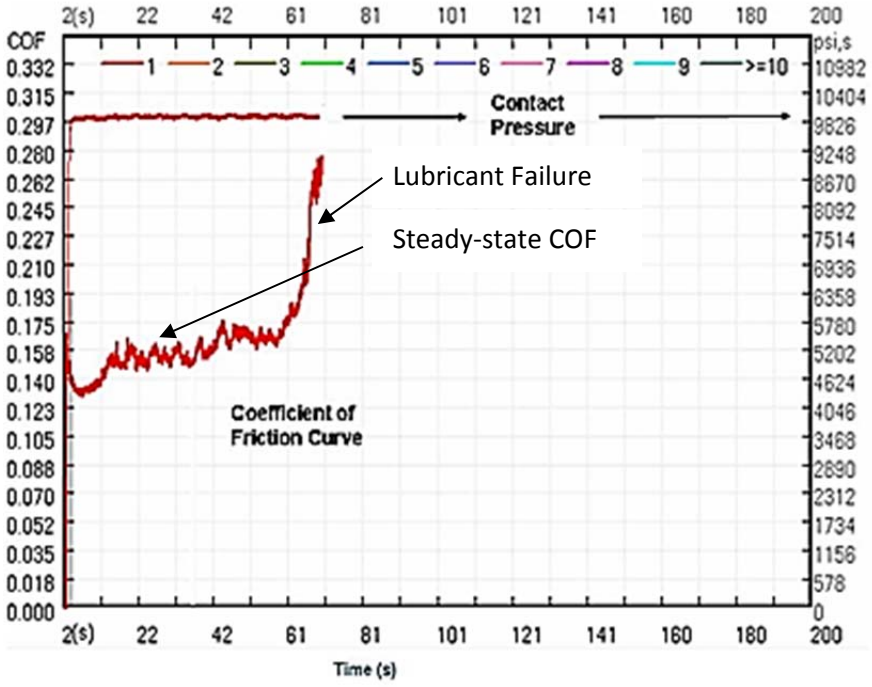

Figure 29: Coefficient of friction and contact pressure curve

2.3.2.1. Analyzing and Reporting Results

The ASTM Recommended Practice for Reporting Friction G117 suggests that friction results are often reported as an average value for the steady state portion of the test. This value represents the contact conditions for the lubricant and is valuable data for comparing process response to a particular lubricant (energy requirements or strain in sheet metal forming). Steady state friction represents the ideal conditions for lubricant performance and is not a good indicator of lubricant effectiveness in reducing adhesive wear. Some tribotests users prefer discreet friction values rather than continuous values (curve) for friction.

The results of candidate screening are difficult to interpret and often require expert interpretation. In the ideal situation, lubricant breakdown is obvious and analysis is easy. However, often there is no clear point of lubricant failure as the friction curve changes during the test. Blau [69] outlined three attributes of transitional friction curves: the shape of the curve, the duration of the event, and the noise in the friction data. He suggested that understanding the origins of these attributes lies in close examination of the friction curves in light of the process being studied and correlation to changes on the contacting surfaces. Similarly, Wiklund and Hutchings reported that rapid irregularities in friction or changes to the derivative of the friction curve indicated the onset of adhesive wear (galling) but that galling was only confirmed by microscopic examination [70].

Since the friction curve contains so much information, it appears to make sense to avoid hardware and software filters during data collection in adhesive wear testing. Vibration and noise are manifestations of friction. External sources of noise are minimized rather than filtering

the signal. Post processing of friction data is used for analysis but the raw data should be retained in its complete form.

The desire to provide a simple quantity to represent lubricant performance means that the richness of the continuous friction data represented by the friction curve is lost and the interpretation subject to bias [71].

The challenge is to retain the full data set and to arrive at a better method of evaluating performance. The next section describes how a computer decision support system is used to extract critical features from the data to help in the lubricant evaluation process.

2.4. Decision Support Systems – Improved Detection Of Lubricant Failure

For many years tribotests such as the TCT have used a single response, COF, as a measure of lubricant performance. The inadequacy of this measure is illustrated in earlier chapters of this work. This is especially true for adhesive failure since friction in some cases decreases with changes to the area of contact (A_{real}) that arise from adhered particles. In these cases adhered particles quickly modify the contact from almost complete conformance (where A_{real} approaches $A_{apparent}$) to a very small area of contact. The changing morphology and chemistry of the surfaces after the onset of adhesive wear means that friction is highly variable.

All too often the richness of friction data curves that were captured by chart recorders and later, data acquisition systems, were reduced to a single number (COF) usually without any indication of variance. The averaging of friction data makes two very different responses appear the same (Figure 30).

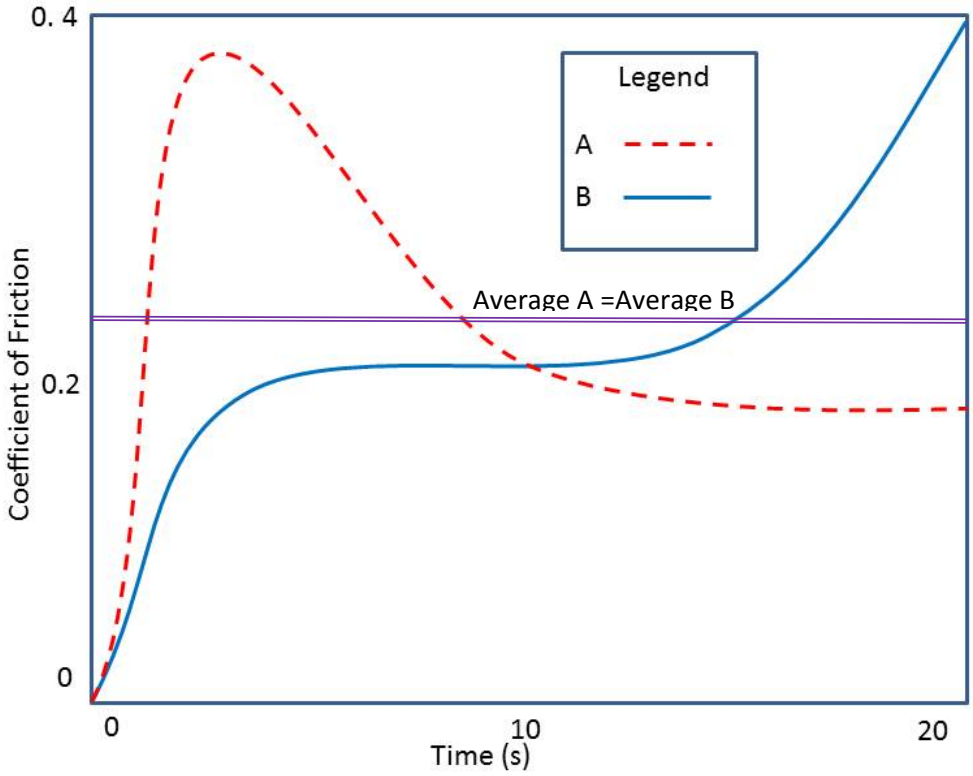

Figure 30: Sample curves showing how two very different friction responses could be reduced to equivalency by averaging.

The cost of a misinterpreted lubricant evaluation is enormous. Lubricant companies rely on their laboratory screening program to identify successful candidates for production trials. A false negative from the TCT eliminating a potential winner represents millions of dollars in lost revenue. Conversely, a false positive leading to a failed production trial could result in the loss of a client. Improving the screening process for lubricants and surface treatments has immediate impact on reducing adhesive wear and its associated costs.

The promise of computer-based expert systems to replace or augment human experts in fault diagnosis is possible in simple and well-behaved systems but is still unrealized in complex and unpredictable systems.

The design of a DSS to improve the lubricant screening process follows the same basic steps as for any DSS.

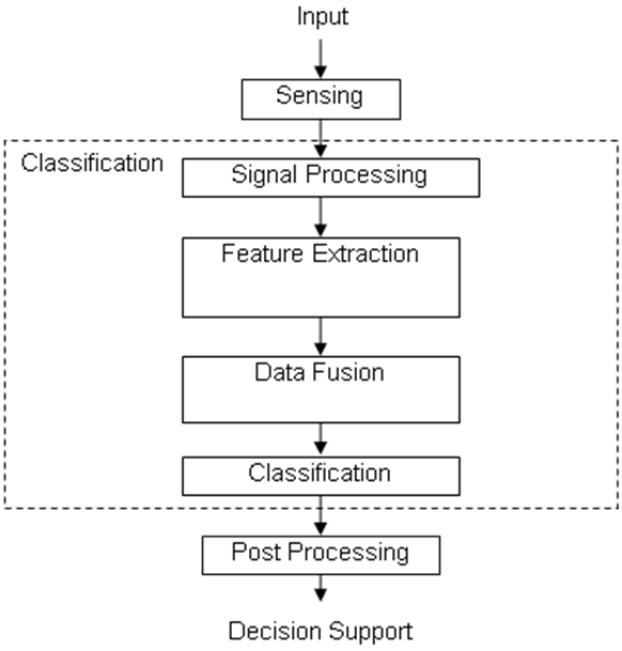

Figure 31: Data flow block diagram for decision support system

2.4.1. Sensing

If the COF by itself is an unreliable indicator of adhesive failure then perhaps the use of other responses, either individually or collectively can improve the detection of adhesive failure in the TCT? Of course increasing the number of responses introduces the "curse of dimensionality" where the data needed to achieve statistical significance increases exponentially with the number of responses being measured. The number of responses was limited to those that proved reliable in other wear studies.

A further constraint in the design of a DSS for the TCT is that the DSS assist the operator in terminating the test as soon as practical after failure is detected so that the failure severity can be observed and recorded. Consequently, only on real-time responses are effective for a DSS to detect adhesive failure and preserve the specimens. Post-test responses are then used to confirm the severity of failure and these responses are used to refine the DSS failure criteria.

2.4.2. Signal Processing

The raw data from the sensors may require processing before feature extraction is performed. AE data is generally presented in terms of events that exceed prescribed thresholds and both measured (amplitude) and calculated values (energy). Other signals such as transmitted torsional force and normal force are combined to create normalized values such as the coefficient of friction. Smoothing algorithms reduce noise from the data but for the purposes of this study smoothing represents a loss of signal and is avoided.

2.4.3. Feature Extraction

Tribotesting for adhesive wear is by nature a progressive rather than steady state process. The lubricated test specimens rotate continuously in contact with each other until the lubricant fails to provide protection from adhesive wear. During this progression features of the data may change such as maxima or minima, signal variation, and average slope. Extracting relevant features from the data will allow changes in them to be correlated with post-test measures of lubricant failure.

2.4.4. Training Dataset Collection

The construction of a DSS for the identification of lubricant failure in the TCT requires a training data set. This data set differs from traditional TCT data in that it contains "healthy" and "unhealthy" data. In our case the healthy data will be collected from tests prior to failure and unhealthy data is collected from tests after failure. In both cases the specimens are separated at the end of data collection to confirm the absence or presence of adhesive wear.

2.4.5. Decision Support System Design

For the task of decision support, the tools of data fusion, signal processing and feature extraction are used to interpret sensory data from signals such as mechanical vibration, electrical conductivity, and temperature. This sensory information is used for supervised training of a range of pattern recognition algorithms for characterising the point of lubricant failure. The decision support system is trained to correlate the sensor data as well as the data history with the point of failure as determined above.

Chapter 3

3. Experimental Methodology

This chapter outlines the methodology used to gather data on the Twist Compression Test (TCT) using novel techniques for measuring the response of two surfaces in sliding contact under an applied normal load. While the instrumentation and data collection/analysis techniques differed from the standard practice (TribSys TCT Instruction Manual [72]), the test procedure, the TCT frame, tooling, and actuators were generally the same as a commercially available TCT (Figure 25). Overall, three separate studies were conducted: a preliminary study, a main study and an extended study. The preliminary study provided a basis for narrowing the experimental parameters in the main study. This chapter outlines the parameters of these studies. The extended study examined the progression of contact and adhesion for one set of conditions by running 21 tests rather than the usual 3 tests. Half of the tests were run to failure while the other half were interrupted before catastrophic adhesion had occurred. The extended study provided both "healthy" and "failed" datasets for training a decision support system (DSS) as described in Chapter 2.4. The matrix in Table 1 summarizes the three experiments: preliminary study, main study, and extended study. In all of these experiments the speed of rotation and contacting materials were held constant (10 rpm, cold-rolled sheet steel, and D2 tool steel annular specimens).

Table 1: Summary of the Experimental Variables for the Preliminary, Main, and Extended Studies

Experiment	Purpose	Interface Pressure	Lubricant Composition	Lubricant Viscosity	Replicates	Total Tests
Preliminary **(Standard TCT)**	Verify the levels of the test parameters and establish a baseline response for a commercial TCT	20 MPa 100 MPa 225 MPa	-Basestock -Ester -Chlorine -Sulfur	-Low -High	3	72
Main **(Experimental TCT)**	Identify data features from multiple sensors and compare responses to lubricant additives	100 MPa	-Basestock -Ester -Chlorine	-Low -High	3	18
Extended **(Experimental TCT)**	Training data set: Interrupt tests to examine surfaces immediately prior to, at the start of, and immediately after failure	100 MPa	-Ester	-Low	-Prefailure 21 -Early failure 4 -Late Failure 21	46

3.1. Experimental Variables

The input variables most often examined in the TCT are the interface pressure, lubricant viscosity, lubricant composition, sheet material, and tool material. The following sections explain the choices of each of the input variables.

3.1.1. Interface Pressure

The apparent interface pressure (hereafter referred to simply as the interface pressure) in the TCT is a function of the applied normal force and the annular specimen contact area. The standard TCT annular specimen geometry has an area of 221 mm^2 (Figure 32). Changes in interface pressure are usually accomplished by varying the normal force. In this study, as in the standard TCT test method, a constant force (and interface pressure) is maintained throughout the test. The real interface pressure is much higher at the initial contact where the full load is borne by a few

asperities and approached the apparent interface pressure as the asperities undergo plastic deformation.

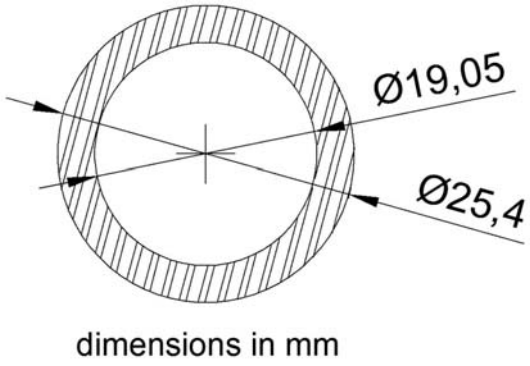

Figure 32: TCT annular specimen apparent contact area – shown hatched

The analyses of data from the preliminary study showed that the 100 MPa interface pressure provided better signal-to-noise ratio than the 20 MPa interface pressure and better discrimination (less saturation) than the 225 MPa interface pressure. The 100 MPa interface pressure was therefore used for the main study and extended testing. While 100 MPa appears to be well below the flow stress of the cold rolled sheet steel (0.6 σ_{yield} or 160 MPa) [73] the real area of contact is typically as low as 20% [74] at the start of the test resulting in a real stress that can exceed 500 MPa. While this stress decreases quickly as the asperities flatten and merge the superimposed frictional shear stress acting on the real area of contact maintains the combined stress above the flow stress.

3.1.2. Lubricant Viscosity

Viscosity is a powerful influence on friction during early stages of contact in the TCT. Higher viscosity lubricants delay the onset of boundary lubrication by resisting depletion during early

contact. This delay may prevent or mute surface reactions that produce beneficial tribofilms. Schey wrote:

> *"The bulk viscosity of the lubricant helps to build a load-carrying film in which the influence of boundary additives becomes less significant…"* [75]

It is useful to understand how lubricant viscosity affects the effectiveness of a formulation in reducing adhesive wear. With commercial formulations this is very difficult since the viscosities rarely are the same. The lubricants formulated for these studies by Mr. Ted McClure of TribSys LLC. The formulations were carefully adjusted by adding base stocks (paraffinic mineral oil) of various viscosities to achieve the target viscosities regardless of the additives in the formulations. Two levels of viscosity were chosen: 93 cSt and 23 cSt @40C as measured using standard : *ASTM D2196 - 10 Standard Test Methods for Rheological Properties of Non-Newtonian Materials by Rotational (Brookfield type) Viscometer*. These were labeled "high" and "low" respectively (Table 2). Both high and low viscosity formulations were used in the preliminary and main study but only the low viscosity formulation was used in the extended study.

3.1.3. Lubricant Composition

Lubricant additives are essential to protect the surfaces once the lubricant film provided by the bulk viscosity of the base stock is lost. Boundary additives protect surfaces with weakly bonded molecules. These films are removed with extensive sliding of the surfaces. When the boundary additives are removed, oxide films on the parent surfaces provide the only protection unless the lubricant includes reactive chemical additives known as EP additives. The three most common EP additives are chlorine, phosphorous, and sulfur. They react with the surface to form compounds that inhibit the adhesion of the contacting surfaces. When these compounds are removed during sliding the freshly exposed surfaces react instantly with the additives in the

lubricant reservoirs and the protection is renewed. Under typical parameters, the best EP additives protect the surfaces from catastrophic adhesive wear for 10 or more revolutions (60 seconds) in the TCT.

The preliminary study included the base stock, a synthetic phosphate ester, a chlorinate paraffin additive (55% MW) and an active sulfur additive (20% MW) (Table 2). The main study included the same lubricant compositions without the sulfur formulation. The reason for not including the sulfur formulation is the main study is discussed with the preliminary study results. The lubricants (with codes) that were selected for the main study are listed in Table 3.

3.1.4. Sheet Material

Cold rolled steel (CRS) is an industry standard. Automotive CRS is textured to retain lubricants during the forming process (Figure 33).

The CRS in the preliminary study responded well to most of the lubricant formulations and showed sensitivity to viscosity. The same sheet material investigated in the preliminary study was used in the main study. Automotive draw-quality (DQ) cold-rolled steel (CRS) is well characterized and is widely used as a standard for comparing lubricant performance. The uncoated 0.8 mm CRS used for this research was obtained from ACT Labs, Detroit Michigan, USA.

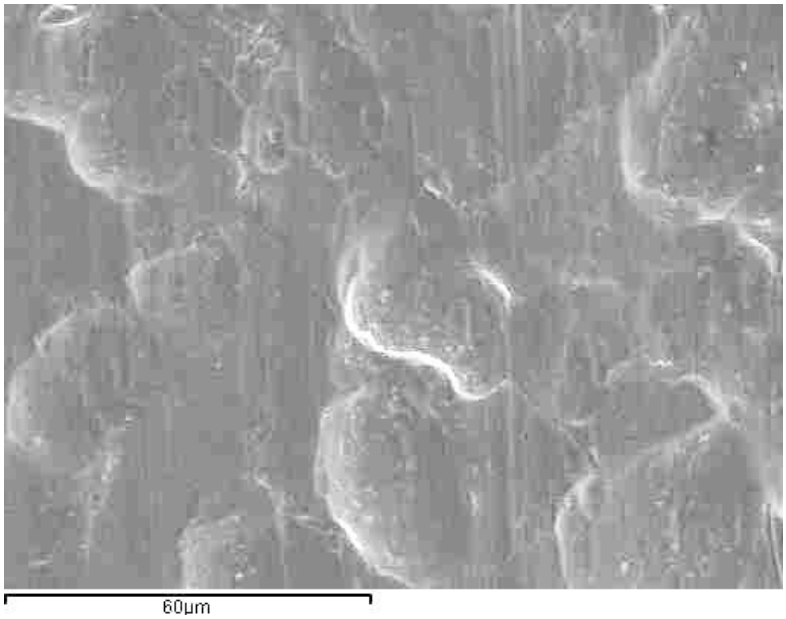

Figure 33: Scanning electron micrograph of as- received cold-rolled steel sheet showing texture left by shot blast rolls.

3.1.5. Tool Material

The standard tool steel for TCT testing is D2 as described in Table 1. D2 was used as the annulus material for all testing. The D2 was heat treated to produce a hardness of 62 Rc. The annular specimens are lapped together at a lapping facility in the USA. In all, 200 specimens were prepared for the three studies. Variations in the lapping process are minimized by restricting the test specimens to those that were processed together.

3.2. Experimental Procedures

The experimental procedures used in the TCT were established to reduce variability in uncontrolled factors. The influence of environmental factors such as temperature and humidity are reduced by running tests as close together as possible. Other more specific controls are described in Appendix 1.

The test procedure including the specimen preservation and data collection are outlined in Appendix 2.

3.3. Preliminary Study Experimental Plan

Studies that are conducted in commercial TCT studies generally use proprietary lubricant formulations with different base stocks and the inherent viscosity the results from the formulation of the additives and base stocks. This makes comparison of fundamental properties (viscosity, EP) between formulations impossible. Lubricants were formulated specifically for this research project to allow for better understanding of the evolution of the contact between the various lubrication regimes. The preliminary TCT experiments were conducted by Mr. Ted McClure at TribSys LLC, Valparaiso and the data were sent to the author for analysis.

Preliminary studies with TCT evaluations are not unique to this study. Before evaluating commercial formulations it is usually necessary to conduct a preliminary study to ensure that the levels of the controlled variables produce meaningful results (e.g. good discrimination between lubricants). If tests are conducted at the wrong normal pressure or if the lubricant viscosity is too high, lubricant additive effects can be masked.

The results of the preliminary study are presented and discussed in this section in the context of establishing the most appropriate levels for the controlled variables for the main study.

3.3.1. Preliminary Study Experimental Variables

The experimental variables examined in tribology experiments are numerous. The fundamental variables in any tribotest are grouped into four general categories as shown in Figure 2.

Each of these categories is further broken down into many subcategories [76]. For the purpose of this research project the variables chosen to be examined were variables most often manipulated by chemists formulating anti-adhesion lubricants, that is:

- lubricant viscosity,
- lubricant composition and in particular anti-adhesion additives
- normal pressure

Other variables such as type of sheet material, test speed, and tool coatings are usually dictated to formulators by the clients they serve. For this study these variables were fixed at basic, well-characterized values. Each test condition is repeated three times. Experience gained over 25 years of TCT use has shown that while variance of the COF is small the time to adhesive failure is governed by stochastic surface features and has a much greater variance. Repeating the test three times using a new annular tool and new sheet specimen for each replicate improves the precision of the time until failure (breakdown) [77].

3.3.2. Choice of variable levels

The variable levels chosen for the preliminary study are outlined in the Table 2. The formulations in the preliminary study were chosen to illuminate the effect of newer additives (ester, and a sulfur compound) compared to the current industry best performer (a chlorinated EP additive).

In addition to four different lubricant compositions, two viscosities were chosen as well as three nominal contact pressures (Table 2). The speed of the rotating annulus was kept constant.

Table 2: Preliminary experiment parameters

Sheet (Material)	1. Cold Rolled Steel (CRS) Grade = AKDQ (aluminum-killed draw quality) Roughness, Ra = 1.5 µm Gauge = 0.8mm
Die (Material)	2. Material: D2 Hardness: 60 HRC Finish: TCT Ra=0.25 µm
Lubricant	
Composition	1. BS: Basestock Only - Paraffinic Oil 2. E: Synthetic Phosphate Ester 3. C: BS 90%, 10% w/w Chlorinated Paraffin 55% MW 4. S: BS 90%, 10% w/w 20% active Sulfur
Viscosity	1. HV High Viscosity 93 cSt @ 40°C 2. LV Low Viscosity 23 cSt. @ 40°C
Process (duty cycle)	
Normal Pressure	1. 20 MPa 2. 100 MPa 3. 225 MPa
Speed	1. 12 mm/s

Table 3: Preliminary Study Test Matrix

Test #	Test Code	Lubricant Composition	Lubricant Viscosity	Normal Pressure (MPa)	Replicates
1	BSLV	Base stock	Low (23 cSt)	20	3
2	BSHV	Base stock	High (93 cSt)	20	3
3	SLV	Sulfur	Low (23 cSt)	20	3
4	SHV	Sulfur	High (93 cSt)	20	3
5	ELV	Ester	Low (23 cSt)	20	3
6	EHV	Ester	High (93 cSt)	20	3
7	CLV	Chlorine	Low (23 cSt)	20	3
8	CHV	Chlorine	High (93 cSt)	20	3
9	BSLV	Base stock	Low (23 cSt)	100	3
10	BSHV	Base stock	High (93 cSt)	100	3
11	SLV	Sulfur	Low (23 cSt)	100	3
12	SHV	Sulfur	High (93 cSt)	100	3
13	ELV	Ester	Low (23 cSt)	100	3
14	EHV	Ester	High (93 cSt)	100	3
15	CLV	Chlorine	Low (23 cSt)	100	3
16	CHV	Chlorine	High (93 cSt)	100	3
17*	BSLV	Base stock	Low (23 cSt)	225	3
18*	BSHV	Base stock	High (93 cSt)	225	3
19	SLV	Sulfur	Low (23 cSt)	225	3
20	SHV	Sulfur	High (93 cSt)	225	3
21*	ELV	Ester	Low (23 cSt)	225	3
22*	EHV	Ester	High (93 cSt)	225	3
23	CLV	Chlorine	Low (23 cSt)	225	3
24	CHV	Chlorine	High (93 cSt)	225	3

* Note these tests failed immediately upon contact

3.4. Main Study Experimental Plan

The main study used a reduced set of the extensive variables explored in the preliminary study (Table 4); however, unlike the preliminary study where only transmitted torsional force and normal force measurements were obtained, in the main study a variety of sensors were used to explore alternative ways of identifying adhesive failure. Real-time measures of surface interaction were recorded and correlated to the post-test surface analysis. The objective of this

analysis was to gain a better understanding of how different sensor outputs respond and correlate to the input variables leading to adhesive wear.

Table 4: Main Study Lubricants with Test Codes

Description	**Low Viscosity**	**High Viscosity**
Base stock (Mineral Oil)	BSLV	BSHV
Chlorinated Paraffin in BS	CLV	CHV
Synthetic Ester	ELV	EHV

3.4.1. Instrumented TCT

A special instrumented TCT was used along with customized DAQ software for improved sample rates and multiple channel sampling. The following sensors were attached as shown in Figure 35 and signals were recorded by the DAQ: transmitted torsional force (r), normal force (z), vibration (r, z) acoustic emission (r), conductivity/resistivity (z) (Figure 34, 36). The transmitted torsional signal and normal sensors were compression load cells as equipped on a commercial TCT. The AE sensor was held in place with a permanent magnet and coupled to the tooling with gel. The radial and normal vibration accelerometers were held in place on the tooling with double sided tape. Finally the digital multimeter (DMM) leads were connected on either side of the two specimens with the lower specimen (sheet) isolated using diaelectric paper. A lack of continuity was verified before the start of the test.

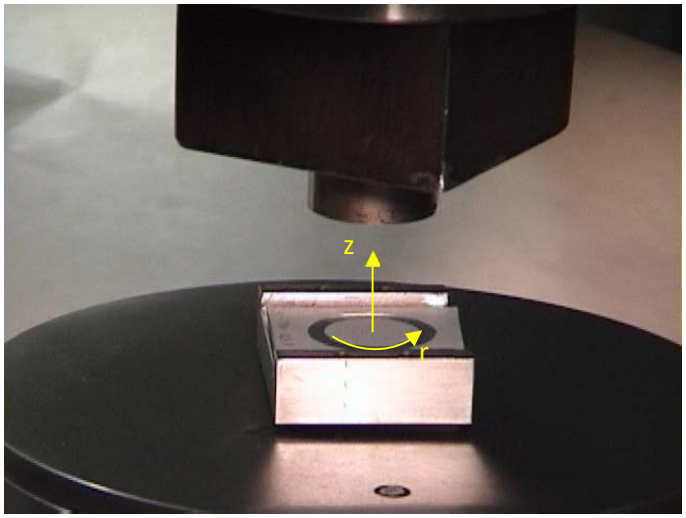

Figure 34: TCT specimens with reference axes

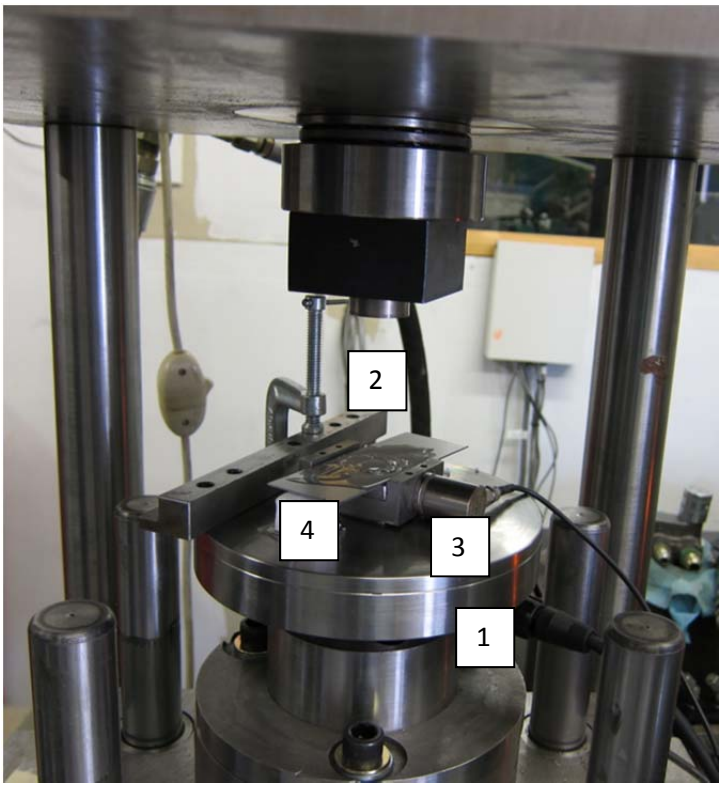

Figure 35: Additional instrumentation for the main study: radial accelerometer (1), normal accelerometer (2), acoustic emission piezoelectric transducer (3), and electrical resistance DMM (4) (note dielectric insulator not shown above).

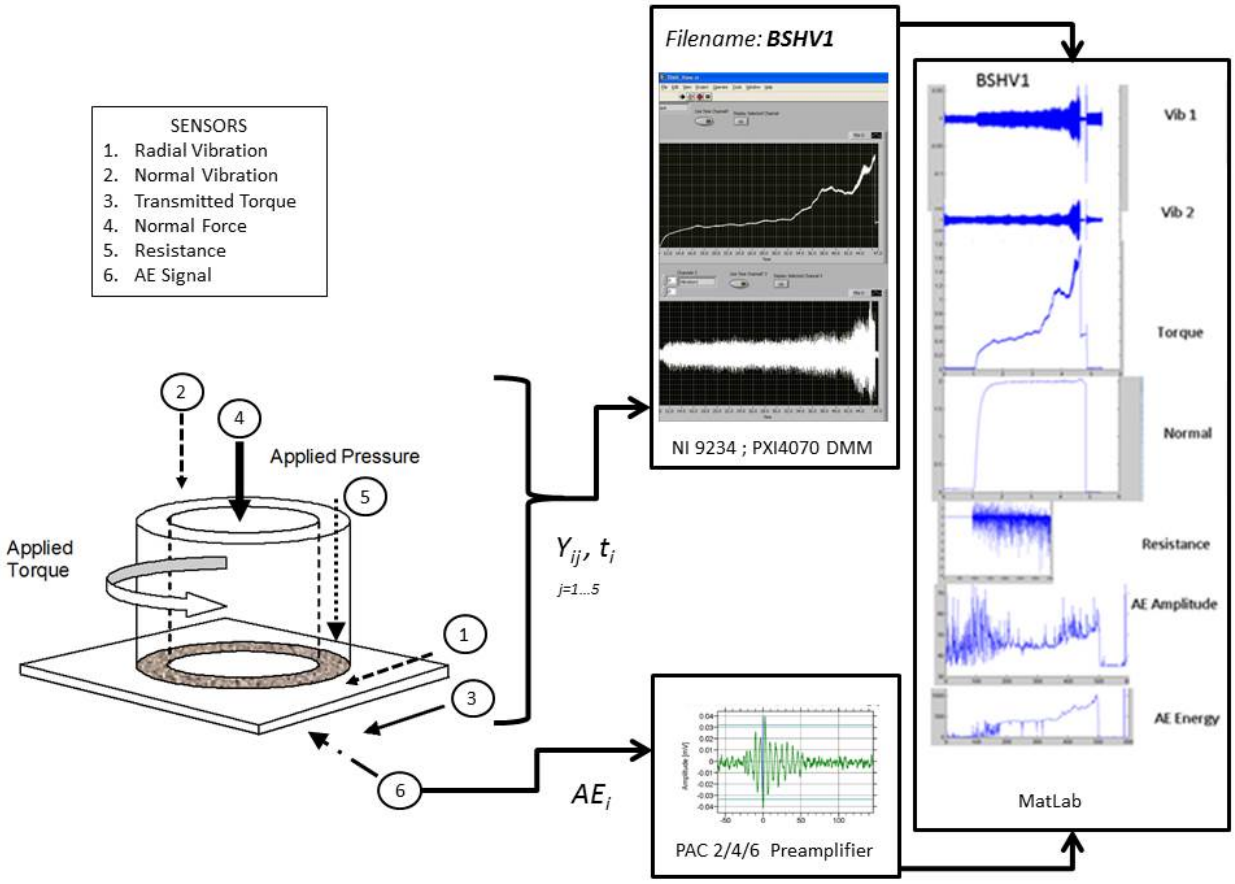

Figure 36: Main Study Data Acquisition Schematic

The following measurements were recorded continuously for each test (Table 5). Load cell output was amplified to produce 0 – 10 V on the DAQ analog input channel.

Table 5: Main Study Instrumentation

Measurement	**Sensor**	**Excitation**	**Output**	**Frequency**
Normal Force	Load Cell	10 V DC	0 to 100 mV	10,000 Hz
Torsional Force	Load Cell	10 V DC	0 to 50 mV	10,000 Hz
Resistance	MMC	None	mΩ	10,000 Hz
Acoustic Emission	Piezoelectric transducer		Various	Various
Vibration R	Accelerometer	IEPE	V	10,000 Hz
Vibration Z	Accelerometer	IEPE	V	10,000 Hz

The raw data was stored and retained independent of subsequent analysis. Analysis of the numerical data was accomplished with MatLab®.

3.4.2. Test Specimens

The annulus (D2 Tool Steel) and flat specimens (CRS Sheet) were preserved following the tests and grouped together (Figure 37) for observation. They were photographed and then stored undisturbed until surface analyses were conducted.

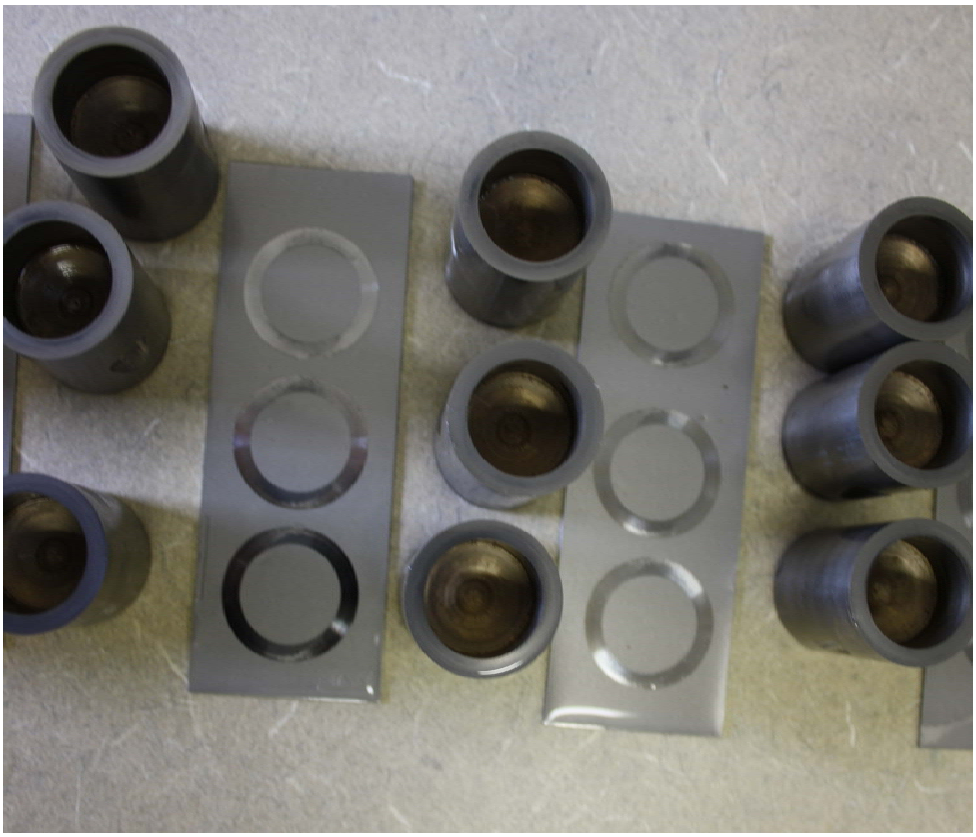

Figure 37: Preservation of TCT specimens after testing.

3.5. Extended Study (Interrupted tests)

A single lubricant (ELV) was chosen for extended testing to identify features near the point of "failure" as identified by the author based on experience.

These areas of interest in the friction curve were identified from the Main Study results. The areas identified in Figure 38 were selected based on the following criteria:

Pre-failure – as late as possible in the test without adhesive failure

Early Failure – as soon after an event that indicates adhesive failure may have occurred

Late Failure – at the point where there is no doubt that adhesive failure has occurred

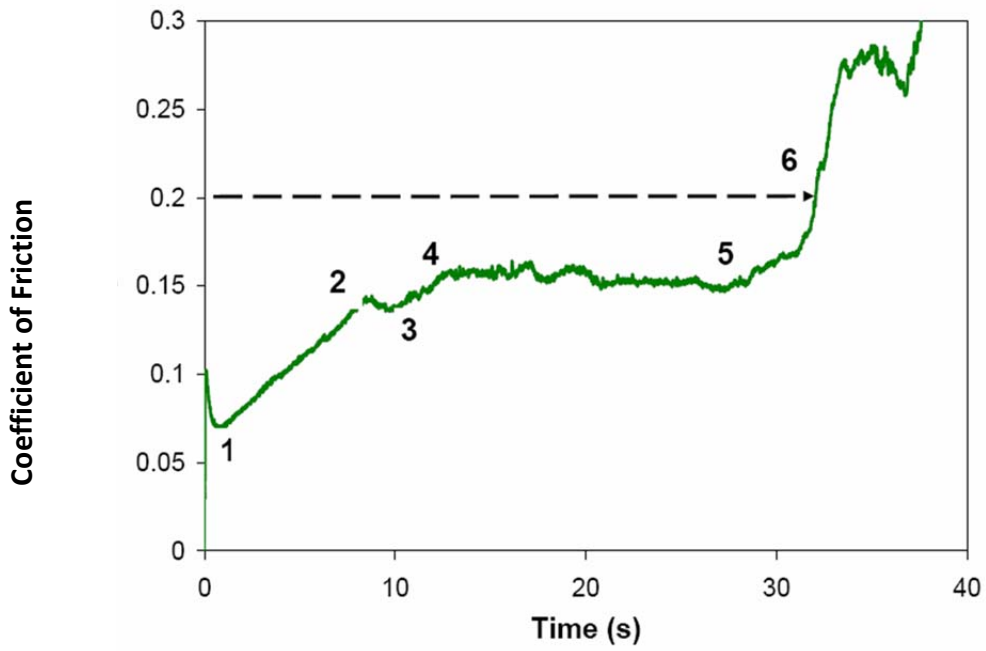

Figure 38 Sample curve with areas of interest: mixed-film lubrication start (1), boundary lubrication start (2), pre-failure (3), EP activation (4), early failure (5), late failure (6).

In Extended Testing, 21 tests were stopped just prior to failure (Pre-failure) and another 21 tests (Late Failure) were stopped when failure was obvious. Another 4 tests were stopped at Early Failure. Fewer tests were conducted at Early Failure due to a limited number of test specimens.

Chapter 4

4. Preliminary Study Results

There were three principal objectives of the preliminary study. The first was to determine the viscosity for the main experiments in the research. The second objective was to determine the appropriate formulations for the lubricants. The third objective was to verify that the contact pressure was appropriate for evaluating the formulations. The scope of the preliminary, main and extended studies was limited to one sheet material, cold rolled steel and one tool material, D2, since these materials are commonly used in sheet metal forming and their behavior is well characterized.

The criteria that these objectives were evaluated on were:

- adhesive failure achieved in a reasonable time (60-90s)
- adhesive failure did not occur immediately (0-4s)
- viscosity and contact pressure levels gave meaningful results

In normal practice preliminary studies are recommended with the TCT when evaluating lubricants or contacting surfaces with no prior TCT history.

Preliminary study experiments were run on a commercially available TCT (Model 3.02) (Figure 25) at the TribSys facility in Valparaiso, Indiana. Lubricants outlined in the previous chapter (Table 2) were formulated specifically for this study. Standard TCT procedures were used in conducting the tests [72]. The results were analyzed to determine if the parameters chosen would yield useful results in the main study.

4.1. The Effect of Lubricant Viscosity

The effects of lubricant viscosity in TCT Tests with the two base stocks (23 cSt and 93 cSt) are seen in the friction curves shown in Figure 39.

a.

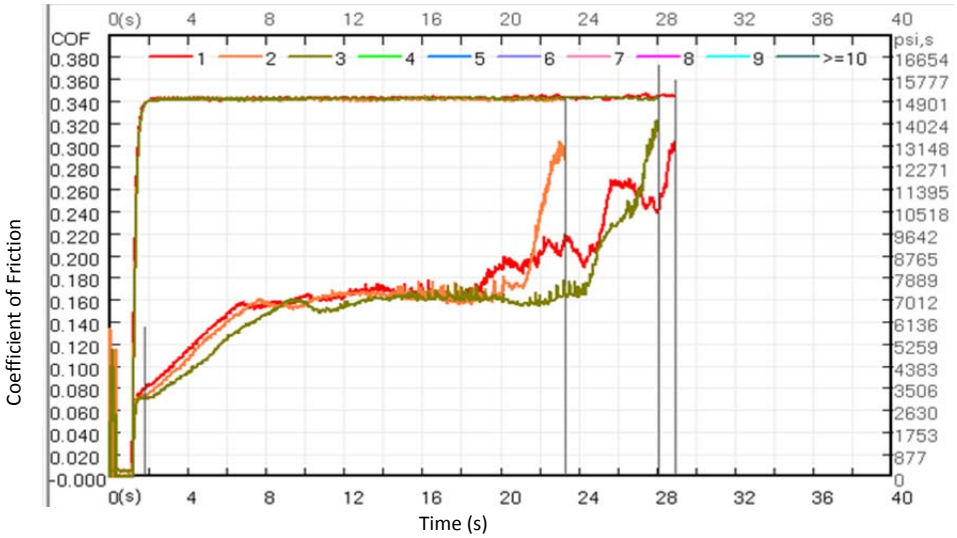

b.

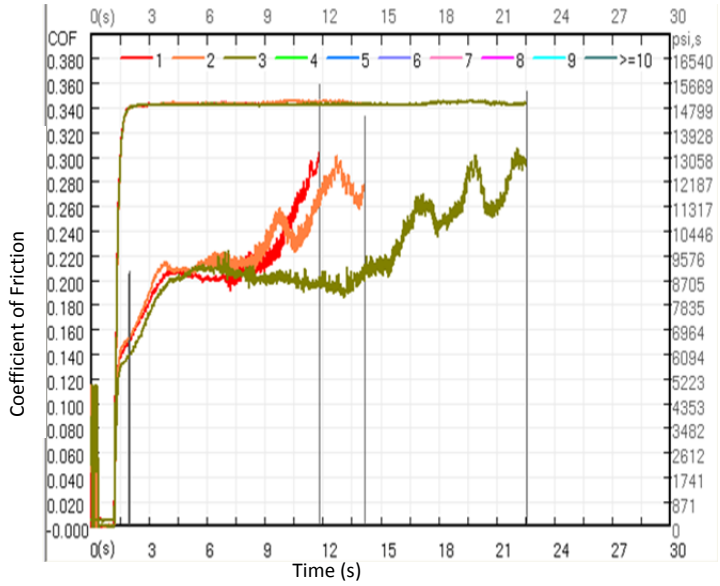

Figure 39: Unfiltered friction data for three replicates of: (a) high viscosity base stock (BSHV); (b) low viscosity base stock (BSLV). The vertical lines can be moved by the operator to select the start and end of a test.

The COF at the point of initial contact is observed to be COF=0.07 for the unformulated high-viscosity (93 cSt) base stock (code: BSHV) and COF=0.13 for the unformulated low-viscosity (23 cSt) base stock (code: BSLV). Lubricant additive and viscosity codes are found in Table 2.

Friction then rises linearly through the mixed film regime to the boundary regime where the COF stabilizes at an average of 0.15 for the BSHV (Figure 39a) and 0.2 for the BSLV (Figure 39b). The end of the boundary regime is traditionally marked by a sudden rise in the COF as adhesive junctions form at the unprotected points of contact. The boundary regime (plateau) lasts approximately 15s for the BSHV (Figure 39a) and only 5s for the BSLV (Figure 39b).

4.2. Effect of Contact Pressure

The effect of contact pressure on the various low viscosity lubricant formulations is shown in Figure 40. The three groups of curves show the effect of increasing pressure on the friction response with continued sliding contact (rotation) for one representative test for each formulation. At the highest contact pressure (225 MPa) even the best lubricants (sulfur and chlorine additives) failed very quickly indicating that this contact pressure was too high for meaningful comparison. At this pressure the base stock and ester lubricant formulation failed immediately and are not shown on the 225 MPa chart. At the lowest contact pressure (20 MPa) the contact pressure was not severe enough to create lubricant starvation in a reasonable time. The light contact pressure was insufficient to stabilize the TCT's self-alignment system as evidenced by the immediate oscillation in the transmitted torsional signal. The 225 MPa contact pressure was too severe for the base stock and ester. The 100 MPa contact pressure showed the best discrimination between the lubricants. While only one representative curve is shown the differences between lubricants at 100 MPa were shown to be significant at a confidence level of 99%. (Appendix 4)

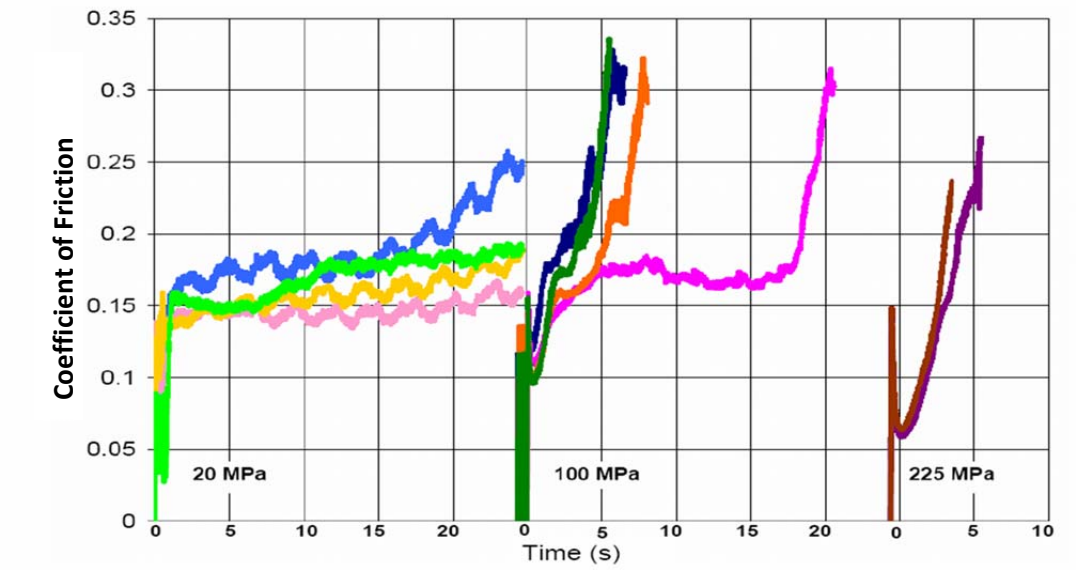

Figure 40: TCT Results- Effect of pressure on friction for various low viscosity lubricant formulations

Note: (light and dark blue=base stock; light and dark green=ester; yellow, orange, brown=sulfur; pink, purple =chlorinate paraffin) at various contact pressures (only sulfur and chlorinated paraffin results are presented for the highest pressure).

4.3. Effect of Lubricant Additive

As discussed in earlier chapters, industrial lubricants were formulated with additives to respond to a variety of surface conditions and performance requirements. The preliminary study TCT data curves were examined and segmented based on the author's estimate of the friction curves to the corresponding lubricant responses (Figure 41).

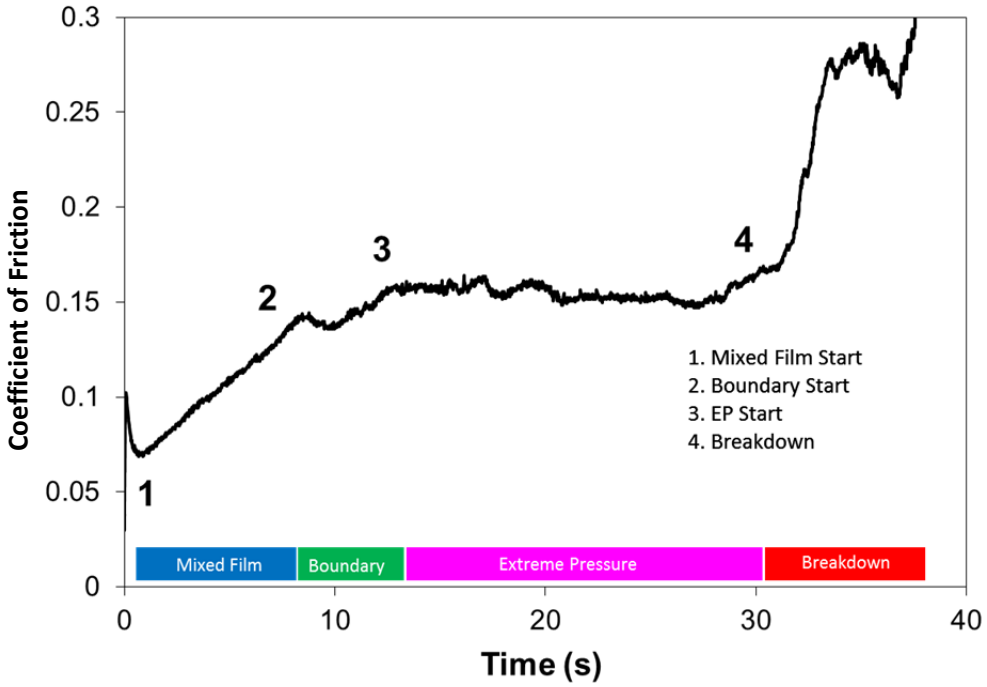

Figure 41: Lubricant responses for a typical TCT friction curve showing the progression of COF with test duration.

The plot shown in Figure 42 shows data points based on these responses for all three replicates of each lubricant formulation. The separation between the viscosity levels for the formulations is most evident in the mixed film response where the COF values do not overlap. This is expected since in mixed film lubrication a portion of the normal force is supported by lubricant pockets and the magnitude of this support is a function of viscosity. As the lubricant is depleted and the support of the bulk lubricant is lost, the difference between low and high viscosity is less. In extreme pressure regime where only reactive films prevent metal to metal contact, the response of the low viscosity chlorine (CLV) formulation performs better (in terms of time to breakdown) than the high viscosity formulations with inferior EP additive protection. Figure 43 displays the individual data points of Figure 42 with lubricant formulation averages. As expected the chlorine (EP) additives were the best performers while the base stock was generally worst.

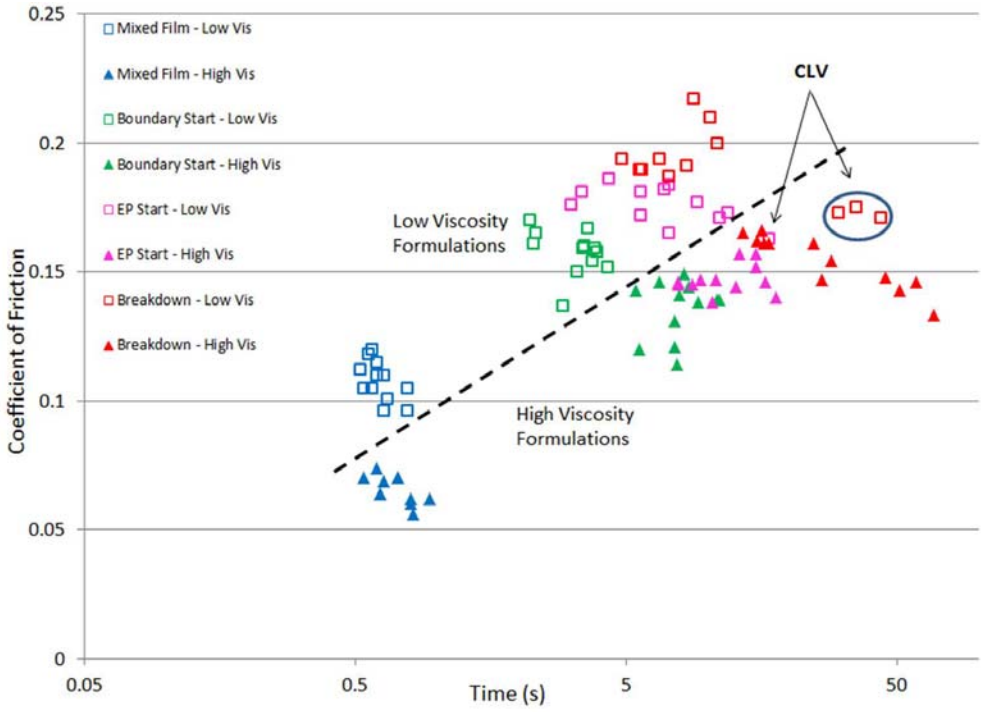

Figure 42: Scatter plot of Preliminary Study data for 100MPa, event time versus COF.

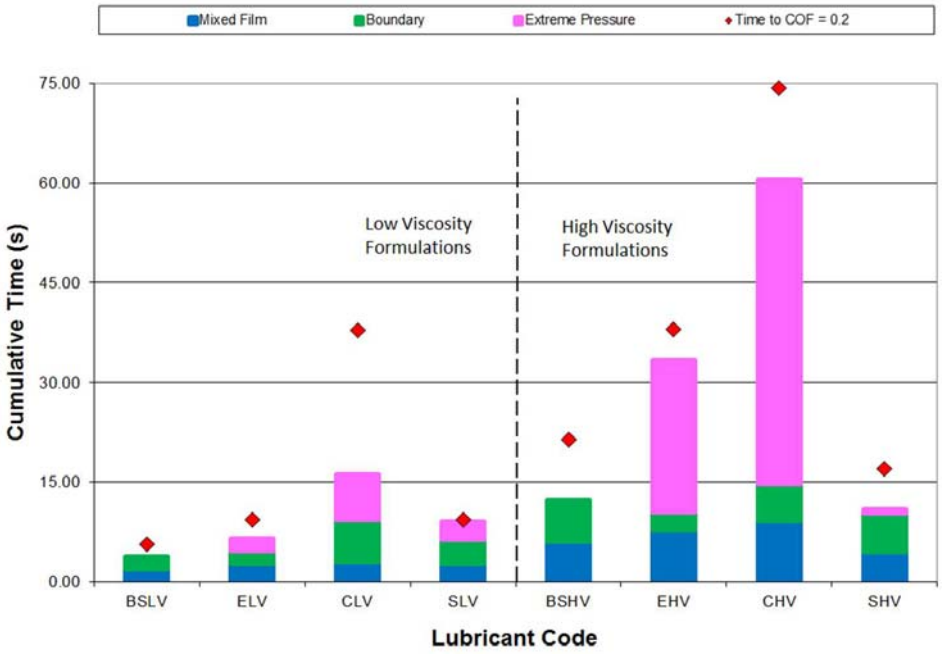

Figure 43: Preliminary Study Average values of event duration versus lubricant formulation

4.4. Discussion and Conclusion from Preliminary Study Results

The preliminary study analysis showed the strength of the time-based rather than COF based ranking for the anti-adhesive wear properties of the formulations (greater time to breakdown means improved effectiveness at reducing adhesive wear). While this approach to evaluating lubricant can be effective, the selection of the point of breakdown requires considerable expertise and is a source of bias. Solving this problem is the main focus of this research so the issue is explored further in later chapters.

In light of the findings of the preliminary study the following refinements to the variables for the main study were decided:

- to conduct all tests at the 100 MPa normal stress level,
- to continue testing at both viscosity levels (23 cSt and 93 cSt),
- to discontinue testing with the sulfur additive while focusing on the low viscosity ester for training data (extended study) since its behavior, in contrast to the low viscosity base stock, exhibited a EP additive response where the boundary regime is extended after a rise in friction (activation).

Chapter 5

5. Main and Extended Study Results

This chapter examines the quantitative, real-time data collected during the main and the extended study in the context of post-test examination of surfaces using a variety of analytical techniques. The hypothesis of this research states that a combination of data from various sensors measuring the real-time response of a tribotest provide better detection of adhesive wear than the coefficient of friction alone. In order to test this hypothesis, real-time sensor data is collected, analyzed, and correlated with post-test specimens collected at the time of interest as indicated by the real-time sensor data.

Prior to presenting the data in each section a brief explanation of the particular technique is presented. The following is a summary of the real time measurements and post-test analytical techniques:

- Real-Time Measurements
    - Friction - torsional force, normal force
    - Vibration - radial, normal accelerometer
    - Acoustic Emission - piezotransducer
    - Electrical Resistance - multimeter
- Surface Analyses (Post-test)
    - Surface features and chemistry - Scanning Electron Microscope with EDX
    - Surface features - Optical Microscope

Note: White Light Interferometry and Attenuated Total Reflectance- Fourier Transform Spectrometry were used on a limited basis and is discussed in the next chapter.

Main Study tests were stopped after obvious failure as indicated by a sudden and sustained rise in friction. Extended tests were stopped prior to failure, early failure, and late failure. Note that "late failure" in the extended tests was sooner than the point chosen in most main study tests. A summary of the experimental conditions outlined in Chapter 3 are presented in Table 6 and 7.

Table 6: Summary of the Experimental Conditions for the Main Study

Lubricant Code	Replicates	Flat Specimen	Annular Specimen	Interface Pressure	Measurement
BSLV BSHV ELV EHV CLV CHV	3	CRS	D2	100MPa	Torsional Force Normal Force Vibration R Vibration Z Acoustic Emission Resistance

Table 7: Summary of the Experimental Conditions for the Extended Study

Lubricant Code	Replicates	Flat Specimen	Annular Specimen	Interface Pressure	Measurement
ELV – Pre-Failure ELV – Early Failure ELV – Late Failure	21 4 21	CRS	D2	100 MPa	Torsional Force Normal Force Vibration R Vibration Z Acoustic Emission

Surface analysis techniques employed on the retained test specimens confirmed the surface conditions at the point at which the test was interrupted. This information was essential for corroborating the presence and severity of adhesive wear with the test measurement leading up to the point of interrupting the test.

The results presented are representative of the complete data collected during the tests and in post-test analyses. The complete results are appended in Appendix 4.

5.1. Real-Time Measurements

Real-time measurements are those measurements that are measured, displayed, and stored as the test is running. The display of real-time data allows for the operator to respond to changes in the surface interactions as indicated by the displayed chart.

5.1.1. Friction

The force resisting sliding (referred to as the frictional force) is often represented as a coefficient of friction (COF, μ) expressed as the ratio of the frictional force to the normal force. In many tribotests the COF is used to evaluate the effectiveness of a lubricant or surface coating at reducing or controlling friction in industrial processes and by extension an indicator of abrasive and adhesive wear. While the use of the coefficient of friction in this manner has advantages, namely establishing normalized quantitative data for a contacting couple, there are disadvantages as well.

It is useful at this point to consider some of the assumptions made about the COF and their validity in light of this discussion. First, the normalized COF removes the context of the contact conditions and implies that friction is independent of these variables. Bowden and Tabor point out that Amonton's Law only holds as long as the contact area continues to grow with increasing load [78] and studies have shown that contact area reaches a maximum, even at high stress, as asperities merge under the applied load [79,80,81].

Secondly, pressurization of a lubricant in a sliding contact causes the friction force to decrease as normal force increases. The pressurized lubricant supports the load and reduces stress on the contacting asperities. In dry sliding, friction was found to be a fairly reliable indicator of adhesive failure [82]; however, in the presence of a lubricant, friction is not a good indication of

adhesive wear [83]. The next section examines friction response from the experiments outlined in Chapter 3.

5.1.1.1. Friction Measurement Results

The friction force data for the experiments conducted in the main and extended studies are left as raw voltages to preserve "noise" and to keep different sensor data at the same scale. A sample calculation of the coefficient of friction from transmitted torsional signal voltage is shown in Appendix 3. Since the apparent contact pressure was held constant (100 MPa) for all tests, the transmitted torsional load cell voltages most closely represent the true unfiltered friction force (Figure 43) and is more easily compared to the signals from other sensors (also voltages). A complete collection of transmitted torsional signal curves representing all of the tests listed in the test matrix can be found in Appendix 4.

While most studies report friction data as a value averaged over the steady state portion of a tribotest, examination of the curves in Figure 44 illustrate the transient nature of friction as lubricant depletion progresses. Reducing these curves to single values would result in a loss in the complexity of the friction response with time.

To understand the response of friction in the TCT it is useful to examine the changes in the response as the lubricant is depleted under the constant normal force and repeated rotations of the annulus over the same apparent area of contact.

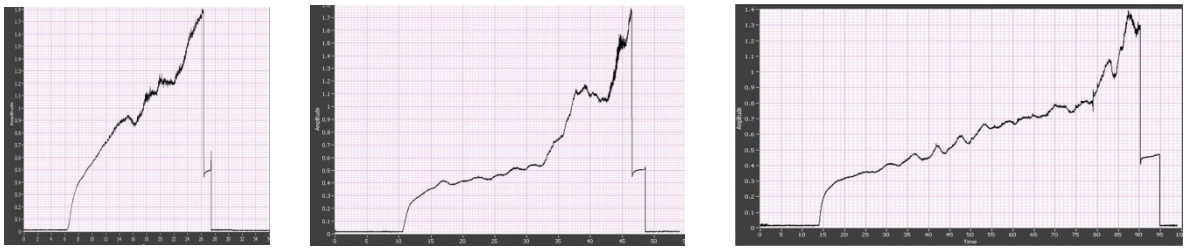

Figure 44: Raw transmitted torsional signal (friction) response (V) for tests with (L-R): Low viscosity base stock, high viscosity base stock, and a chlorine additive in high viscosity base stock. The curves are shown to illustrate the complexity of the friction response and how reducing these curves to a single COF value would be difficult.

In Chapter 2 the three lubrication regimes described by the Stribeck Curve (Figure 14) were introduced. They are repeated here in the context of the TCT test:

I. Hydrodynamic – the rotating annulus approaches the stationary, lubricated test specimen and as the contact pressure builds the lubricant is squeezed until the surfaces come into contact (i.e. the lubricant film thickness approaches zero).

II. **Mixed-film lubrication** - the combined support of the lubricant trapped between asperities and the asperity plateaux support the normal load (i.e. the stress in the asperities is lower than the limiting flow stress of the softer surface.

III. **Boundary lubrication** - friction remains constant with weakly-adhered lubricant films protecting the surfaces. These films reform if there is adequate lubricant supply and temperatures are not too high. Once metal transfer dominates the surface interaction the measurement of friction becomes difficult since the contact between surfaces is now governed by adhered particles.

The typical TCT test follows the sequence outlined in the previous section and the test is stopped after friction rises above the point of obvious lubricant failure. The commercially available

TribSys TCT analysis software approximates the point of failure with an algorithm in the data acquisition software based on the slope of the COF curve. The user can override the software if they think that the point of failure as defined by the software algorithm is not representative. In most cases where the operator overrides the software a threshold, (ie COF=0.2) is used to reduce operator bias.

We expect to see an increase in time-to-breakdown (t_{BD}) with increasing EP additive effectiveness or stated as a null hypothesis(there is no difference between EP formulations and the base stock of the same viscosity):

$$\text{Ho: } t_{BD(basestock)} = t_{BD(ester)} = t_{BD(chlorinate\ paraffin)}$$

Prior to analyzing the data using statistical tests three assumptions were made [84]:

1. The errors are independent (the errors in one observation are not influenced by errors in another observation)
2. The variance of the errors is the same among all groups
3. The errors are normally distributed

To ensure independence of the errors (1), test specimens were randomly selected from one batch of annular tools and one batch of steel sheet. The uniformity of error variance between groups (2) allows the Student-t test to be used to compare means between groups. Uniformity was ensured by using formulations of the same viscosity and using simple formulations that produced expected responses in the preliminary study (at 100 MPa). Finally, the assumption that the errors are normally distributed (3) was tested and the results shown in Figure 45. The linearity of the plot of residuals indicates that the assumption of Normality is valid [85].

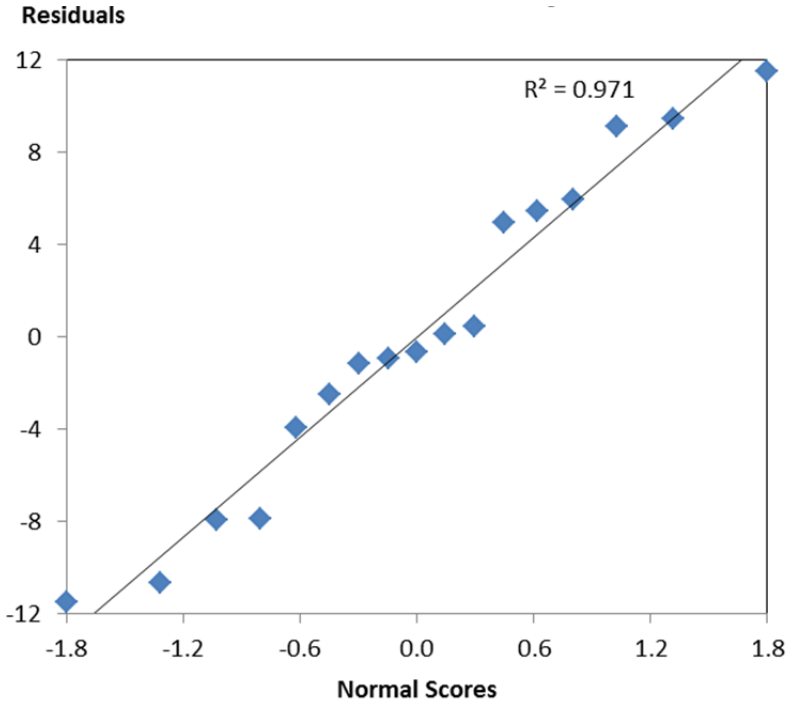

Figure 45: Normal probability plot of Main Study residuals with linear fit.

The results of the main study were compiled using the time-to-breakdown as defined by the COF=0.2 criterion and are presented in Figure 46 and Table 8. The results show that as expected increased viscosity (**LV=low viscosity, **HV=high viscosity) plays a strong role in delaying failure while additive packages further delay failure. Both of these effects were significant at a 99% level. Interaction between viscosity and additive was found to be not significant (see ANOVA Table, Appendix 4) The synthetic ester doubled the time to failure with both the low (ELV) and high viscosity (EHV). The high viscosity chlorinate paraffin additive (CHV) improved the time to failure over the EHV by 28% while the lower viscosity formulation showed a 113% improvement over the ELV response. The improved performance with the CLV is not unexpected since the low viscosity base allows the temperature of activation (necessary for EP additives) to be achieved sooner.

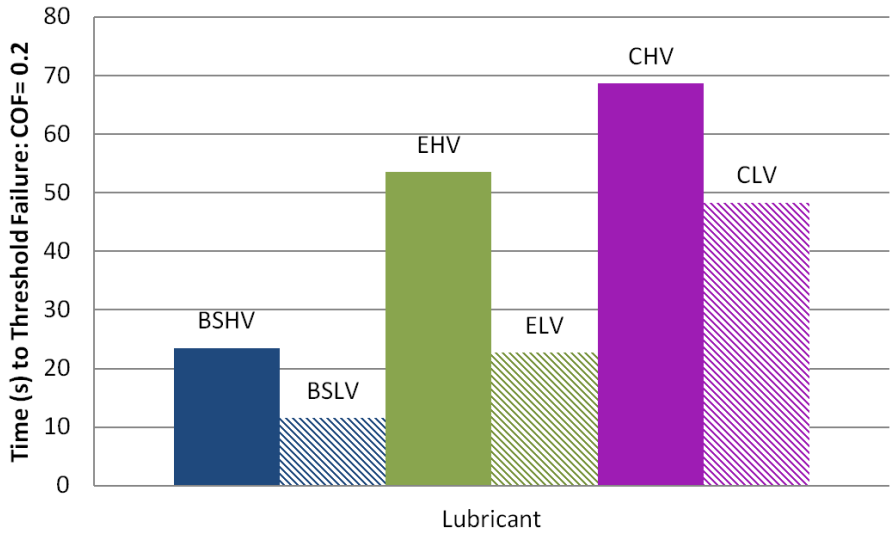

Figure 46: Main study results based on failure Criterion: COF=0.2 (1.0V)

Table 8: Main study results with failure criterion: COF=0.2 (1.0V)

Lubricant	Number of Reps	Time-to-Breakdown	
		Average	Std Dev
BSHV	3	23.5	5.6
BSLV	3	11.5	0.5
EHV	3	53.5	4.5
ELV	3	22.7	3.5
CHV	3	68.7	11.6
CLV	3	48.3	8.5

5.1.1.2. Identifying lubricant failure through interrupted tests

In the extended study it was necessary to produce data for healthy (unfailed) test specimens as well as failed specimens to both test the hypothesis. To accomplish this objective, 21 tests were run with one lubricant (ELV) to the end of mixed film and the start of boundary lubrication to establish the surface conditions at a point sufficiently long into the test but before the transmitted torsional response displayed typical signs of adhesive wear (increased amplitude). An equal number of tests were run to the point of obvious failure as characterized by a sudden and sustained rise in transmitted torsional force. Four tests were then run and stopped during the period between these two states to understand the surface conditions during EP activation. These tests would be used as an intermediate condition between un-failed and failed lubricant. Figure 47 shows one sample curve from each of these groups and Figure 48 shows the how the variability between the transmitted torsional signal curves increases dramatically for the tests here labeled as “Late Failure”. It is interesting that the variability (noise) within the individual curves increases as the tests progress. This “noise” is examined by subtracting a filtered friction curve (determined using a 20 point moving average) from the raw friction data (Figure 47 inset). Figure 47 shows how the transmitted torsional signal amplitude (in this case rectified to show all amplitude values as positive) generally increases as the TCT test progresses, with sudden increases the transmitted torsional signal amplitude curve corresponding to lubricant regime changes as indicated by the transmitted torsional signal curve.

Furthermore, Figure 49 compares the results of different transmitted torsional signal curve features as identified on the raw friction curve (inset).

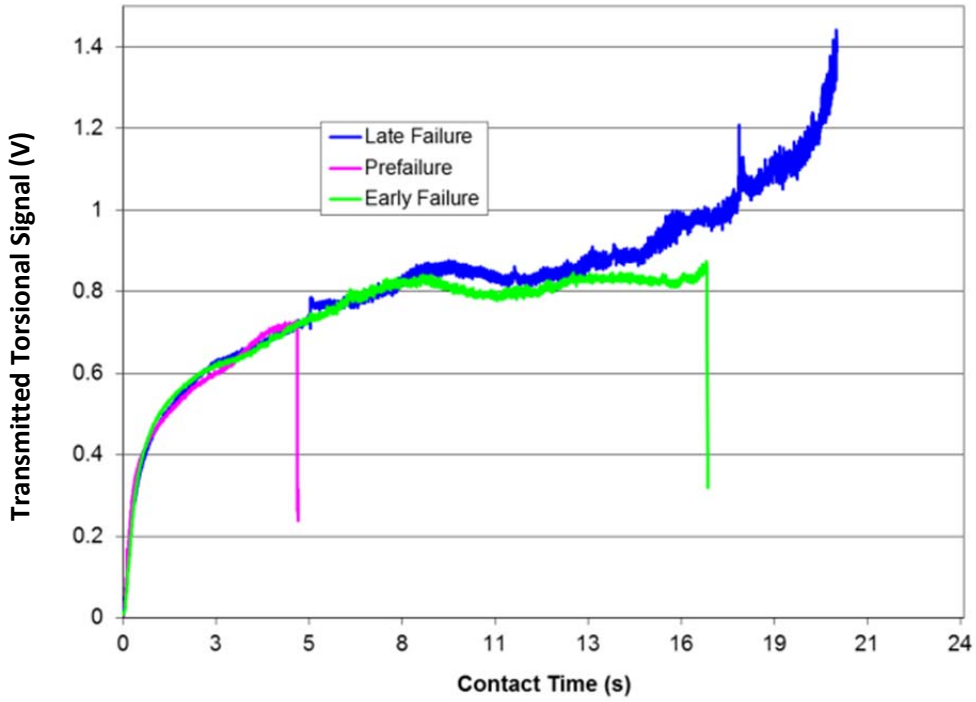

Figure 47: Typical curves from each type of interrupted test in the extended study.

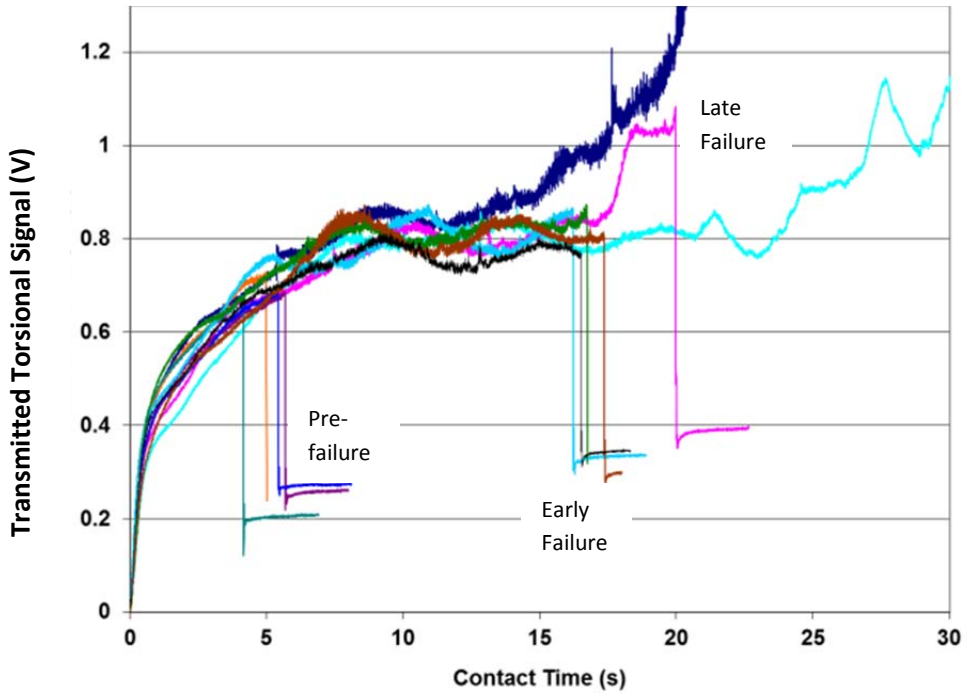

Figure 48: Increase in variability as the tests approach failure both between curves and within each curve.

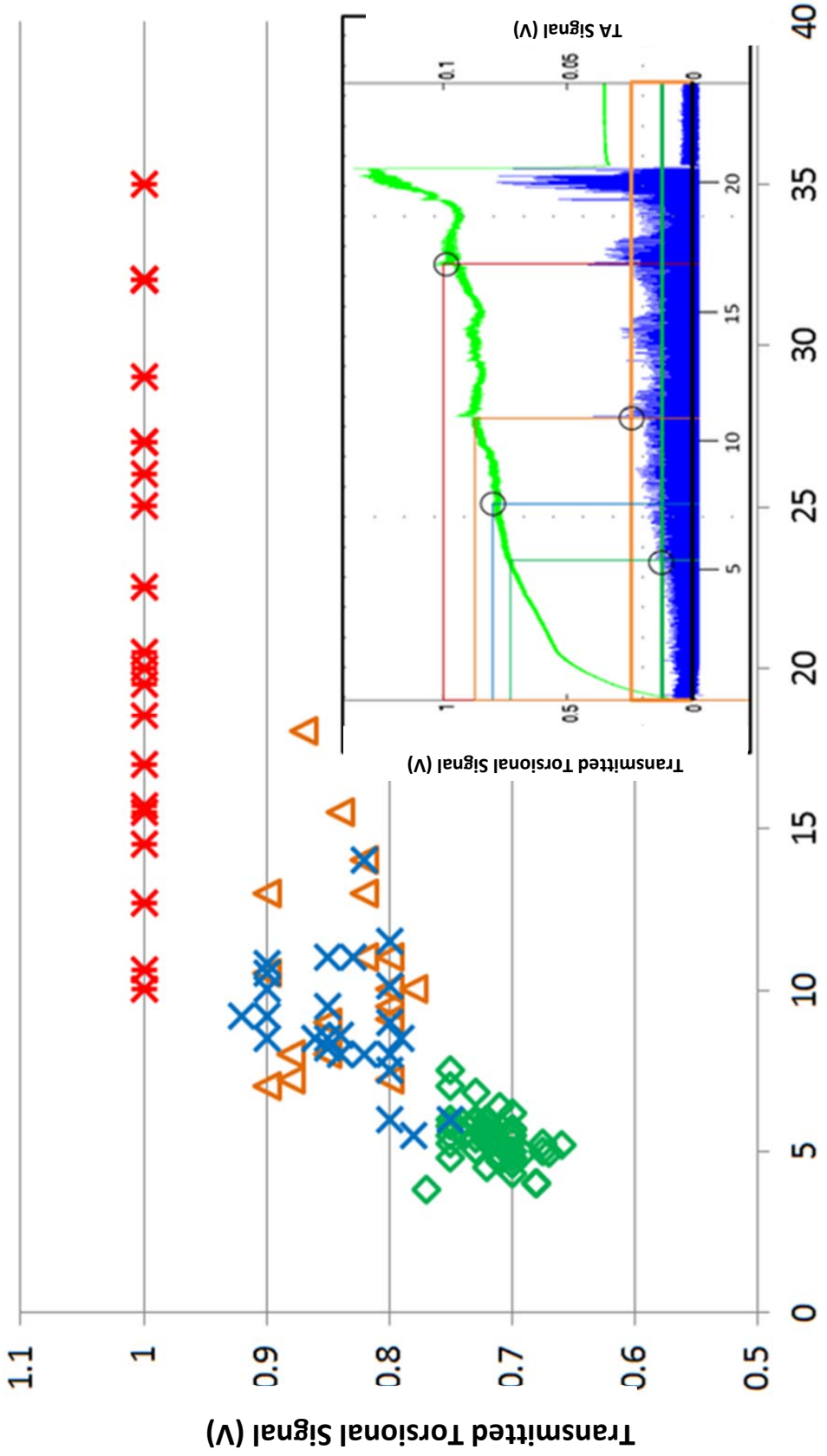

Figure 49: Extended test results for all extended study tests (see Table 9). Note the red and blue symbols refer to the transmitted torsional signal (inset: light green) while the orange and green symbols refer to the transmitted torsional signal amplitude (TA signal) curve (inset: dark blue)

The green diamonds and yellow triangles represent transmitted torsional signal and time when the "noise" or transmitted torsional signal amplitude exceeded 0.0125 V and 0.025 V respectively. The blue X's represent the plateau or first maxima in the curve ($\Delta COF/\Delta t=0$). Finally the red X's represent the time when the COF exceeded 0.2 or a transmitted torsional signal = 1.0 V (the standard threshold used today).

One sees in Figure 49 that the increase in variability with time that was seen in the raw transmitted torsional signal curves is repeated in the data points representing the four criteria and is characteristic of the stochastic nature of adhesive wear. Once the severity of adhesive wear increases beyond light scuffing the variability doubles.

Table 9: Extended Study Results

Criterion	Number of Data Points	Time to Failure		Adhesive Wear Severity
		Average	Std Dev	
TA=0.0125V	46	5.4	0.8	Light scoring
Plateau	25	9.0	1.8	Light scuffing
TA=0.025V	19	11.2	3.8	Moderate
COF=0.2 (Transmitted torsional signal =1.0V)	21	22.0	7.4	Heavy

Finally, the correlation between the standard transmitted torsional signal threshold and the transmitted torsional signal amplitude, i.e. plotting the time for the amplitude of an individual sample to exceed 0.025 V versus the time for the magnitude of the transmitted torsional signal of that same sample to exceed 1.0 V (COF=0.2) showed a strong positive correlation (Figure 50).

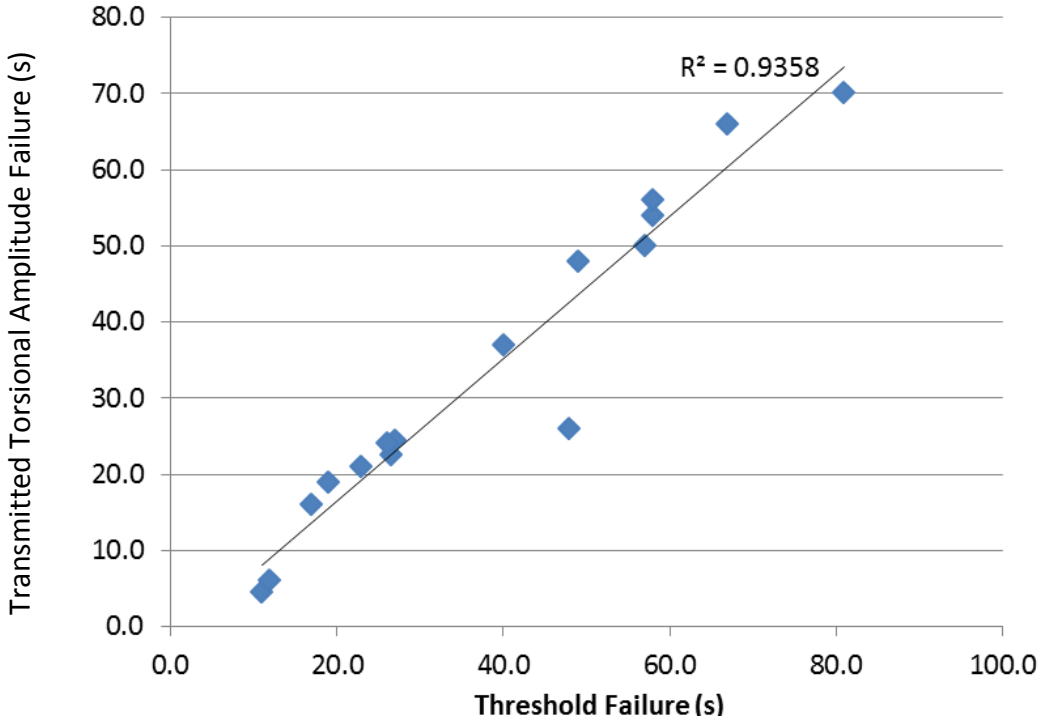

Figure 50: Correlation between transmitted torsional amplitude failures (>0.025 V) and standard transmitted torsional signal threshold failures (COF =0.2). Each marker represents the transmitted torsional signal threshold and transmitted torsional signal amplitude of a single test.

The implication of the strength of this correlation is the ability to use transmitted torsional signal amplitude as a second feature of the same data to confirm adhesive failure. Using a transmitted torsional signal amplitude limit of 0.025 V as a measure of lubricant failure yielded a time to failure that is in all cases sooner than the COF threshold of 0.2 (1.0 V). The advantage of ending the test earlier is that the specimen sustained less post – failure damage and thus makes interpretation of the nature of failure easier.

5.1.2. Vibration

Vibration is often identified with friction. The relative motion of two surfaces is marked by a series of resistance and release causing vibrations both normal to, and in the direction of, sliding.

Raw vibration signal data is recorded as a voltage as a function of time and is described by Amick [86] as:

> "*Time domain data are representations of physical motion, wherein motion is quantified as a set of amplitudes as a function of time."*

Amick goes on to remark:

> *"The severity of instantaneous amplitude can be characterized by a maximum value over some period of time, either as 0-to-peak (the maximum absolute value) or peak-to-peak (the absolute sum of positive and negative peak amplitudes)."*

Extremes of this phenomenon are known as stick-slip and under certain conditions when stick-slip occurs in the TCT it produces a "ringing" tone. Two accelerometers were placed to capture both radial and normal components of the vibration signal generated from the TCT test. There were no attempts to filter the vibration signals since the identification of noise in the signal is extremely difficult in tribotests.

5.1.2.1. Vibration Measurements

Representative curves of data collected from radially (r) and normally (z) oriented accelerometers for lubricant: ELV (interrupted) are shown in Figure 51 (a) and (b).

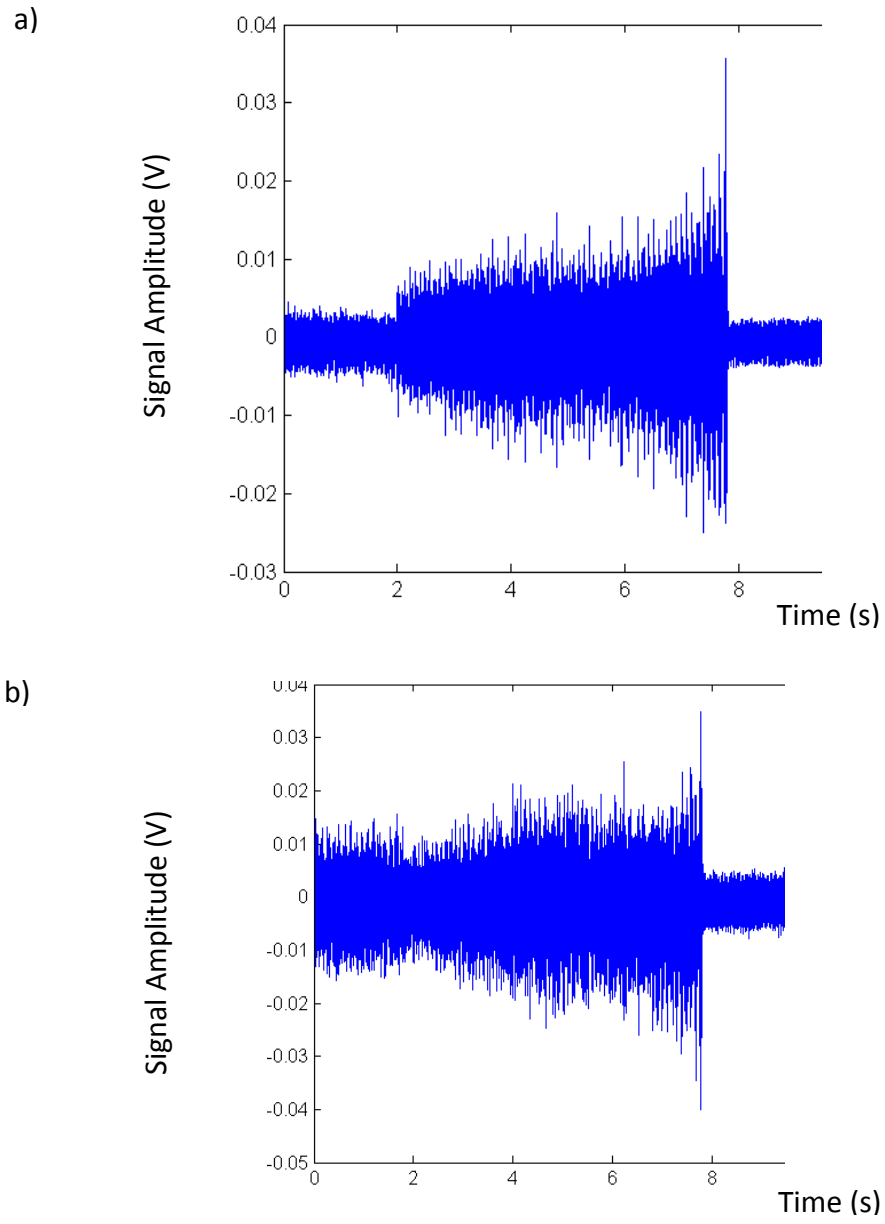

Figure 49: Typical TCT vibration signals (amplitude versus time) collected for a) radial vibration; b) normal vibration (ELV interrupted test)

Note that for both vibration signals, and especially the normal vibration signal (Vibration2), the "noise" in the signal prior to contact (at 2s) is greater than the noise following the test (at 8s). The higher background noise prior to contact in the test is thought to be due to the motion of the hydraulic actuator and hydraulic motor prior to the test. These hydraulic components are not active at the end of the test where the background vibration is reduced. The narrowing of the normal vibration signal amplitude at the 2s mark indicates the point where the test begins as the contact pressure develops between the two specimens and the hydraulic ram stops moving. For both radial and normal vibration signal, from the 2s point to the 8s point the magnitude of the amplitude is due to vibrations generated by surface contact. The amplitude of both vibration signals increased during the test with, possibly due to an increase in the severity of adhesion.

The normal component of the vibration signal appears to be more complex (responding to unknown variables) than the radial component and hence a less robust indicator of lubricant failure due to adhesive wear. Like the transmitted torsional signal amplitude, the ease of setting limits on the amplitude of the radial vibration signal means that this signal could be used to indicate the progression of adhesive wear (Figure 52). Rectifying the vibration signal and filtering of the data to remove transient spikes using a RMS transformation may improve its usefulness in lubricant failure analysis.

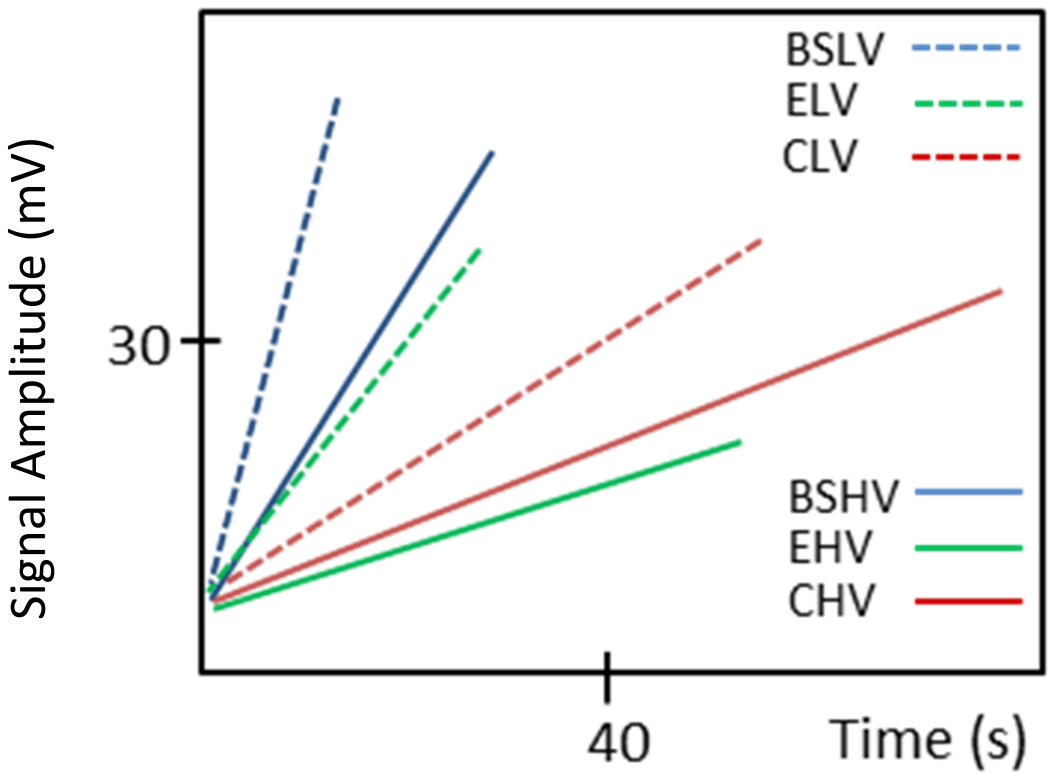

Figure 50: Trends in radial vibration signal amplitude with time in the TCT

5.1.3. Acoustic Emission (AE)

Acoustic emission data are collected and recorded as events under various parameters such as energy, amplitude, etc. (Figure 53). Analyses of AE signals emanating from two contacting surfaces is not easy given the complexity of the interface. The introduction of noise from the mechanical system rather than the interface presents further challenges.

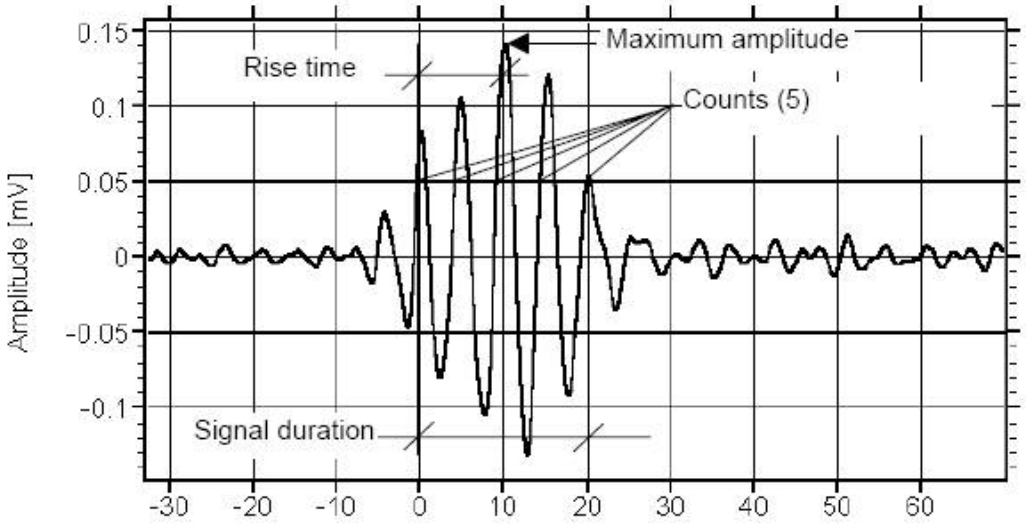

Figure 51: Features of Transient Signals (source: Vallen AE Manual[83])

Holt et. al. noted that in the forming of steel the number of detectable AE events are small and that sources of background noise must be limited [87] .

In the analysis of AE data for crack detection [88], AE bursts are categorized as wanted and unwanted. The unwanted bursts include electrical noise (short signals) and friction noise (low amplitude, long duration signals). In our case the "wanted" bursts include the friction noise and, since this will be a function of the lubricant effectiveness, should be an indicator of the surface condition.

5.1.3.1. AE Measurements

Figure 53 shows typical signals for a range of AE parameters collected during a single test (ELV interrupted before failure). These AE parameters are compared to the transmitted torsional signal and radial vibration signal for the same test. Unlike the typical AE burst shown in Figure 53, the AE signal generated from the TCT (Figure 54) are continuous bursts super-imposed with discrete bursts. Various AE parameters are displayed in individual panels. The transmitted torsional signal and radial vibration signal amplitude (upper left) are shown for comparison.

One can see that for the most of the AE parameters: Amplitude (Fig 54b), RMS (Fig 54c) Absolute Energy (Fig 54d), Average Frequency (Fig 54e) and Energy (relative) (Fig 54f) the majority of the AE response occurs during the mixed-film portion of the curve (see transmitted torsional signal curve). It is during the mixed-film regime, where asperities are being flattened, that the greatest plastic deformation occurs. It appears from the Rise Time curve (Fig 54g) that the rise time does on average increase during the test but there does not be any indication of impending lubricant failure in the rise time.

Qualitative comparison the various AE parameters between replicates of the same test and between different lubricants showed that variability within tests was too great to provide a robust discrimination between lubricant formulations. Interrupted tests (Figure 55) for one lubricant show excellent repeatability for the transmitted torsional signals (10 curves) but poor repeatability for the AE Absolute Energy signals (4 curves marked E in the legend) during mixed-film lubrication.

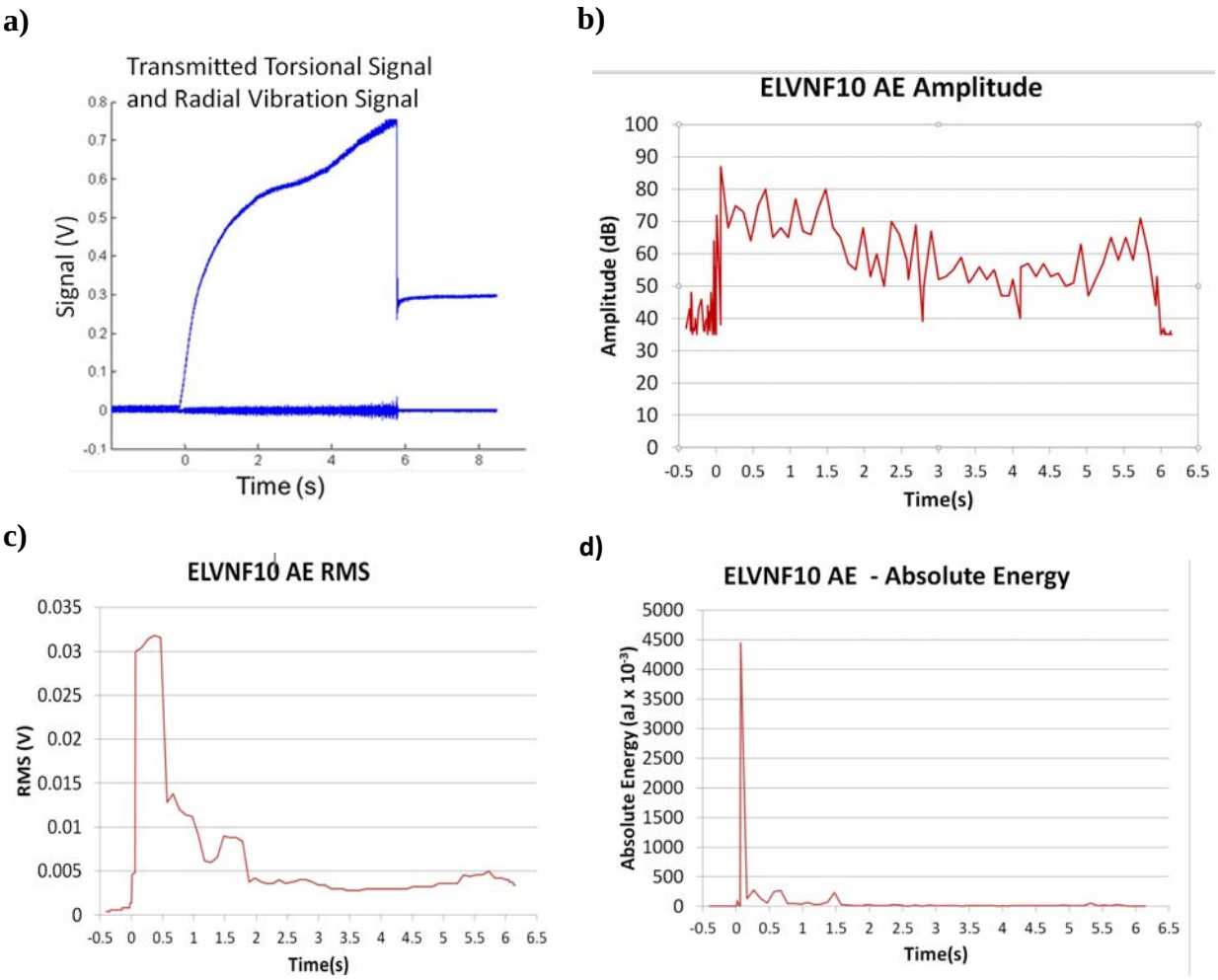

Figure 52: AE parameters (b-d) for ELV interrupted test (not failed) compared to Transmitted torsional signal and Radial Vibration signal (a).

Continued on next page

e)

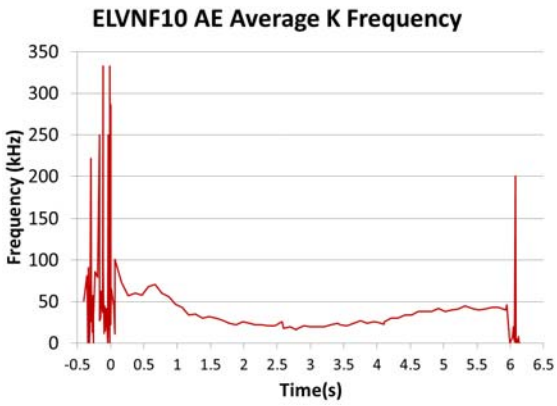

f)

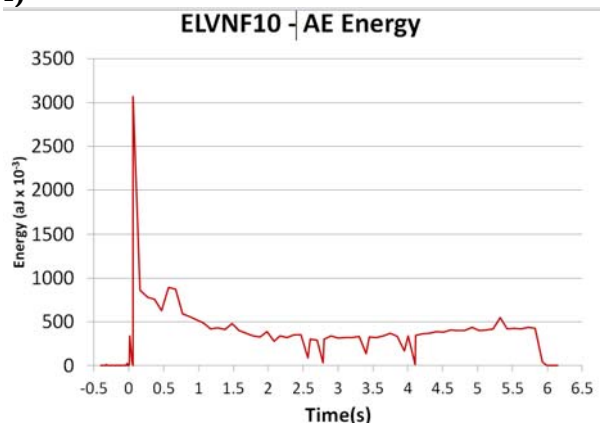

g)

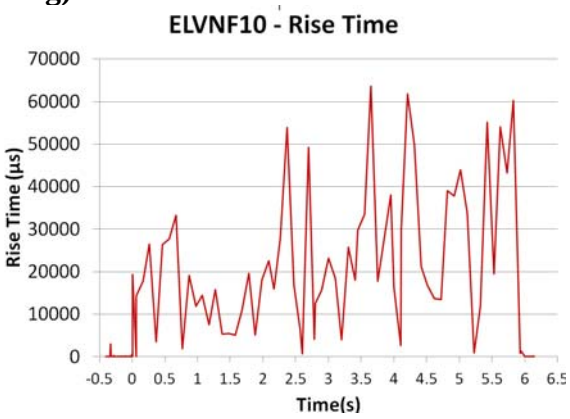

Figure 53 continued: AE parameters for ELV interrupted test (not failed): e) Average K Frequency, f) Energy, and g) Rise Time.

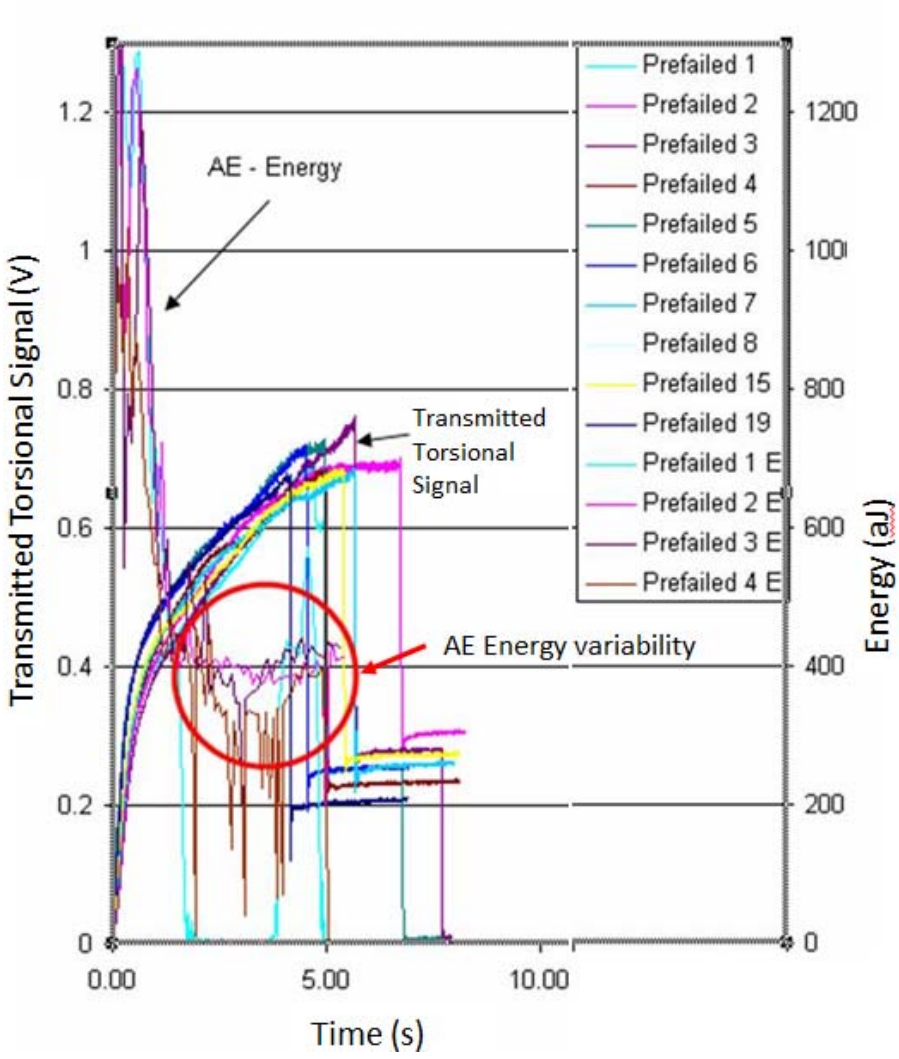

Figure 54: TCT Curves for ELV interrupted tests comparing transmitted torsional signal with variability in AE Energy (red circle).

Given the lack of response to adhesive wear events by acoustic emission signal (seen in the transmitted torsional signal and vibration signal responses), it is not clear from the data collected in this study how AE could be used as an indication of lubricant failure to adhesive wear.

5.1.4. Electrical Resistance

Electrical conductivity of contacting surfaces was studied by Archard for the purpose of improving electrical switches [89]. Several tribology researchers realized that it would be useful as a means of measuring the degree of contact between sliding surfaces.

Cameron describes the need to measure film thickness for thin films and the specialized surfaces required for most laboratory techniques. He suggested two contact measurement methods for industrial (garden variety) surfaces one involving resistance measurement across the gap and the second involving voltage discharge [90]. The voltage discharge method might generate sparking and thereby changing the surface chemistry so was not considered further in this study. The resistance method was used earlier by this author with some success to study diamond-like coatings under dry sliding.

5.1.4.1. Electrical Resistance Measurements

Despite a very accurate sensor (National Instruments PCI 4070 - 6.5 Digit DMM) grounding of the signal occurred very early in the contact of the sliding surfaces and by the time the transmitted torsional signal threshold of 1.0V was achieved there the surfaces were completely grounded (red arrow) (Figure 56). The use of resistance as a measure of adhesive failure in these experiments proved futile. The findings related to using resistance as an indicator of adhesive wear were further supported by the conclusions of Bowden and Tabor who point out in their study:

"…Thus electrical resistance measurements provide a very sensitive means of discriminating between complete fluid lubrication and the smallest amount of metallic contact. The main disadvantage of this method is that it does not make a clear distinction between metallic contact and metal surfaces covered with boundary films." [91]

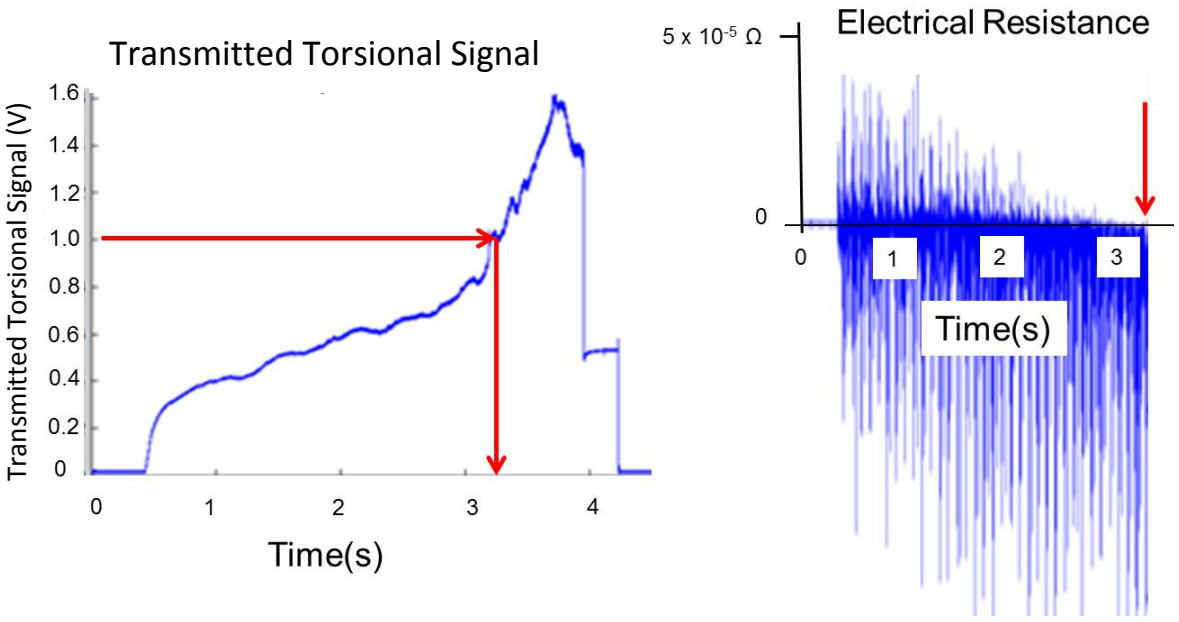

Figure 55: Resistance measurements compared to transmitted torsional signal for ELV

5.2. Surface Analyses (Post-Test)

5.2.1. Optical Microscope

Low magnification optical imaging is useful in detecting adhesive wear such galling, scoring and plowing. On the annular tool, adhered metal particles appear white on a matte gray background (Figure 57). On the flat sheet specimens optical microscopy revealed physical changes to the contact area (flattened area = shiny) using incident light (Figure 58). A burnished (shiny) contact area shows up black since the low angle light is reflected away from the objective of the microscope.

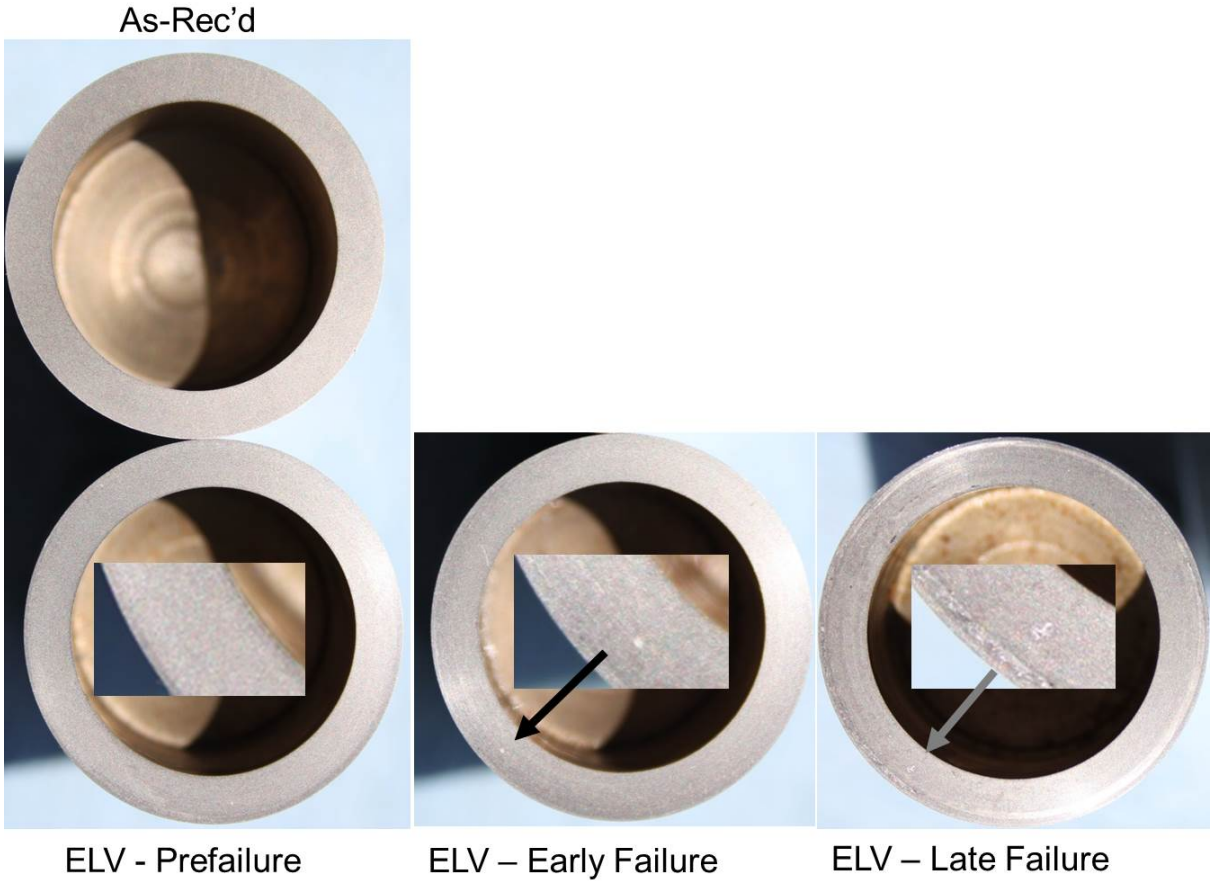

Figure 56: Adhered sheet particles on annular specimens (arrows)

The total reflection of light from the burnished track in Figure 58a indicates that the contact area is approaching 100%. In the early and late failure specimens the damage from adhesive wear produced roughening of the burnished area. The adhesive wear appears lighter than the darker burnished surface (Figure 58 b, c).

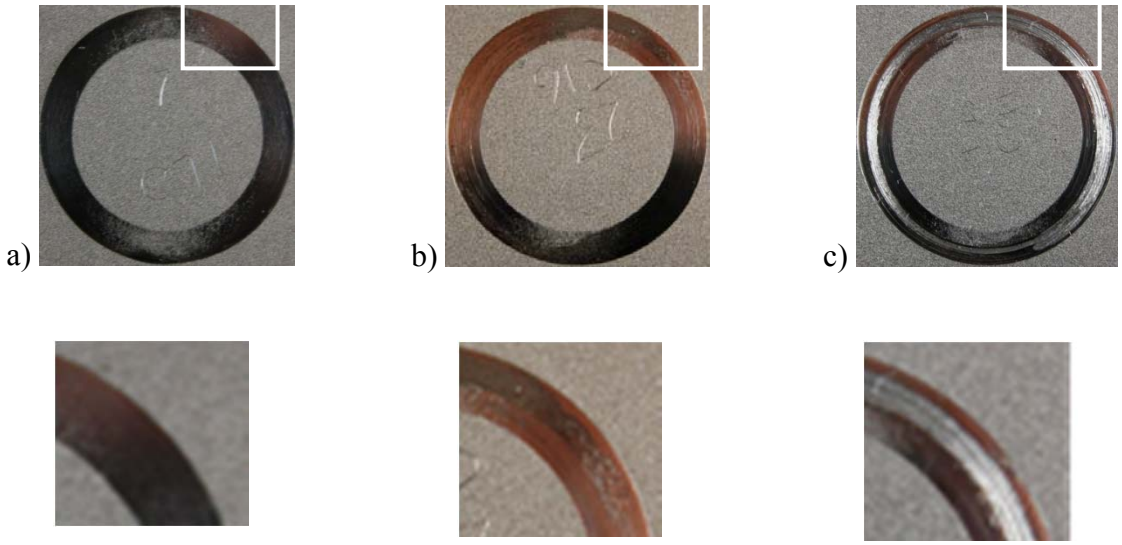

Figure 57: Optical imaging of contact area (a.) pre-failure, (b.) early failure, (c.) late failure. There is no obvious damage in a) despite high % real to apparent contact area, (b.) shows signs of scuffing and (c.) shows heavy metal transfer (light band in dark region).

5.2.2. Scanning Election Microscope (SEM)

The SEM is a valuable tool for tribological investigations. It allows the contacting surfaces of the post-test specimens to be examined at an appropriate scale and depth of field that is most relevant for understanding wear mechanisms (millimeters to microns) that are not possible with optical microscopy. However, the considerable specimen preparation and high cost of machine time limit the analysis to confirming optical microscope analyses. An SEM equipped with elemental analysis (EDX) provides an opportunity to confirm the origin of adhered particles observed with the optical microscope.

The specimens of the TCT were designed to fit into the vacuum chamber of an SEM so that the risk of damage during specimen preparation would be reduced.

One drawback with the conventional SEM is that it operates under high vacuum and surfaces must be thoroughly cleaned otherwise oils will darken and volatize.

It is critical that the TCT test is terminated at the point of interest otherwise the specimen surface does not correspond to the measured test data. Examination of sheet specimens from the extended testing study show the changes in the cold-rolled sheet surface.

The as-received texture of the sheet (imparted by the ground and shot-blast rolls) is seen in Figure 59A. After sliding contact and prior to failure (Figure 59B), the contact area is smooth

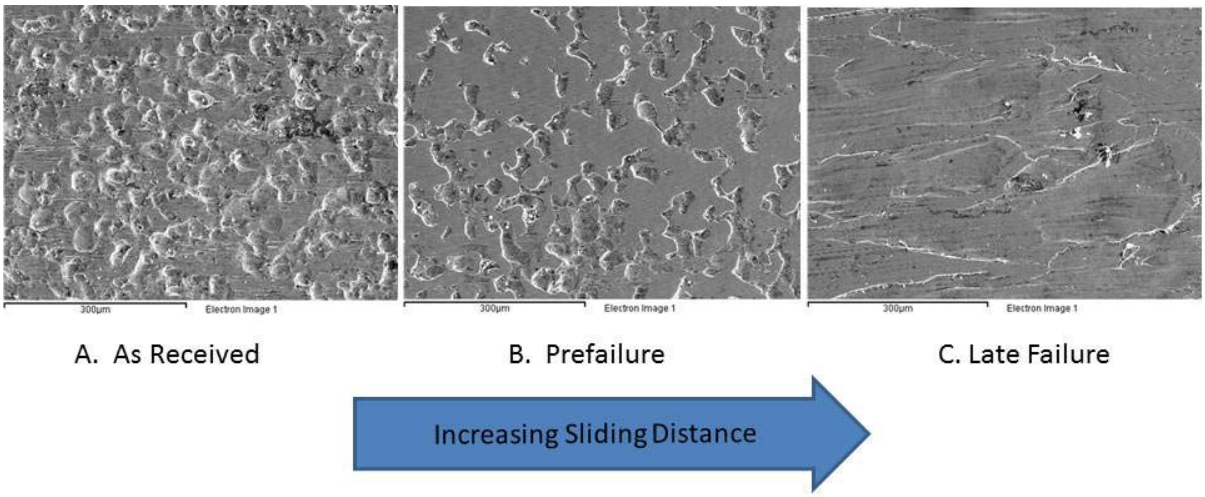

Figure 58: Sheet surface a) As-rec'd, b Pre-failure (note: burnishing and lubricant pockets), C. Late adhesive failure (smearing of surface). Cold-rolled sheet with low viscosity lubricant.

and isolated lubricant pockets are seen. These pockets are excellent reservoirs for pressurized lubricant. Figure 59C. shows the surface after failure. The lubricant reservoirs are gone and the

surface is roughened and smeared (particles and feathered edges are seen), a consequence of metal transfer to and from the annular tool (shown in the next section).

5.2.3. Energy Dispersive X-Ray Spectroscopy (EDX)

Energy Dispersive X-Ray spectroscopy measures X-rays released from a surface resulting from of an incident beam of electrons directed at the surface.

The spectra shown in Figure 60 illustrate the effectiveness in identifying the presence and source of adhesive wear particles on a surface. The peaks in the spectrum (Figure 60b) show the elements present where there is an absence of adhered particles on an annular tool (Spectrum 1). These elements correspond well to the AISI D2 tool steel published composition specifications [92, 93] as shown in Table 10. Analysis of the adhered metal particles (Figure 60 c.) show a predominance of iron and very little of the D2 alloying elements (V and Cr). The x-rays emitted from the surface represent the composition of the particle. Since these x-rays are generated at a depth of about 2um [94] analysis of thin adhesion layers may include elements in the substrate. The presence of trace chromium in the particle analysis (Spectrum 2) is thought to originate from the underlying substrate.

a.

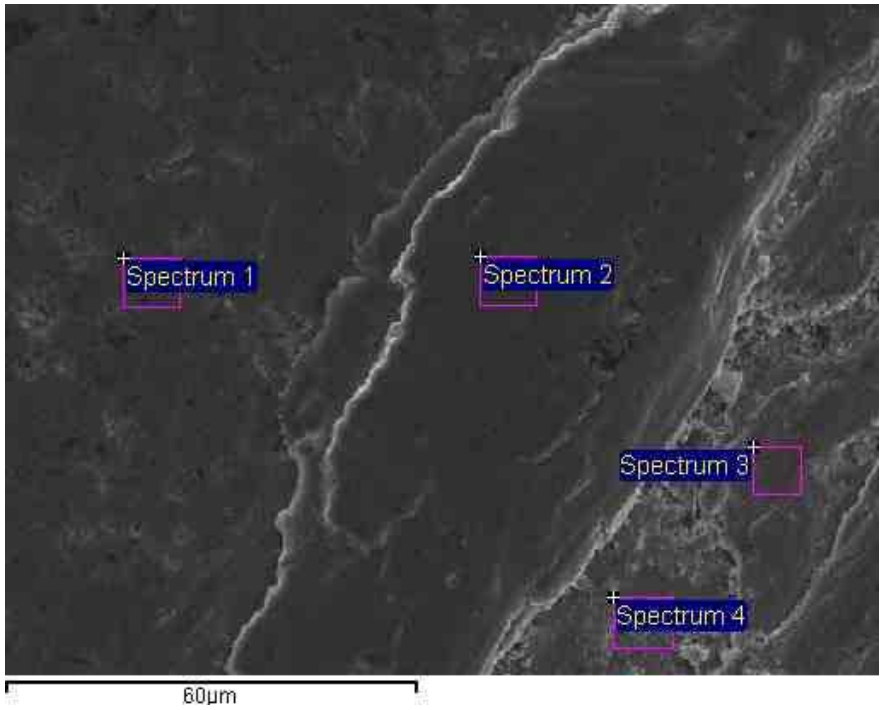

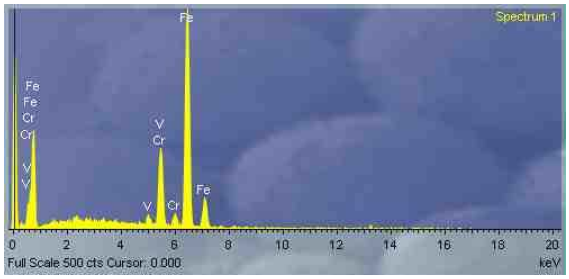

b.

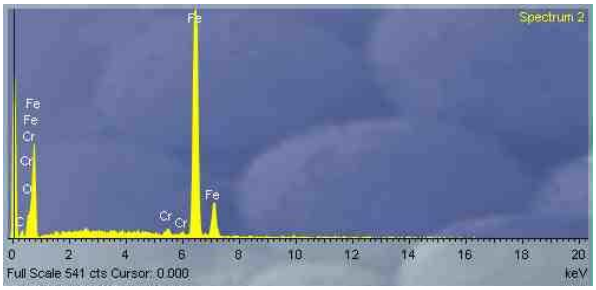

c.

Figure 59: EDX analyses of an annular (D2 tool steel) specimen with corresponding spectra for the bare tool steel (b. Spectrum 1) and mild steel adhesion particles (c. Spectrum 2)

Table 10: Typical Elemental Analysis of the Sheet and Annulus

Sheet: AISI 1008 *(weight %, balance iron)* [92]

C	*Mn*	*P*	*S*
0.10max.	*0.30-0.50*	*≤0.040*	*≤0.050*

Annulus: AISI – D2 *(weight %, balance iron)* [93]

C	*Mn*	*Si*	*Cr*
1.50	*0.50*	*0.30*	*12.00*
Mo	*V*	*Fe*	
0.80	*0.90*	*84.00*	

5.3. Reliability of Transmitted Torsional Signal Amplitude as Indicator of Lubricant Failure

While Figure 47 shows how the transmitted torsional signal amplitude mirrors the evolution of adhesive wear for one lubricant additive at one viscosity (ELV), it does not indicate the reliability of transmitted torsional signal amplitude to indicate differences in adhesive wear between different lubricant formulations. Figure 61 shows that all lubricants tested exhibited an increase in transmitted torsional signal amplitude as they reached boundary lubrication. In the absence of anti-adhesive wear additives, the transmitted torsional signal amplitude increased dramatically. With the formulated lubricants the change in transmitted torsional signal amplitude varied. It appears from comparison of the transmitted torsional signal and transmitted torsional signal amplitude curves that transmitted torsional signal amplitude is an effective indicator of the activation and exhaustion of lubricant additives can be inferred using this response (Figure 61).

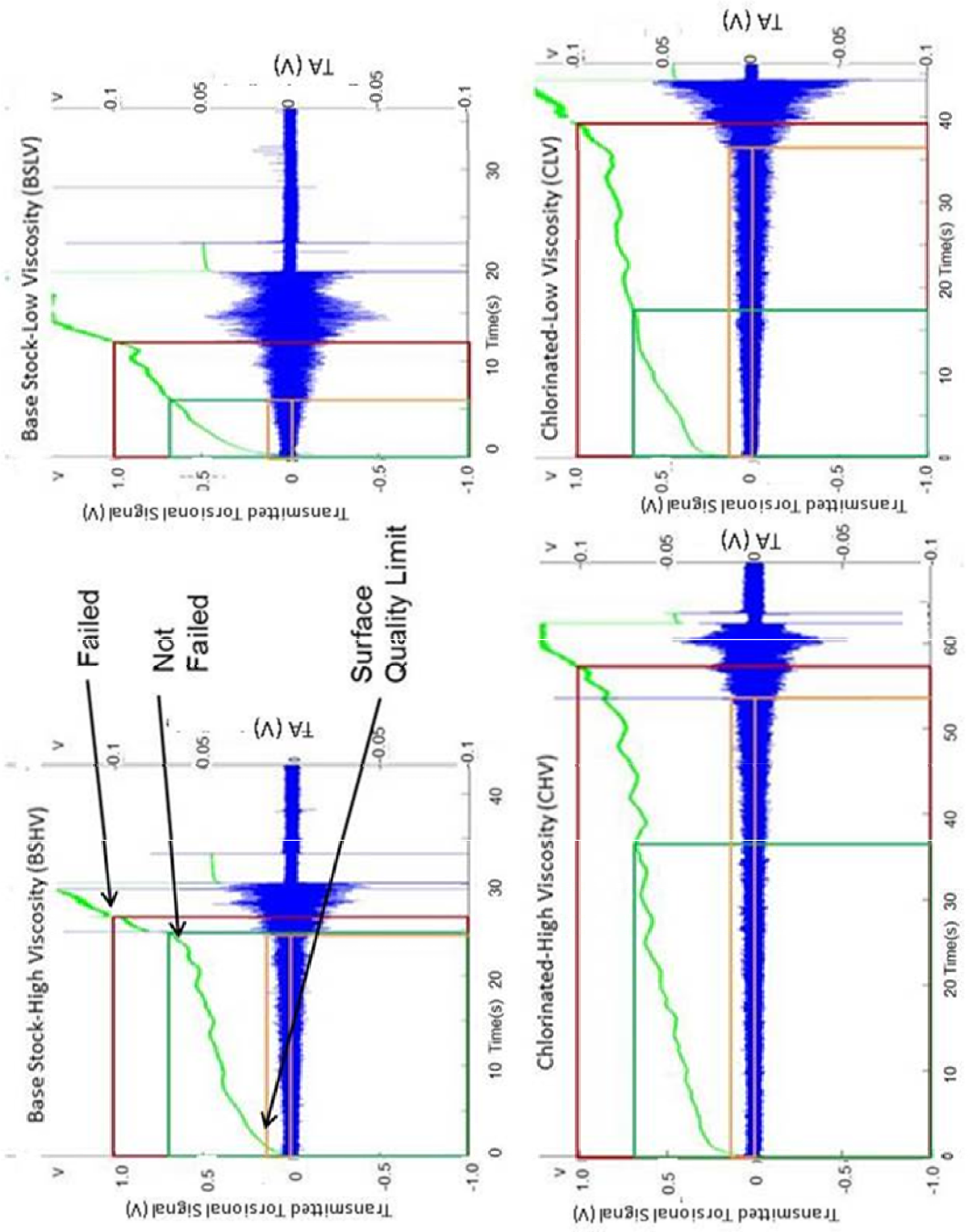

Figure 60: Comparing Viscosity and EP additive effect with Transmitted torsional signal and Transmitted torsional signal Amplitude (TA). The extension of the orange box (limit = 0.0125 V) with the CHV and CLV shows the effect of the EP additive (chlorinated paraffin) on adhesive failure.

Transmitted torsional signal threshold values of 0.7 V and 1.0 V are shown for comparison. The TA limit of 0.0125 V corresponds to the 0.7 V threshold of the unformulated lubricant and the 1.0 V threshold of the EP formulation.

Chapter 6

6. Discussion and Conclusions

In this chapter the analyses of the data from the main and extended studies are discussed in the context of providing a solution to the problem outlined in earlier chapters. That is, what measures will improve the process for identifying adhesive failure during lubricant evaluation? This discussion involves examining the process of adhesive failure and then assesses how the tribotest responses relate to that process.

6.1. The Catastrophic Adhesion Mechanism

Perhaps the most important part of this discussion is to arrive at a basis for evaluating anti-adhesive wear strategies. In an ideal world the best strategy to avoid adhesive wear is to maintain separation of the surfaces. In this "ideal" case, failure would be measured by initial contact of the two surfaces. Unfortunately in many industries surfaces come into direct contact with each other leading to opportunities for adhesive wear. The situations where surfaces contact are often not part of the engineering design since they occur outside of the operating parameters. An exception to this is metal stamping where during the normal course of the process the surfaces come together unless separated by a physical barrier such as a polymeric film. These surfaces invariably suffer some damage as a result of this contact.

Realistically a new definition of failure must be based on the degree of damage caused by adhesive wear. Hence, our discussion starts where the ideal world ends:

> *"In normal running the surface roughnesses that break through the film and interfere with each other are protected by a layer of surface active molecules. In oils these molecules are obtained from materials existing in the oils*

> *themselves. In extreme conditions the naturally occurring oil molecules no longer protect the surfaces and agents having more endurance have to be added to the lubricant. The extreme conditions are almost exclusively produced by high temperatures. Pressure (or load) by itself is of very little consequence. Once this protective layer of molecules vanishes the chance asperity contact causes welding, leading to the destruction of the whole system."* *A. Cameron* [95]

The initial contact of two lubricated sliding surfaces at some relative velocity means that the normal load is borne by only the tallest asperities. The very high stress causes particles to detach from the asperity tips of the softer material as junctions form and fracture. As Cameron noted, the formation of these junctions is the onset of failure. And, since the junctions form very early on with the contact of the tallest asperities, failure should be defined in real world rather than absolute terms.

Initially adhesive debris particles are often 1μm or smaller and may adhere to the asperities of either surface or act as a 3rd body interacting with the two main surfaces until they find refuge in a valley (Figure 62a) or are transported to the edge of the contact.

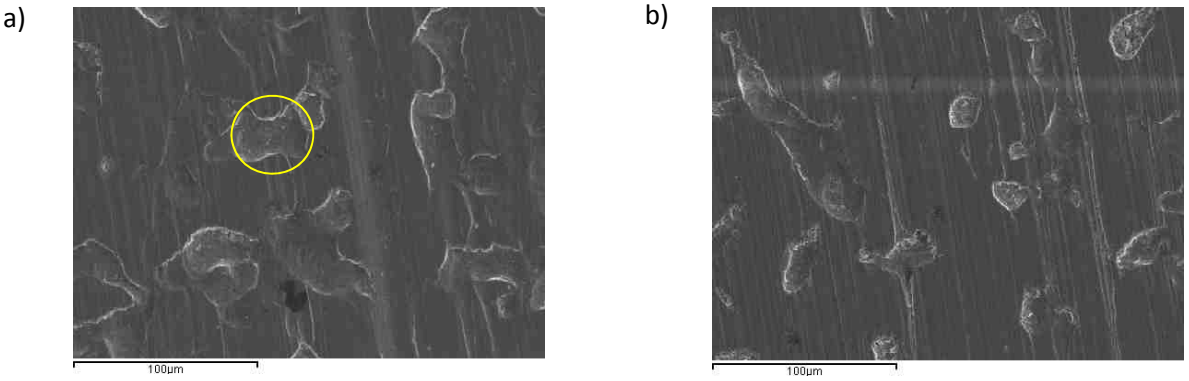

Figure 61: a) Small particles can be seen in the valleys of the lightly contacted sheet; b) The valleys are sealed and the pressurization of the lubricant in these pockets supports the normal force hence reducing stress.

The small wear particles that adhere to the surface have minimal impact on increasing the magnitude of the friction force; however the energy that is required to shear the junctions is

reflected in an increase in oscillations of the friction force [96]. This is an important point and is discussed later in the context of defining adhesive failure.

If the surface texture is optimal, pressurized lubricant pockets form between the load bearing plateaus of the softer surface (Figure 62 b) and friction is stable. (Figure 41, p81) [97, 98]. However, the stability of the level of friction is tenuous and depends on the nature of the contact. The newly formed plateaux, being nascent surfaces, are highly reactive and large scale adhesion is inevitable without a barrier. Fortunately the lubricant reservoirs provide a source of lubricant additives that are carried into the contact by the sliding motion where they may form tribofilms such as metallic soaps [99]. When continued sliding has exhausted the additive supply or surface temperatures are above the melting point of the tribofilm, the small adhered particles may agglomerate on one or both surfaces to form new asperities. At this point one of two things is probable:

1. These new asperities are now the highest peaks and either deform, delaminate or, if they form on the harder surface, plow the plateaux of the softer surface. The process of agglomeration, plowing and delamination of particles results in an increase in surface temperature and a variation in the friction force know as stick-slip [100]. In stick-slip the magnitude of the friction amplitude change is governed by many factors including the size of the adhered particles and the strength of the bond to the parent surface. When the accumulated damage exceeds the surface quality required by the process or impedes the movement of the surface then catastrophic adhesion has occurred.

2. Alternatively, as the size of the adhered particles increase, contact stress and flash temperatures increase there is the potential for forming halides, phosphides, or sulfides with

EP additives in the lubricant [101]. These anti-weld compounds interfere with the adhesion process by creating contaminant reaction products that prevent welding thus delaying catastrophic adhesion.

6.2. Identifying Lubricant Failure

The formulation of lubricants for specific applications requires a real world failure criterion that matches the conditions of failure in the application of interest. Some processes, such as the forming of stainless steel kitchen sinks, tolerate some scoring or scuffing as long as the adhesive wear damage does not exceed the depth of surface finishing (Figure 63). Adhesive wear damage, beyond the depth able to be removed by surface finishing, results in the sink being scrapped.

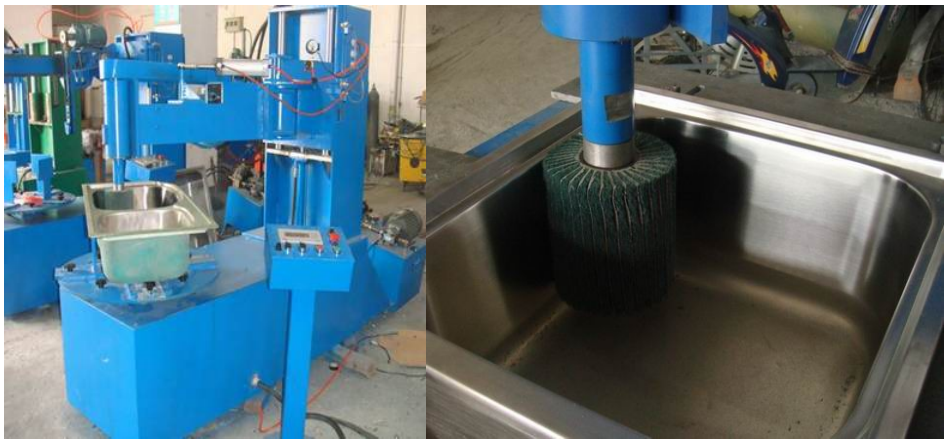

Figure 62: Grinding of the inside of a deep drawn stainless steel sink [102]

Other processes may be more or less sensitive to surface damage so it is important that the formulation chemists interpreting tribotest results have an understanding of the degree of damage that is tolerable in the process of interest.

6.3. Tribotest Responses as Indicators of Lubricant Failure

This section compares the experiment responses that were the focus of this study to the *status quo* (transmitted torsional signal threshold) and their potential to improve the evaluation of lubricant formulations in the TCT.

6.3.1. The Limitations Of The Magnitude Of Friction

The lubricants examined in this study represented a variety of formulations at two viscosities. In these experiments viscosity clearly had a powerful effect on the magnitude of friction (transmitted torsional signal). The reduced transmitted torsional signal levels gave no indication of the ability of the lubricant to resist adhesive wear. This was seen in the superior performance of low viscosity formulations at resisting adhesion over the high viscosity base stock (Figure 45, p. 91).

This was also observed by Bowden and Tabor:

> *"...substances which give the same coefficient of friction are not necessarily equally efficient as lubricants"* 103]

The data and analyses show that the magnitude of the friction force changes considerably during testing (Figure 48). These levels may correlate to the different lubrication regimes, in particular, mixed-film and boundary lubrication (Figure 41). After lubricant depletion the film thickness is zero and the regimes as defined by the Stribeck curve (Figure 14) are no longer valid. At this point the level of friction is governed by the shear strength of either tribofilms on the surfaces or the underlying substrates at asperity junctions. As these levels change the friction force which in some cases will be lower when the substrate fails. Trying to identify lubricant failure based on the magnitude of friction in real time is not reliable.

6.3.2. Vibration

Vibration signal response in both the normal and radial directions gave indications of lubricant failure increasing in amplitude with the progression of adhesive wear. The radial vibration signal was more sensitive than the normal vibration signal; however, the amplitude increased with the observed adhesive wear but only up until scuffing in 2/3 of the cases.

The radial vibration signal response (amplitude) generally correlated to the various levels of the transmitted torsional signal threshold 0.7V corresponding to pre-failure, 0.8V corresponding to early failure, and 1.0V corresponding to late failure (Figure 64).

The radial vibration signal limits were conservatively set at values that would ensure the worst case scenario for the pre-failure and early failure did not exceed the time to failure based on the transmitted torsional signal for these categories. The vibration signal response has much greater variability for the pre-failure and early failure and appears to saturate as adhesive wear increases with only a few late failure tests reaching an amplitude greater than 0.025V. While radial vibration signal may appear to be inferior to transmitted torsional signal threshold as an indicator of lubricant failure it may be useful as an indicator of adhesive failure in cases where measuring transmitted torsional signal is not practical. The placement and isolation of the vibration sensors on the TCT could be refined to improve the signal-to-noise ratio.

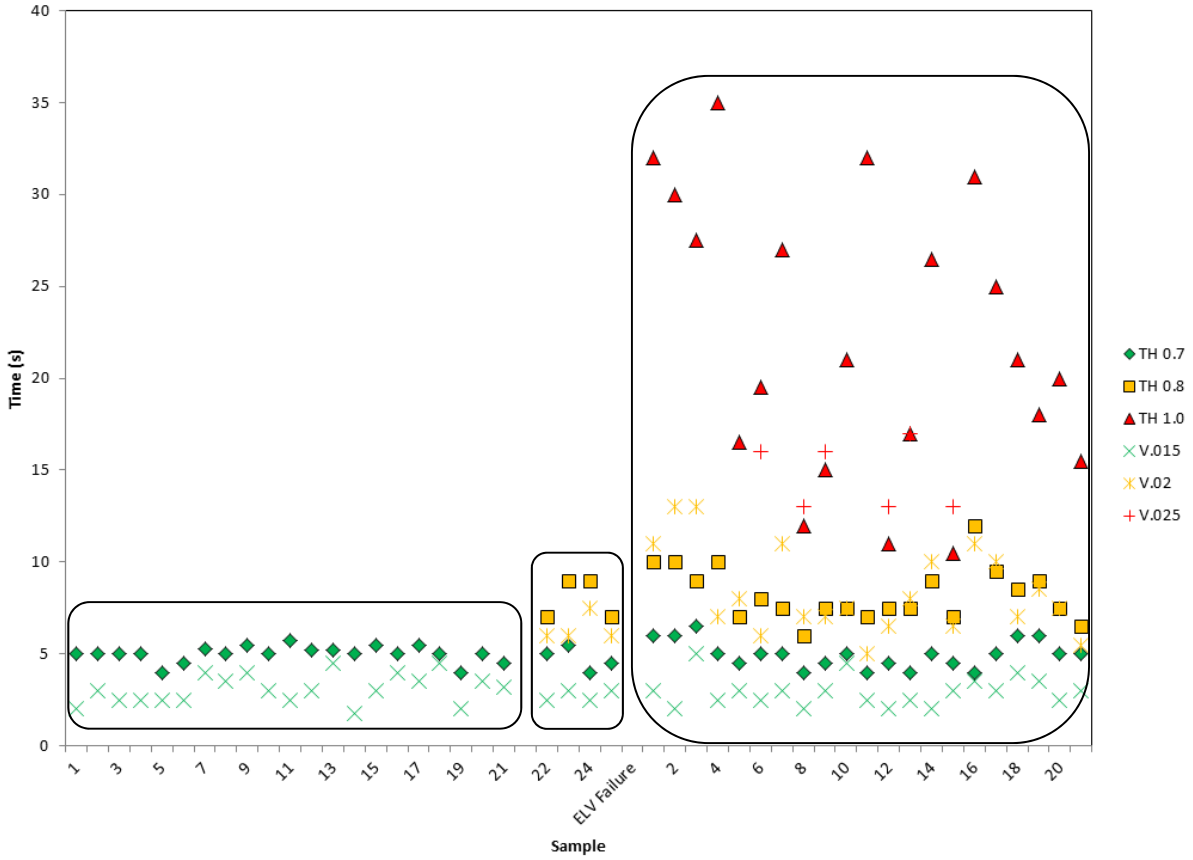

Figure 63: Chart showing transmitted torsional signal threshold (solid symbols) and radial vibration signal amplitude values corresponding to no failure (green), scuffing (yellow), and catastrophic adhesion (red).

Note: ELV – 1- 21(on left) tests stopped just prior to failure, 22-25 tests stopped at the first sign of failure, and 1-21(on right) tests stopped only after obvious failure.

6.3.3. Electrical Resistance

Other researchers have reported promising results using electrical resistance as a measure of lubricant failure. These studies were not conducted at the severity of the conditions encountered in this study. Electrical resistance proved to be ineffective in measuring contact severity saturating shortly after full contact pressure was achieved during mixed film lubrication. Experimental results show that electrical resistance proved to be a poor indicator of lubricant performance in boundary lubrication. Spikes observed during boundary lubrication were

attributed to momentary separation during stick-slip. In their seminal work, Bowden and Tabor reported in 1950:

> *"Thus electrical resistance measurements provide a very sensitive means at discriminating between complete fluid lubrication and the smallest amount of metal contact. The main disadvantage is that it does not make a clear distinction between metallic contact and the contact between metallic surfaces covered with boundary films."* [104]

6.3.4. Acoustic Emission

AE signals are useful in detecting momentary contact between surfaces where asperity contact generates a burst of energy. In the presence of plastic deformation these asperity interactions are superimposed on a continuous level of energy that accompanies plastic deformation [105]. In the TCT where massive plastic deformation occurs during the progression to catastrophic adhesive wear, the severity of asperity contact is lost. The number of contacting elements (asperities) is large and continually changing as asperities flatten and adhesive wear particles form. Determining adhesive failure from AE data is complex and will require a thorough sensitivity analysis to prove the effectiveness of the technique. For the purposes of this study AE does not hold the promise of transmitted torsional signal amplitude or radial vibration signal in achieving improvement over current practice (transmitted torsional signal threshold).

6.3.5. Transmitted torsional signal (Friction) Amplitude

Extended tests for one lubricant condition (Low Viscosity Ester, ELV) indicate that indeed adhered particle size and resulting adhesive wear damage correlated well to transmitted torsional signal amplitude. Esters are the reaction products of organic acids and alcohols. They are thermally stable (Figure 17, p36) and some varieties (e.g. polyglycols) impart a viscosity boost at

the interface by separating from water. They also deliver EP additive properties to the contacting surfaces [106].

As the surface of the softer sheet steel deforms under the combined normal stress and shear stress the lubricant undergoes changes that are reflected in both the magnitude of friction (transmitted torsional signal) and amplitude of this signal. The magnitude of the transmitted torsional signal is a composite term and therefore identifying adhesive failure of the sheet surface is difficult. Increases in transmitted torsional signal may be due to the formation of a high shear strength molecular layer or an increase in plowing. The amplitude of the transmitted torsional signal is characteristic of particles welding and breaking loose. As the lubricant becomes depleted these events become more severe and less predictable.

Following the simple adhesion theory of friction developed by Bowden and Tabor [107] where the force resisting sliding (f) for most metals is composed of an adhesion term and a plowing term. ($f= A \tau + p$) where A is the real area of contact, τ is the critical shear stress and p is the resistance of the softer material to plowing by the asperities of the harder surface. The plowing term is ignored for light to moderate contact (where plowing is much smaller than adhesion) and so the friction force can be expressed as $f=A\tau$ and since the coefficient of friction is $\mu= f/N$; thus $\mu= \tau /\sigma$; where σ is the yield stress of the material. For most metals this ratio is 1:5 or $\mu=0.2$. This is the maximum friction before plowing becomes significant.

The friction threshold of COF = 0.2 as an indication of catastrophic lubricant failure is recommended to TCT users as a means of reducing bias in comparing lubricant performance (note that in this study a transmitted torsional signal of 1.0V equates to a COF of 0.2). However, as Halling points out: this simplified friction model does not take into account the effect of

combined stresses reducing the critical flow stress and the effect of contaminant films on the critical shear stress [108] . We must therefore be cautious in the use of the friction threshold method for determining catastrophic adhesive failure.

Going back to the mechanism of adhesion discussed at the start of this chapter, if it is assumed that the amplitude of the transmitted torsional signal is an indicator of the degree of adhesive wear, then for a given contact couple and lubricant it is possible to identify the failure of a lubricant to protect against adhesive wear with just the transmitted torsional signal amplitude.

6.4. Post-Test Confirmation Of Failure

It was shown in the previous chapter (Section 5.2) how post-test analyses such as optical microscopy, SEM (Figure 65), and EDX are necessary to confirm that adhesive failure has occurred and how it is critical to stop the test at the moment of interest to preserve the surfaces at that time. The complexity of tribotesting and the nature of adhesive wear dictate that post-test analysis is necessary especially when working with unfamiliar materials or lubricants.

Two analytical tools were used on a very limited basis to assess their capability to be used to evaluate adhesive wear. The two tools were Scanning White Light Interferometry (SWLI) and Attenuated Total Reflectance spectroscopy (ATR). The following sections report on the use of these tools to analyze adhesive wear on metallic surfaces.

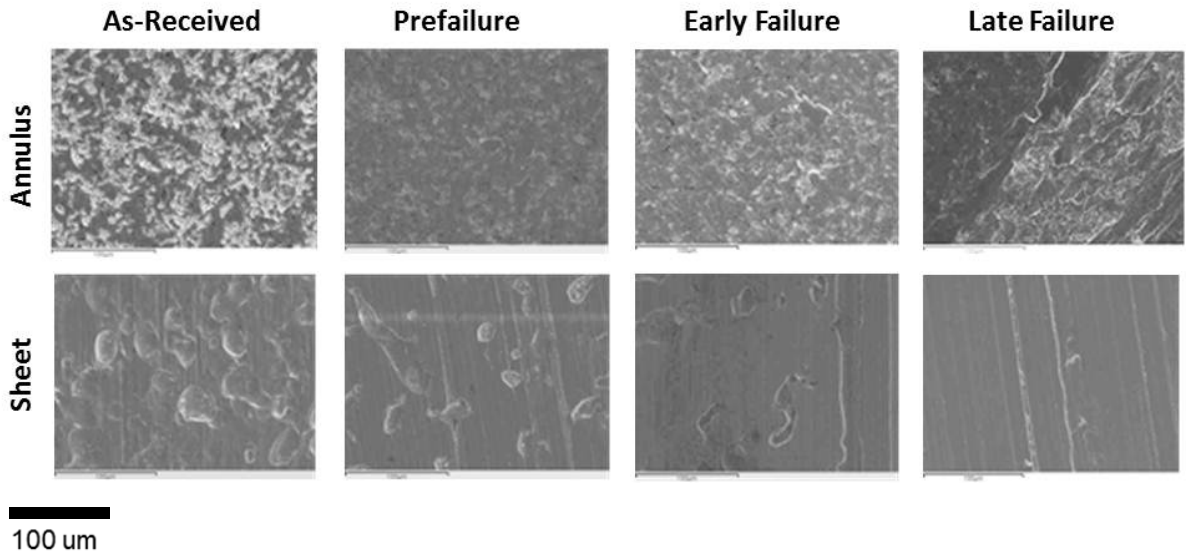

Figure 64: SEM photographs of annulus and sheet specimens for the Extended Study

6.4.1. 3D Surface Imaging With Scanning White Light Interferometry (SWLI)

The quantification of surface roughness has improved dramatically over the past 20 years with the development of 3D, non-contacting, scanning techniques. The technique of interferometry involves the splitting of a beam of achromatic light into a sample beam and a reference beam and thus producing interference fringes when the path of the sample beam differs from the reference beam [109]. 3D Surface SWLI imaging equipment uses this principle to provide very high vertical resolution over a broad sample area. Even broader samples can be scanned using stitching techniques.

Not only can general roughness parameters (as described in section 2.2.6.2) be determined but 2D profiles can be positioned to reveal individual surface features. The technique described here would use the 2D profile to quantify lubricant failure where an individual feature exceeds quality limits for a particular process (Section 6.2).

A Zygo ZeScope was used to examine Extended Study specimens before and after testing to reveal changes to the surface topography. A 3D map was generated from non-contacting surface scans. 2D profiles were determined radially across the width of the annular track using a wave filter of 0.25 mm and a stylus filter of 1.0μm.

The roughness profile of the lapped annular tool (D2 R_c 61) is shown in Figure 66a with the roughness profile of the as-received sheet (upper left) shown next to a burnished area (lower right) in Figure 66b. The tallest asperities (peak-to-valley height) of the sheet are about five times taller than those of the annular tool (note the different scales on the profiles). The 2D profile below the 3D map shows the complete flattening of the surface in the burnished zone where the average sheet roughness (Ra) is reduced to that of the annular tool. The deep lubricant

reservoirs of the as-received sheet are gone and without lubricant replenishment adhesive failure is imminent. Figure 66c reveals the wear track of the annulus on the sheet at the onset of adhesive failure. Pieces of the sheet surface are being ripped out when they weld to the harder annular tool surface and are removed during further sliding where the reattach to the sheet surface.

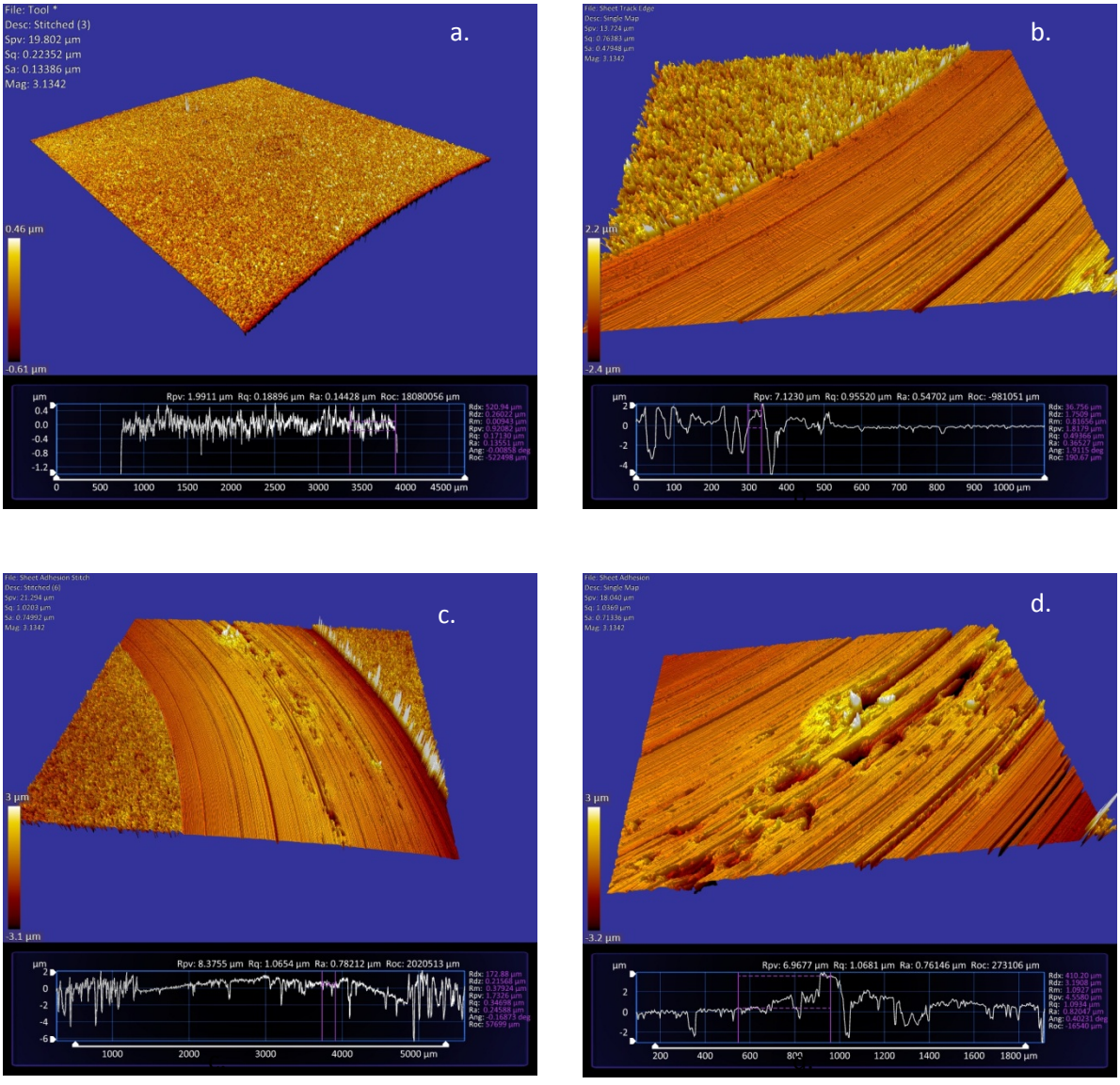

Figure 65: Surface profile map using white light interferometry: a. Lapped annular tool; b. Prefailure burnished and light scoring; c. early failure – scuffing; and d. late failure. Note: Calibration - NIST SRM2073a (Sinusoidal 3 -100)

Figure 66d shows the protuberances typical of catastrophic adhesive wear (galling) on a sheet specimen from late failure extended test. They are caused by pieces of sheet material detaching from the annular tool surface and reattaching to the sheet. The 2D profile in 66d shows the height of one protuberance to be about 4.5μm above the burnished surface and as such and the normal force is carried on by these points leading to higher stress and more adhesive wear. The size of these protruberences is reflected in the increase in the transmitted torsional signal amplitude response from prefailure to late failure. (Figures 48-50)

When the entire contact area is populated by a few of these protuberances, oscillation of the sheet specimen in the self-aligning holder is seen in the friction force curve The period of this oscillation is usually the same as the speed of rotation. The periodic oscilation of the transmitted torsional signal curves coincides with the observed adhesive wear in the SEM and SWLI corresponding to “Early failure” and “Late failure” seen in Figure 66c-d.

6.4.2. Attenuated Total Reflectance Fourier Transform Spectroscopy (ATR-FTIR)

Tribologists have theorized about the reaction of chemicals in the lubricant with contacting surfaces during sliding. Cameron wrote of anti-wear and anti-weld properties of lubricants when he identified the blocking of EP additive reactions by oiliness additives at low temperatures. Above a critical temperature sulfur and other anti-wear additives reacted to form protective anti-wear films. When the temperature rose to the point where these films no longer provided protection, the same additives reacted with the freshly exposed surface to form anti-weld compounds such as sulfides, chlorides, and phosphides and thus preventing scuffing [110].

Sheet metal specimens were placed in a Perkins-Elmer ATR-FTIR spectrometer to determine whether the chemical reaction compounds were present on test specimens,. ATR-FTIR has an

advantage over traditional FT-IR techniques because specimen preparation is so much easier and more flexible. The sheet surface was placed in contact with the crystal through which a infrared beam is passed. An evanescent wave is generated by the reflection of the IR beam within the crystal. This wave extends into the sample 0.5μm to 5 μm. When the sample absorbs energy from the wave it is attenuated and the differences from the internally reflected wave can be measured and used to characterize the changes to the IR spectrum [111].

In this study sheet specimens were scanned both with forming oil in place and after cleaning with IPA. Characteristic spectra of the IPA on an untested area of the sheet steel were collected to remove the IR signals of the cleaning residue from the spectrum gathered from the tested areas.

It was found that reacted surface films were more reliably detected with the cleaned specimens than those specimens with the residual forming lubricant. Online IR databases allow analyses of ATR-FTIR Spectra by fitting known substance spectra and synthesizing spectra that match more complex substances [111, 112]. Figure 67 shows such an analysis [112]. The first specimen shows the as-rec'd CRS sheet surface exposed to low viscosity chlorinated paraffin (CLV) but saw no contact with the tool. The spectrum collected from the specimen (Fig 67a. green) is overlaid with a synthesized spectrum (pink) for 10% chlorinated paraffin and 90% mineral oil. Note that the synthesized spectra are flat baseline while the uncorrected experimental spectra are curved.

a.

b.

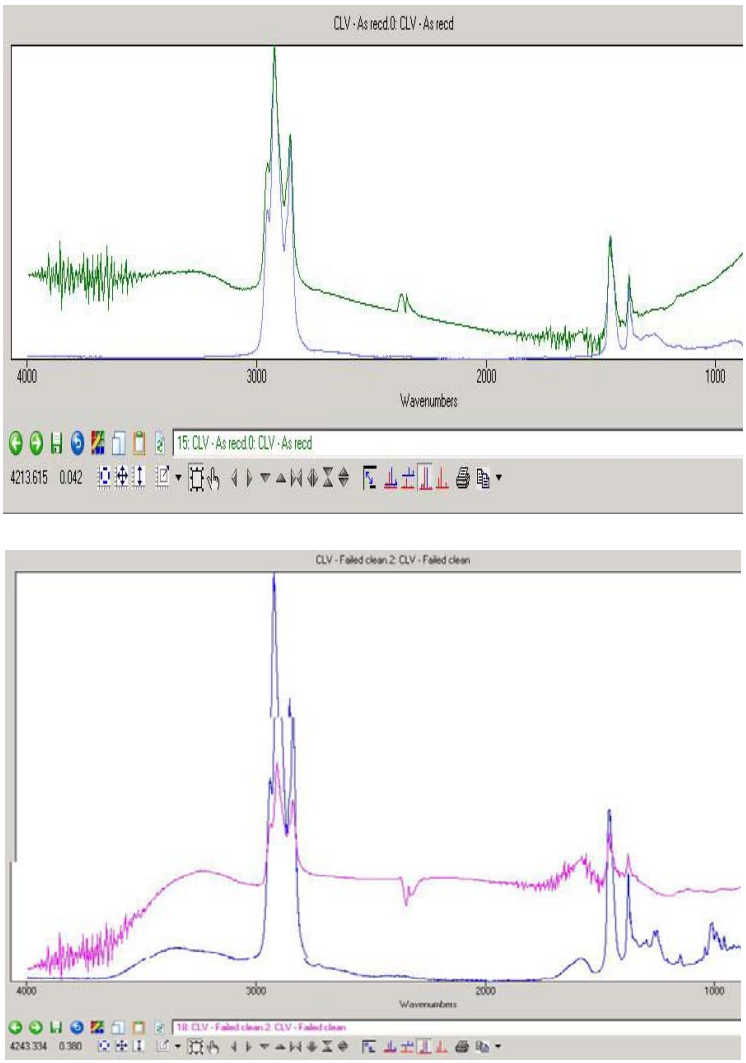

Figure 66 a) ATR-FTIR spectrum for as-rec'd with CLV (green) and synthesized IR spectrum for 90% mineral oil and 10% chloroparaffin (flat); b) ATR-FTIR Spectrum (pink) with synthesized IR spectrum (.8X(.9 min oil +.1 chloroparaffin)+ .2 Iron hydroxide gamma)

The pink spectrum shown in Fig 67b shows the same lubricant (CLV) after TCT testing to failure. The blue spectrum shows a synthesized spectrum of 8% chlorinated paraffin in 72% mineral oil with a 20% iron hydroxide (gamma). The spectra in Figure 68 reveal increasing and decreasing of peaks of several CLV spectra. The different spectra represent different areas of contact from the same test specimen (CLV) that were selected based on severity of contact. The

black peak (lightest contact) and subsequent increasing contact intensity (green, blue) is contrasted to the pink spectrum (as received).

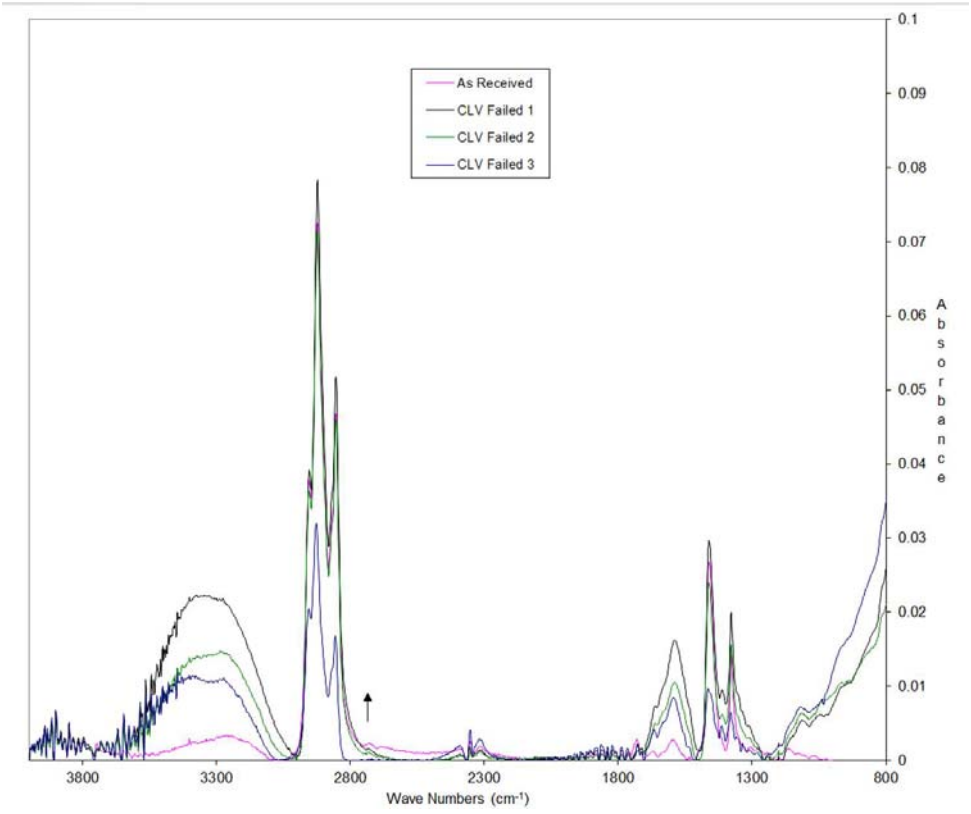

Figure 67: ATR-FTIR Spectra for surface films corresponding to varying degrees of contact on a single test specimen ranging in severity from no contact (As-received) to severe contact (CLV failed 3). The lubricant CLV is a well-known EP additive (chlorinated paraffin).

The differences in spectra peak intensity could be due to real differences in reaction products or could be due to sampling error (i.e. variation in crystal contact force). A thorough sensitivity analysis of this technique would be necessary to validate the use of this technique in identifying lubricant additive activation.

From this limited investigation it appears that the ATR-FTIR spectra can be used to identify the creation and depletion of a chemical species (iron hydroxide) on a surface. This analytical tool

could be used by lubricant developers to better understand how the additives are responding to changing conditions and to better understand interaction between additives in a formulation. Furthermore, ATR-FTIR analysis of actual production parts could be used to verify TCT test conditions and to quantify surface temperatures in forming (based on tabulated activation/deactivation temperature data, Figure 17).

6.5. Extension to a Decision Support System

In this research simple lubricant formulations with matching viscosities were used to reduce complex interactions and conflicting lubrication mechanisms. In real applications lubricant formulations are far more complex and less well-behaved. It is expected that each formulator will develop a knowledge base of lubricant responses correlated to post-test surface analyses with which to train a decision support system to identify lubricant failure in their target market. Lakanen et al showed that the Extended Study data could be successfully used to identify lubricant failure in a DSS [113].

They created five feature vectors from the torque, vibration, and acoustic emission data to find the best method of identifying catastrophic failure. Of the five feature vectors they found that the feature vector made of 3 simple statistical features of transmitted torsional signal data was the most effective in identifying failure (Table 11). A twenty feature autoregression model of the torque data performed the worst. Acoustic emissions showed some promise in identifying failed tests but were less reliable with healthy specimens probably due to background noise and pre-adhesion asperity interaction.

It is important to note that the Lakenen et al study used a failure criterion that allowed more surface damage than would be tolerated in most processes.

The work by Lakanen shows that TCT test data can yield powerful feature vectors for identifying healthy and failed test specimens but it is the identification of a failure criterion that is the most important step in using a Decision Support System as a tool in the evaluation of strategies for reducing adhesive wear.

Table 11: Neural network classification of healthy and failed TCT tests using five feature vectors. [113]

Features	Total Number of Features	RMS error Healthy	RMS error Failed
Acoustic Emission (AE)	13	0.3782	0.2229
Auto-Regressive 20 Model (AR20)	20	0.7363	0.2167
Vibration	4	0.4467	5.0940×10^{-5}
Torque	3	0.0029	2.9289×10^{-5}
Torque and Vibration Features	7	0.0269	6.6471×10^{-7}

6.6. Conclusion

This research tested the hypothesis that a combination of data from various sensors measuring the real-time response of a tribotest provides better detection of adhesive wear than the coefficient of friction alone.

Analyses of the data from a variety of real-time measurements were correlated to post-test analysis of specimens and found to reveal that the real-time data were representative of physical changes to the surfaces such as sheet topography and the extent of adhesive wear particles. These changes governed and were governed by lubricant distribution and chemical reactions on the surfaces.

While the magnitude of the transmitted torsional signal (friction force) is indicative of sheet topography and lubricant regime, the amplitude of the transmitted torsional signal (friction force) is indicative of the size and extent of adhered particles.

SEM and EDX analyses confirmed that damage to the surface by the adhered particles progresses from scoring, to scuffing, to plowing of the softer surface and it is only the last of these stages where damage is reliably indicated by the magnitude of the transmitted torsional force. The amplitude of the transmitted torsional force and the vibration signal of the specimen holder both are superior indicators of the severity of damage to the sheet surface.

Resistance was not effective at indicating adhesive wear and acoustic emissions (AE) were more difficult to relate to the adhesive wear mechanism than transmitted torsional force amplitude or vibration. It is possible that with improved instrumentation and analyses AE would be more effective.

In terms of ease of use both AE and vibration sensors have a significant advantage over force sensors in that they are used in-situ without the mechanical isolation required to measure transmitted torsional force.

The preservation of the specimens at the time of failure is critical to confirm the presence of adhesive wear. The development of a decision support system using an appropriate feature vector of real-time data will be necessary to choose the point of failure and stop the test. While the limited data set examined in this study showed that one response (transmitted torsional force amplitude) was more effective than the status quo in determining lubricant failure, other materials and lubricant combinations may require advanced signal processing and feature extraction techniques in combination with multivariate data representation to gain improved sensitivity of the failure detection DSS.

References

1. http://www.catminestarsystem.com/articles/health-technologies-reducing-unscheduled-downtime , accessed 2013-07-11
2. H. Gurgenci, 2001 –Maintenance Mining Machinery, accessed 2013-07-11 http://www.mech.uq.edu.au/courses/mmme2104/chap11/maintenance.htm
3. J. Schey, *Tribology of Metalworking*, ASM Publications, Metals Park, OH, 1983, pg 96
4. L. Vitos, "An atomistic approach to the initiation mechanism of galling", *Computational Materials Science* 37 (2006) p.193–197
5. Definition: lubricant - *Oxford Dictionary http://www.oxforddictionaries.com/,* accessed 2013-07-11
6. Definition: lubricating – *Oxford Dictionary* http://www.oxforddictionaries.com/, accessed 2013-07-11
7. Definition: surface treatment (finishing) *Wikipedia*, http://en.wikipedia.org/, accessed 2013-07-11
8. US Dept of Education – DSS definition
9. A. Zalounina, "A stochastic model of susceptibility to antibiotic therapy–The effects of cross-resistance and treatment history" *Artificial Intelligence in Medicine* (2007) 40, 57—63
10. E. Stein, "A knowledge-based system to improve the quality and efficiency of titanium melting", Expert Systems with Applications 24 (2003) 239–246
11. M. Pechenizkiy, "Feature extraction for classification in the data mining process", *Information Theories & Applications*, Vol.10, 2010 p.274
12. J. Schey, *Tribology of Metalworking*, ASM Publications, Metals Park, OH, 1983 p.239
13. https://uni.edu/newsroom/unis-abil-to-announce-major-railways-complete-conversion-to-soy-based-grease, Accessed 2014/06/16
14. T. Hakala, Presentation: Nanoparticles *KEM - 31.5530*, 2011
15. Photo: Scoop bucket - ajspecialists.com/scans/line_boring_bucket_eyes.jpg
16. J. Schey, *Tribology of Metalworking*, ASM Publications, Metals Park, OH, 1983 – p 95
17. Y Meged Modeling of the initial stage in vibratory cavitation erosion tests by use of a Weibull distribution, *Wear* 01/2002; 253(9):914-923
18. D.J. Wilkins, Bathtub curve, Accessed 2011-08-15: [http://www.weibull.com/hotwire/issue21/hottopics21.htm]
19. N. Runciman, N. Vagenas, " Maintenance characteristics of mobile mining equipment at Falconbridge Strathcona mine", *Mine Planning and Equipment Selection 1995*, Singhal et al (eds), Blakerna, Netherlands, 1995
20. K-H., Zum Gahr, *Microstructure and Wear of Materials*, Elsevier, 1987

21. G. Deiter, *Engineering Design*, McGraw-Hill, 1983, p. 267

22. C. Poli, "Design for Stamping: a Group Technology-based Approach", *Concurrent Engineering* December 1993 1: 203-212,

23. C. Walford, "Wind turbine reliability: understanding and minimizing wind turbine operation and maintenance costs" Sandia Report: SAND2006-1100 Printed March 2006

24. J. Ribrant, L. Bertling, "Survey of Failures in Wind Power Systems With Focus on Swedish Wind Power Plants During 1997–2005", *IEEE Transactions on Energy Conversion* 04/2007

25. I.R. McColl, et al "Lubricated fretting wear of a high-strength eutectoid steel rope wire, *Wear* Volume 185, Issues 1-2, June 1995, p. 203-212

26. L. Grabill, J. Malkowski, "Pressurized lubrication system", US Patent 4,368,802, 1983

27. V. Reddy et al. "Analysis of rail wear data for evaluation of lubrication performance" *Proceedings Austrib 06 - International Tribology Conference*, Brisbane, 2006

28. *Aviation Investigation Report A09A0016* Main Gearbox Malfunction / Collision With Water Cougar Helicopters Inc. Sikorsky s-92a, C-GZCH St. John's, Newfoundland and Labrador, 35 NM E 12 March 2009

29. F. Capra, *The Science of Leonardo*, Doubleday, 2007

30. Early friction models: www.tribology-abc.com, accessed 2011-09-15

31. http://www.engineershandbook.com/Tables/frictioncoefficients.htm, accessed 2011-09-16

32. F. Bowden, D. Tabor, *The Friction and Lubrication of Solids*, Clarendon Press, Oxford, UK, 1950, p. 87

33. Ibid, p.88

34. Ibid, p.88

35. Ibid, p.89

36. G. Dalton, Proceedings of the IDDRG Biennial Congress, Ann Arbor, MI, 2000

37. G. Dalton, unpublished report

38. G. Dalton, "Improving The Effectiveness Of Tribotests By Identifying Lubricant Failure Features", *Proceedings of the ASME/STLE International Joint Tribology Conference*, IJTC2009-15074, 2009

39. A. Valkonen, "Oil film pressure in hydraulic journal bearings", Doctoral Dissertation. Helzinki University of Technology, TKK Dissertations 196, Espoo 2009.

40. J. Schey, *Tribology in Metalworking: Friction, Lubrication, and Wear*, ASM, Metals Park, Ohio 1983, p. 32; p.102-4

41. F. Bowden, D. Tabor, *The Friction and Lubrication of Solids*, Clarendon Press, Oxford, UK, 1950, p.91-5

42. J. Schey, *Tribology in Metalworking: Friction, Lubrication, and Wear*, ASM, Metals Park, Ohio 1983, p. 32

43. Ibid p. 50

44. http://www.metalformingfacts.com/fluids/extreme-pressure-additives.html accessed 2011/11/27

45. A. Cameron, *Basic Lubrication Theory*, Longman Group, 1970, p.171

46. ibid, p.173

47. ibid, p.173

48. J. Schey, *Tribology in Metalworking: Friction, Lubrication, and Wear*, ASM, Metals Park, Ohio 1983, p.105

49. D. Markov, D. Kelly, "Mechanisms Of Adhesion-Initiated Catastrophic Wear: Pure Sliding", *Wear* 239, 2000, p189-210

50. H. Yoshizawa, et al. "Recent Advances In Molecular Level Understanding Of Adhesion, Friction, And Lubrication", *Wear* 168, 1993, pp161-166

51. J. Kumpulainen, "Factors Influencing Friction And Galling Behavior of Sheet Metal", *Proc. 13th Biennial Congress IDDRG*, , 1984, pp. 476-490

52. J. Schey, *Tribology in Metalworking: Friction, Lubrication, and Wear*, ASM, Metals Park, Ohio 1983, p.547

53. "Surface Texture – ANSI B46.1-2002," Published by ASME

54. ASME B46 Committee on Surface Texture Panel Discussion, IJTC 2012

55. T.Vorberger, J. Raja "Surface Finish Metrology Tutorial" NISTIR 89-4088

56. SAE J911-1998 Cold Rolled Sheet Steel, SAE Standard

57. J. Schey, *Tribology in Metalworking: Friction, Lubrication, and Wear*, ASM, Metals Park, Ohio 1983, p.107

58. A. Cameron, *Basic Lubrication Theory*, Longman Group, 1970, p173

59. J. Halling, *Principles of Tribology*, MacMillan Press Ltd, 1975, 119

60. A. Berman, *Origin and Characterization of Different Stick-Slip Friction Mechanisms*, Langmuir 1996, 12, p4559-4563

61. G. Fox-Rabinovich, et al., Physical and Mechanical Properties to Characterize Tribological Compatibility of Heavily Loaded Tribosystems (HLTS), in *Self-Organization During Friction*, G. Fox-Rabinovich, G. Totten eds. Taylor & Francis, Boca Raton, FL, 2007, p.127

62. J. Schey, *Tribology in Metalworking: Friction, Lubrication, and Wear*, ASM, Metals Park, Ohio 1983, p. 39

63. *Definition:galling*, G40-10, ASTM G02 standards, Volume 03.02, ASTM International, W. Conshohocken, PA, 2011

64. T. Donaghy, Innovation to Benefit Our World, Our Environment, and Our Future, *Tribology and Lubrication Technology*, Nov 2010, p 36.

65. J. Schey, in Proc. *4th Int. Conf. Production Engineering, Jpn. Soc. Prec. Eng.* Toyko, 1980, pp.102-115.

66. J. Schey, A Critical Review of the Applicability of Tribotesters to Sheet Metal working, *SAE 970714*, 1997

67. B. Podgornik, et al. Comparison Between Different Test Methods For Evaluation Of Galling Properties Of Surface Engineered Tool Surfaces, *Wear 257* (2004) 843–851

68. J. Schey, *Tribology in Metalworking: Friction, Lubrication, and Wear*, ASM, Metals Park, Ohio 1983, p.208

69. P. Blau, *Friction and Wear Transitions of Materials*, Noyes Publications, 1989

70. U. Wiklund, I. Hutchings, Investigation of surface treatments for galling protection of titanium alloys, *Wear 251* (2001) 1034-1041,.

71. G. Dalton, New Friction Model for Sheet Metal Forming, *SAE 010081*, 2001

72. TribSys TCT Instruction Manual, 2005

73. J. Schey, *Tribology in Metalworking: Friction, Lubrication, and Wear*, ASM, Metals Park, Ohio 1983, p 15

74. G. Dalton, "Effect of Bead Finish on Friction in the Drawbead Simulator", MASc Thesis, U Waterloo, 1991

75. J. Schey, *Tribology in Metalworking: Friction, Lubrication, and Wear*, ASM, Metals Park, Ohio 1983, p 59

76. ibid, p.78

77. O. Davies, ed. *The Design and Analysis of Industrial Experiments*, 2nd Ed. Longman Press, 1956, NY, p. 20

78. F. Bowden, D. Tabor, *The Friction and Lubrication of Solids*, Clarendon Press, Oxford, UK, 1950, p. 99

79. M. Liewald, S. Wagner, D. Becker, *Influence of Surface Topography on the Tribological Behaviour of Aluminum Alloy 5182 with EDT Surface*. Springer, 2010

80. J. Schey, *Tribology in Metalworking: Friction, Lubrication, and Wear*, ASM, Metals Park, Ohio 1983, p.

81. G. Dalton, and J. Schey, " Effect of bead finish on friction and galling in the drawbead test," *SAE Technical Paper No. 920632,* 1992

82. A. Kovalchenko, et al., Scuffing tendencies of different metals against copper under non-lubricated conditions, *Wear 271* , 2011, 2998-3006

83. D. Tabor, in Preface to Paperback Edition Bowden and Tabor 1950, 1986 p. ix

84. O. Davies, ed. The Design and Analysis of Industrial Experiments, 2nd Ed. Longman Press, 1956, NY, p. 42

85. ibid, p. 46

86. H. Amick, Vibration Data Representation for Advanced Technology Facilities Reprinted from *Proceedings of 12th ASCE Engineering Mechanics Conference*, La Jolla, California, May 17-20, 1998, pp. 306-309

87. Holt, Goddard, Palmer, "Methods of measurement and assessment of the acoustic emission activity from the deformation of low alloy steels", NDT International, Volume 14, Issue 2, Pages 49-53

88. Pressure Vessel failure Monitoring, Acoustic Emission Manual, Vallen System Gmbh, Munich, 1998

89. J. Archard, Contact and Rubbing of Flat Surface, *J. Appl. Phys.* Vol 24 (8) 1953 p981–988.

90. A. Cameron, *Basic Lubrication Theory*, Longman Grp Ltd, London, UK 1970

91. F. Bowden, D. Tabor, *The Friction and Lubrication of Solids*, Clarendon Press, Oxford, UK, 1950, pg. 247.

92. http://www.matweb.com/search/datasheet.aspx?matguid=145867c159894de286d4803a0fc0fe0f&ckck=1, accessed 2014/01/17

93. http://www.cartech.com/toolsteelspowder.aspx?id=2432, accessed 2014/01/17

94. B. Gabriel, *SEM: A User's Manual for Material Science*, ASM Publishing, Metals Park, OH 1985

95. A. Cameron, *Basic Lubrication Theory*, Longman Grp Ltd, London, UK 1970, p 1

96. J. Schey, *Tribology in Metalworking: Friction, Lubrication, and Wear*, ASM, Metals Park, Ohio 1983, p 59

97. M. Liewald, et al. *Influence of Surface Topography on the Tribological Behaviour of Aluminum Alloy 5182 with EDT Surface*. Springer, 2010

98. J. Schey, *Tribology in Metalworking: Friction, Lubrication, and Wear*, ASM, Metals Park, Ohio 1983, p. 141

99. A. Cameron, *Basic Lubrication Theory*, Longman Grp Ltd, London, UK 1970, p. 171

100. ibid, p. 173

101. Photo: "The Effects of Grinding" retrieved from: http://www.ennaide.com/enProductShow.asp?id=579

102. F. Bowden, D. Tabor, *The Friction and Lubrication of Solids*, Clarendon Press, Oxford, UK, 1950, p.189

103. ibid p.247

104. H. Benabdallah, D. Aguilar, Acoustic Emission and Its Relationship with Friction and Wear for Sliding Contact, *Tribology Transactions*, 51: 738-747, 2008

105. Ted McClure, TribSys LLC, private communications May, 2013

106. J. Halling, *Principles of Tribology*, MacMillan Press Ltd, London, UK 1975, p. 80

107. ibid, p. 92

108. L. Deck, P. de Groot, High-speed noncontact profiler based on scanning white-light interferometry, *APPLIED OPTICS* / Vol. 33, No. 31 / 1 November 1994, p7334-8

109. A. Cameron, *Basic Lubrication Theory*, Longman Grp Ltd, London, UK 1970 p 171-3

110. http://web.archive.org/web/20070216065646/http://las.perkinelmer.com/content/TechnicalInfo/TCH_FTIRATR.pdf

111. http://www.perkinelmer.com/catalog/category/id/ftir%20software

112. Essentialftir v. 1.50, Operant LLC, http://www.essentialftir.com/download.shtml

113. G. Lakanen et al., "Adhesion Detection Using the Twist Compression Test and Neural Networks", unpublished

Appendices

Appendix 1. TCT Specimen Preparation

Several measures should be taken to ensure that specimens were prepared in a way that reduced bias and operator error. First, it is critical to control specimens and to ensure they are the specimens matching their labels. Because the surface properties can vary significantly between the two sides of the steel sheet, care was taken to orient specimens from a single sheet in a consistent manner. In order to reduce potential influences from variations in the tooling of the TCT, a single batch of annular tools are used. While the finishing technique was nominally the same, using test specimens that were prepared at different times introduces the possibility if an uncontrolled variable. Lubricant specimens were labeled and only the lubricant being tested was opened. The following outlines some of the specifics related to preparation and handling of specimens before and after testing.

1. Annulus - machined, hardened and tempered to Rc 61 ±1, lapped with SiC powder to Ra = 0.10μm, identified with a diamond engraver, degreased with mineral spirits and cleaned with nonpolar solvent.

2. Flat –flat and scratch free. Orientation (same side) of master sheet was identified, sheared, deburred, test code marked with an engraver, degreased with mineral spirits and then cleaned with a nonpolar solvent, lubricated just prior to testing (within 60s).

3. Lubricant – additive levels by wt %, balanced viscosity by adjusting base stock, labelled jar and lid with unique code and date. Only opened one bottle at a time and used a new disposable pipette to apply the lube for each test.

Appendix 2. TCT Test Procedure

The following procedure was followed for all tests:

1. Prepare specimens - degrease and clean annular specimens ensuring they were free of nicks and no lint remains.
2. Entered test parameters in TCT DAQ interface and calibrated pressure on TCT Unit.
3. Loaded sheet specimen and annular specimen in their respective holders. Applied a few drops of lubricant with a disposable pipette to the sheet specimen and distributed it uniformly.
4. Started the test and watched the display to terminate the test after breakdown had occurred. A test was stopped as soon as possible after breakdown had occurred to preserve the specimens.
5. Removed the specimens and wrote the annular tool number within the contact ring of the sheet specimen for post-test analysis.
6. Repeated steps 3-5 using fresh sheet and annular specimens for a total of 3 replicates for each lubricant.

Appendix 3 – Friction Force and COF Calculation From Sensor Voltage

TCT Spec	Imperial	Metric
OD inch (mm)	1.0000	25.4000
ID inch (mm)	0.7500	19.0500
Area in^2 (mm^2)	0.3436	221.6845
Moment Arm inch (mm)	0.4419	11.2253

Centroid of Annulus

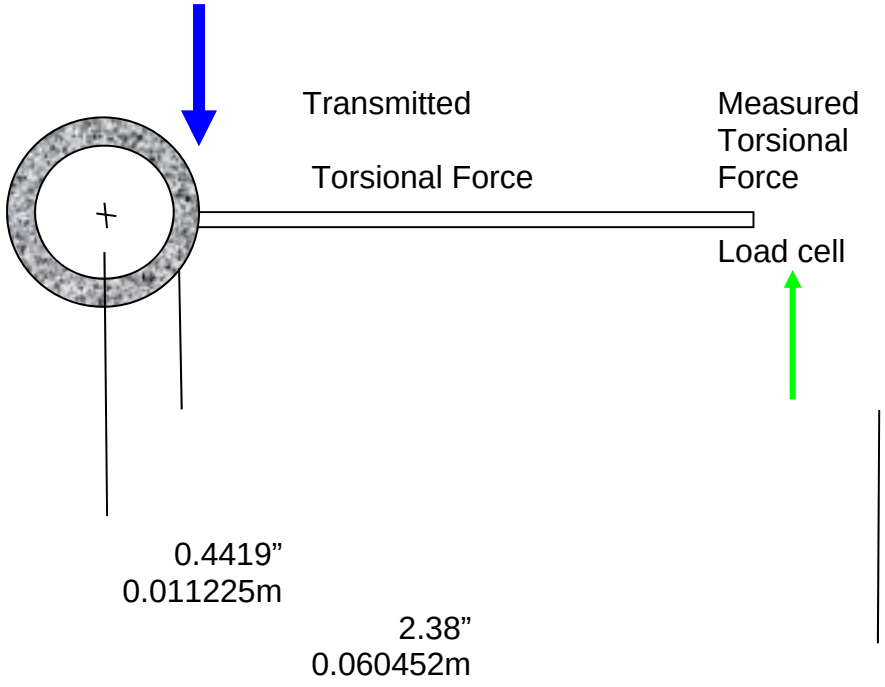

Transmitted Torsion=measured torsion x torque applier arm/ specimen arm

Conv Factor (V>F)	193.1043	lbs/V	0.858970524	kN/V
measured Torsion	193.1043	lbs	0.8590	kN
Torque applier rad	2.38	in	0.0605	m
Specimen rad	0.4419	in	0.0112	m
Transmitted Torsion	1039.929	lbs	4.625835646	kN
ratio	5.385325		5.3853	

Hence a load cell measurement of 1 volt = frictional force acting at the centroid of 4.626 kN

At 100MPa contact stress

COF = (4.626kN/V*1000N/kN)/(221.6845mm^2*100N/mm^2) = 0.208/V

Or 1V transmitted torsional force at 100MPa ~ COF = 0.2

Appendix 4- Main Study ANOVA Table

Anova: Two-Factor With Replication

Main Study Results - Time-to-breakdown (COF=0.2)

SUMMARY	BaseStock	Ester	Chlorine	Total
Low Visc				
Count	3	3	3	9
Sum	34.5	68	145	247.5
Average	11.5	22.66667	48.33333	27.5
Variance	0.25	12.33333	72.33333	288.75
High Visc				
Count	3	3	3	9
Sum	70.5	160.5	206	437
Average	23.5	53.5	68.66667	48.55556
Variance	31.75	20.25	134.3333	442.8403
Total				
Count	6	6	6	
Sum	105	228.5	351	
Average	17.5	38.08333	58.5	
Variance	56	298.2417	206.7	

ANOVA

Source of Variation	*SS*	*df*	*MS*	*F*	*P-value*	*F crit*
Sample	1995.014	1	1995.014	44.12934	2.38E-05	9.330212
Columns	5043.028	2	2521.514	55.77542	8.39E-07	6.926608
Interaction	267.1944	2	133.5972	2.955146	0.090463	6.926608
Within	542.5	12	45.20833			
Total	7847.736	17				

Appendix 5 - TCT Sensor Curves from DAQ

Main Study (3 lubes, 2 visosities) : A5 – Main Study.pdf

Extended Study (ELV pre-failure); A5 – ELV Prefailure.pdf

Extended Study (ELV early failure); A5 – ELV early failure.pdf

Extended Study (ELV late failure); A5 – ELV Failure.pdf